KEMIAN LAITOS
JYVÄSKYLÄN YLIOPISTO

Peptide-based transient gels

M.Sc. thesis

University of Jyväskylä

Department of Chemistry

04.04.2023

Jenni Rive

Abstract

The literature part of this master's thesis deals with transient gels and their potential applications. Special emphasis was put on peptide-based transient gels and their properties.

The experimental part of the thesis focuses on the effect of chemically active organic solvents and acid concentration on the temporal self-assembly, the gelation mechanism and the network of in situ formed organogels. In this study, the amino acid-based precursor gelator (Boc-Phe-Phe-O*t*Bu) was used to form organogels. The selective deprotection reaction of the Boc group in the attendance of the *tert*-butyl group was the driving force of the gelation. The effects of organic solvents on gelation and the structure of the gels were investigated by NMR and FT-IR spectroscopy, mass spectrometry, scanning electron microscopy (SEM), and various other experiments on the gels. The organic solvents used were shown to support the formation of gels, participate in the gelation process and affect the spatiotemporal properties of the gel.

Tiivistelmä

Tämän pro gradu -tutkielman kirjallisuusosa käsittelee transientteja geelejä ja niiden mahdollisia sovelluksia tulevaisuudessa. Transientit geelit ovat epätasapainotilassa ja niiden itsejärjestäytymistä sekä hajoamista voidaan säädellä ennalta ohjatusti erilaisten kemiallisten polttoaineiden tai valon avulla. Kirjallisuusosassa perehdyttiin tarkemmin peptidipohjaisiintransienttigeeleihin ja niiden ominaisuuksiin sekä valmistamiseen.

Tutkielman kokeellisessa osassa tutkittiin kemiallisesti aktiivisten orgaanisten liuottimien ja happopitoisuuden vaikutusta geelien itsejärjestäytymiseen, geeliytymismekanismiin ja muodostuvien organogeelien rakenteeseen. Tässä tutkimuksessa organogeelien muodostamiseen käytettiin aminohappopohjaista prekursorigelaattoria (Boc-Phe-Phe-O*t*Bu). Boc-suojaryhmän selektiivinen poisto *tert*-butyyliryhmän läsnä ollessa aiheutti geeliytymisen. Orgaanisten liuottimien vaikutuksia geeliytymiseen ja geelien rakenteeseen tutkittiin NMR- ja FT-IR-spektroskopialla, massaspektrometrialla, pyyhkäisyelektronimikroskopialla (SEM) ja erilaisilla geeleille tehdyillä kokeilla. Käytettyjen orgaanisten liuottimien osoitettiin tukevan geelien muodostumista, osallistuvan geeliytymisprosessiin sekä vaikuttavan geelin spatiotemporaalisiin ominaisuuksiin.

Preface

The experimental part of this master's thesis was done from June 2022 to August 2022 at the Nanoscience Center of the University of Jyväskylä. The literature part was done from September 2022 to April 2023. Professor Maija Nissinen acted as supervisor for my master's thesis, and postdoctoral researcher Efstratios Sitsanidis supervised the experimental work. I would like to thank them both for their guidance and advice during the work. I would also like to thank docent Tanja Lahtinen for acting as the second examiner of the thesis.

Table of Contents

Abbreviations

$AcCH_2CO_2tBu$	*tert*-Butyl acetoacetate
Ala	Alanine
Asp	Aspartic acid
ATP	Adenosine triphosphate
Boc	*tert*-Butyloxycarbonyl
Boc-Phe-Phe-OtBu	Boc-*L*-phenylalanyl-*L*-phenylalanine *tert*-butyl ester
CGC	Critical gelation concentration
CH_3OtBu	*tert*-Butyl methyl ether
$ClCH_2CO_2tBu$	*tert*-Butyl chloroacetate
CSH	Cysteine thiol
CSSC	Cysteine disulfide
DBC	Dibenzoyl-*L*-cystine
DBD-$(OMe)_2$	Dibenzoyl-*L*-cystine ester form
DF-OMe	Aspartame
DMF	Dimethylformamide
DMSO	Dimethyl sulfoxide
DTT	Dithiothreitol
Fmoc	Fluorenylmethyloxycarbonyl
FT-IR	Fourier-transform infrared spectroscopy
GHEC	Glycerol hydroxyethyl cellulose
Glu	Glutamic acid
Gly	Glycine
HCO_2tBu	*tert*-Butyl formate

HEC	Hydroxyethyl cellulose
His	Histidine
HR-MS	High-resolution mass spectrometry
Ile	Isoleucine
Leu	Leucine
LMW	Low molecular weight
LMWG	Low molecular weight gelator
Lys	Lysine
MC	Merocyanine
Nap	Naphthalene
PG	Partial gel
Phe	Phenylalanine
Phe-Phe	Diphenylalanine
Phe-Phe-OtBu	*L*-phenylalanyl-*L*-phenylalanine *tert*-butyl ester
SEM	Scanning electron microscopy
Sol	Solution
SP	Spiropyran
SPR	Surface plasmon resonance spectroscopy
SSG	Self-supporting gel
tBuOAc	*Ter*t-butyl acetate
TCA	Trichloroacetic acid
TLC	Thin-layer chromatography
Tyr	Tyrosine
Val	Valine

LITERATURE PART

1 Introduction

A gel is a system that consists of at least two different components, one of which is solid and the other liquid. The gel consists mostly of liquid and has some of the properties of liquid components, but it still behaves in some parts like a solid substance.[1] Gels can be roughly separated into chemical and physical gels. Physical gels are also called supramolecular gels and are prepared from low molecular weight gelators (LMWG) or polymers, which act as gelators. Gelation occurs through supramolecular self-assembly by non-covalent interactions. Chemical gels are based on covalent bonds, i.e. strong interactions.[2] Physical gels have gained increasing recognition over the last decades due to their diverse use in various areas, such as tissue engineering, cell culture, catalysis or antimicrobial and self-healing materials.[2,3]

Most synthetic materials, for example gels, are in the equilibrium state. However, structures and materials can also appear in a non-equilibrium state, where energy and matter are exchanged with the environment. Actually, various natural structures cannot be in equilibrium because they are thermodynamically unstable.[4] Many living systems in nature self-assemble from building blocks and are in a state of imbalance. Self-assembly processes are controlled by the energy obtained from the reaction cycle and from the outside.[5]

Creating artificial non-equilibrium gel assemblies, i.e. transient gels, is becoming more common in molecular self-assembly and supramolecular chemistry. These dynamic transient gel assemblies have many useful properties compared to their equilibrium counterparts, such as the capability to be managed over space and time or heal themselves. Such properties would create significant steps towards the synthesis of artificial life.[6] Stimulus-sensitive supramolecular gelators are ideal building blocks for designing synthetic materials with autonomous time-dependent properties that mimic living systems, especially if they constitute of biologically relevant components.[7]

Transient gels can be prepared using many different gelators, for example, peptide-based gelators. In this case, various amino acids act as building blocks, and the properties of the gel can be changed and controlled easily by simply changing the amino acids.[2] Peptide-based transient gels can be achieved

by reaction cycles that use either chemical fuel or light as energy.[6] Such transient peptide-based gels could be used, for example, to mimic and express the function of proteins or to craft remoldable items.[8] Transient gels generally also have many potential future applications, for example, in regenerative medicine and material chemistry.[8,9]

2 Low molecular weight gelators

Gels can be roughly separated into chemical and physical gels (Figure 1). LMWGs belong to physical gels defined by dynamic cross-links continuously being formed and broken.[10] LMWGs are small molecules that can form gels by self-assembling in aqueous or organic solutions. If the LMWG forms a gel in water, it is called a hydrogel, and if in an organic solvent, it is called an organogel. LMWGs form three-dimensional structures while gelling. These structures stick together by different weak interactions, like π–π stacking, hydrogen bonding and van der Waals forces.[11]

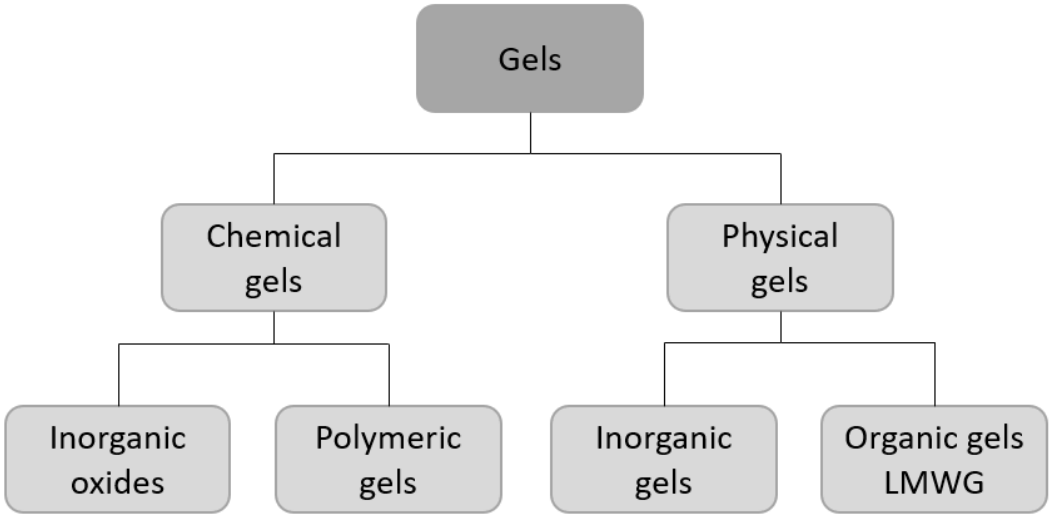

Figure 1. A rough classification of gels.[10]

LMWGs are often chiral. Most often, LMWGs include multiple stereogenic centers, thus exhibiting many different stereoisomers, generally showing different behavior during gelation. The spatial arrangement of the various diastereomers strongly affects their ability to create weak interactions. Because of this, modifying the configuration of one stereocenter can greatly affect the properties of the gel, such as the stiffness and the gelation temperature.[10]

LMWGs have recently attracted interest owing to their potential as simple and low-cost matrices which can be used in many different chemical, industrial and medical applications.[11] The LMWGs have properties that cannot easily be achieved with polymeric gelators, such as response to various

external stimuli.[2] Despite the rapid increase in LMWGs research recently, it is still challenging to foresee if a specific compound gels or not.[11]

2.1 Peptide-based gelators

A few properties are required for a gelator: (i) the compound must be partially insoluble in the solvent; (ii) the molecule must include functional groups which form weak interactions, such as π–π stacking interactions, hydrogen bonds, hydrophobic forces, and van der Waals forces; (iii) non-covalent interactions must be directed, guiding to the assembly of nanoscale fibers. For example, chiral peptide-based gelators have these properties.[10]

Peptides are made from amino acid monomers and are one of the most used LMWG components. Peptides constituting less than ten amino acids belong to LMWGs. Usually, peptide-based gelators used in gelation are shorter, such as di- or tripeptides, because they self-assemble more easily. Peptide-based gelators can act as organogelators or hydrogelators depending on their structure, which enables them to self-assemble through different weak interactions. These weak interactions form ordered supramolecular structures capable of trapping and immobilizing various solvent molecules.[10] The non-covalent gelator-gelator and solvent-gelator interactions provide good qualities, such as reversible phase transitions and sensitivity to various external stimulation.[2]

Peptide-based gelators have aroused interest due to their bioactive functionality, biodegradability and biocompatibility.[12] They are also easy to produce in large amounts and modify chemically and biologically.[10] They can be used, for example, to support cell growth.[11] LMW peptide gelators are also of interest because they can mimic the complex self-assembly of peptides in a simpler way. Understanding the folding or misfolding of peptide chains helps to understand how they can be used in real-life applications, such as preventing the formation of amyloid plaque that occurs in Alzheimer's disease.[11] Figure 2 shows the most common amino acids used in peptide-based gelators.

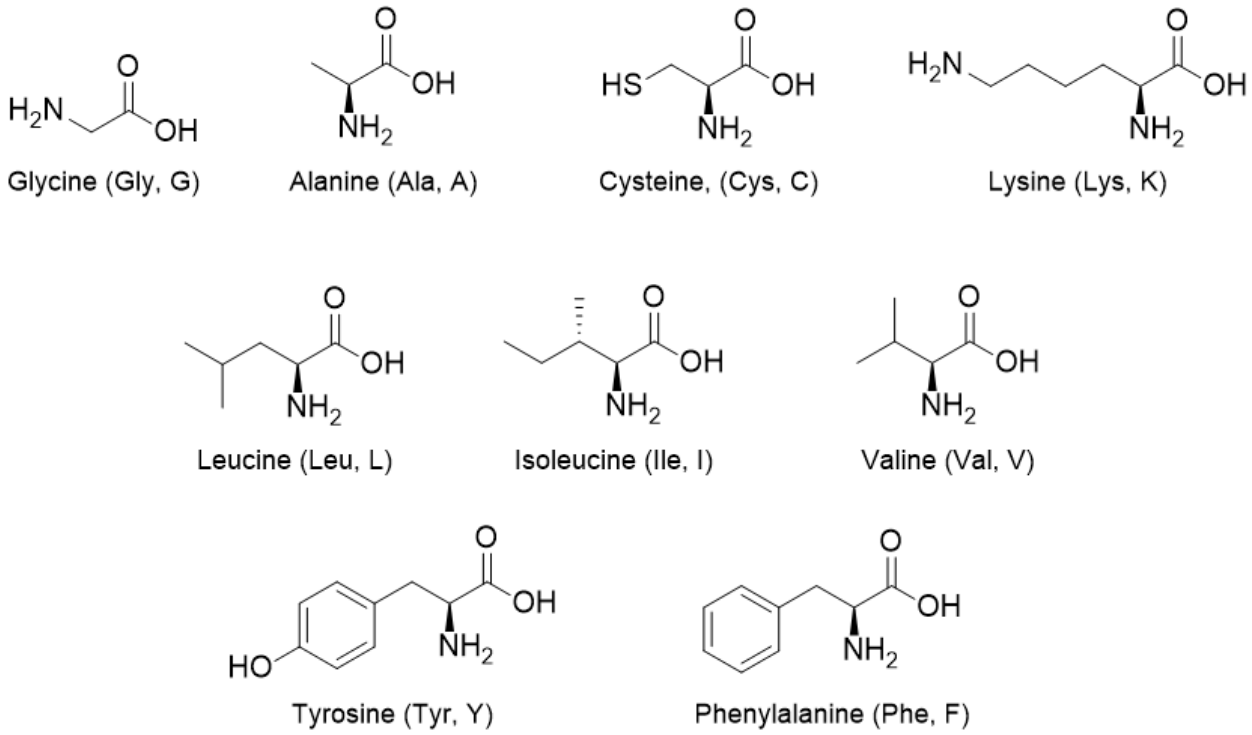

Figure 2. Common amino acids used in peptide-based gelators.

2.2 Characteristics of peptide-based gelators

Peptides are interesting gelators due to their side chains and free amino and carboxyl ends, which offer the opportunity to modify their functions by simply changing amino acids.[11,12] Peptide-based gelators can form gels with side chains capable of forming hydrophobic interactions and π–π stacking interactions, as shown by many studies of amino acids with aromatic side chains.

Among the monomers, phenylalanine (Phe; Figure 3) and its various derivatives are highly effective gelators. Phe is a relevant amino acid, and for the hydrophobicity of the aromatic side chain, it is categorised as a neutral and non-polar amino acid. Effective gelation in many different solvents is due to the π–π interactions and hydrophobicity induced by the phenyl group and the hydrogen bonds of the amide group.[2] The importance of the phenyl ring was noticed when research revealed that using other α-amino acids, such as leucine (Leu), alanine (Ala), histidine (His), and tryptophan (Trp), did not result in gelation with a metal cation.[13] When coordinating Phe with Cu(II) and dissolving the coordination complex in water, a hydrogel formed quickly, while gelation did not occur using other

amino acids. Phe has also been shown to be the only one of all 22 naturally occurring amino acids capable of forming supramolecular gels with a free N-terminus.[2] Chemical elaboration of Phe at the N- or C-terminus has allowed the development of many LMWGs for various applications.[2] Diphenylalanine (Phe-Phe (**2**); Figure 3) is, on the other hand, one of the earliest studied dipeptide gelators. Diphenylalanine can form gels in chloroform and aromatic solvents, for example in toluene, but not in solvents like acetone, methanol and cyclohexane.[11]

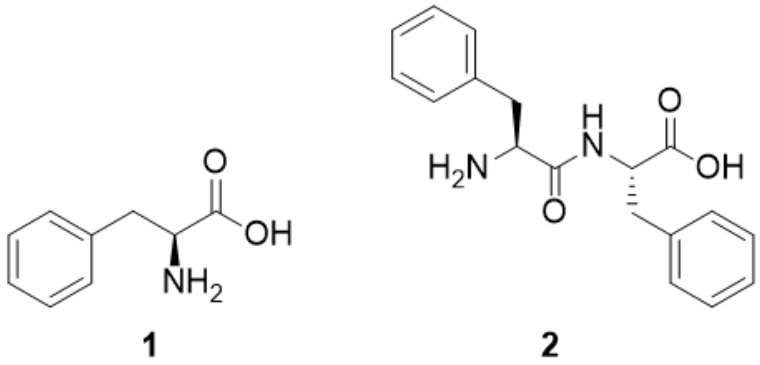

1 **2**

Figure 3. Structures of phenylalanine (Phe; **1**) and diphenylalanine (Phe-Phe; **2**).

The simplest approach to making peptide-based gelators is to attach an aromatic group to amino acids. In these gelators, the polar parts of amino acids are combined with hydrophobic side chains or N-protecting group. Aromatic groups, such as fluorenylmethyloxycarbonyl (Fmoc) and naphthalene (Nap; Figure 4), are effective and common in hydrogelators.[14,15] Studies have shown that Phe–Phe alone forms nanotubes or vesicles in an aqueous solution, while Fmoc–Phe–Phe forms extensive fibrillar structures that combine eventually to form hydrogels.[11] Other dipeptides have also been found to form gels when they contain such aromatic protecting groups. Therefore, gelation seems to work better when the gelator contains an aromatic protecting group, like Nap or Fmoc, at the N-terminus of the dipeptide.[10,11]

Other protecting groups have also been successfully used to form gels and modify gelators. The removal of *tert*-butyloxycarbonyl protection group (Boc group; Figure 4) has been used to form organogel in an active organic solvent[16] and to transform organogel into hydrogel with the help of pH change.[16,17] To form organogel in an active solvent, deprotection of the Boc group from Boc-Phe-Phe-O*t*Bu with acid was used, leading to a mixture of Phe-Phe-O*t*Bu and Phe-Phe (**2**). The balance between the two components resulted in a transient organogel.[16]

In another example, Boc protection at the primary amine of different peptide-based amphiphilic precursors led to efficient organogelators. However, deprotection of the Boc group under acidic conditions produced amphiphiles that could gel in water. Based on this observation, it was possible to convert the organogel into a hydrogel by simple protection and deprotection by changing the pH.[17]

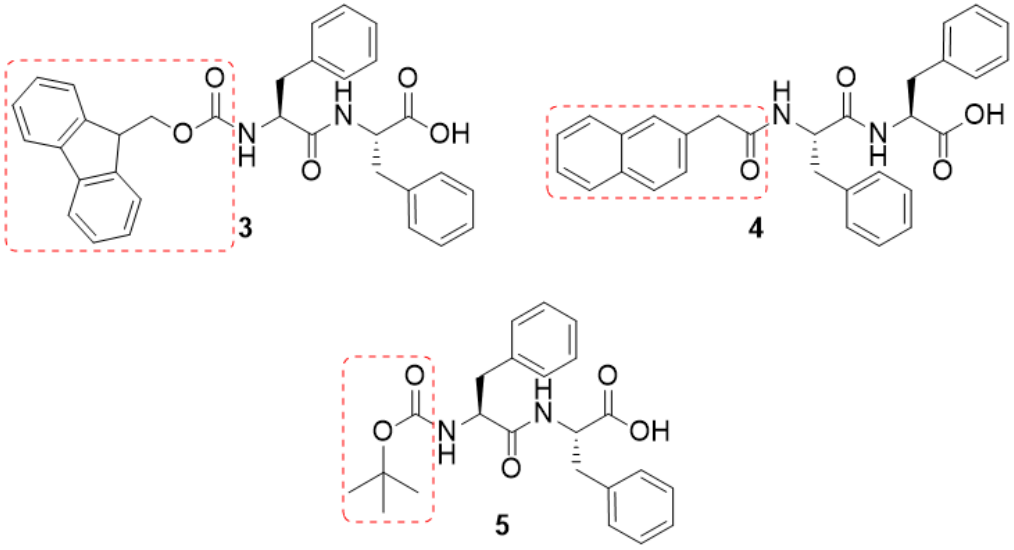

Figure 4. Structures of N-protected dipeptides: Fmoc-Phe-Phe **(3)**, Nap-Phe-Phe **(4)** and Boc-Phe-Phe **(5)**. Protecting groups are separated with a red line.

Fmoc is widely used in peptides as an N-terminus protecting group and guiding group for self-assembly.[12] The self-assembly of Fmoc-dipeptides is driven by π–π interactions and hydrogen bonding via the fluorenyl ring's π -electrons.[10] Gelation of Fmoc-Phe-Phe can be triggered by, for example, altering the pH of the solution or by adding water to the solution.

Yang *et al.*[18] noticed in their study of multicomponent supramolecular hydrogels that phenyl groups can improve the strength and elasticity of the gel. This was noticed when replacing the aliphatic side chain of the peptide gelators with an aromatic one. An increase in π - π stacking seems to increase the elasticity of the gel.[11] Bowerman *et al.*[19] found that peptides containing cyclohexyl alanine were better hydrogelators than the corresponding phenylalanine peptides. This suggests that hydrophobicity is more important than aromaticity in gelation.[11] The same effect was also noticed when amphiphilic the hydrogel formation of bola-amino acid derivatives were investigated. Bola-amino acid derivates have hydrophilic groups at both ends of the hydrophobic chain. Replacing valine with the more

hydrophobic isoleucine moiety greatly affected the gelation. The required amount of gelator decreased, and the aggregation properties of the gel improved.[20]

Debnath *et al.*[21] found, when studying the antimicrobial features of Fmoc-protected dipeptides functionalized with a pyridinium unit at the C-terminus, that the amino acid sequence affected the antimicrobial properties of the dipeptide. Many of the selected dipeptides proved to be highly bactericidal, and the best Fmoc-protected dipeptides contained an L-phenylalanine unit at the N-terminus. However, changing L-phenylalanine to the C-terminus of the dipeptide significantly reduced its antimicrobial features.

2.3 Gelation of peptide-based gelators

The gelation process of peptide-based gelators can be initiated using various external stimuli, such as light, temperature, pH, ionic stimuli or enzymes. The chemical functions and properties of gels can also be manipulated by simply changing their primary building blocks, i.e. amino acids.[2]

Peptide-based gelators self-assemble into a gel via different weak interactions, such as hydrogen bonding (Figure 5), π–π stacking and van der Waals forces. Hydrogen bonding is an essential part of the self-assembly process in gelation.[11] For example, self-organization of the phenyl moiety creates microvoids that can immobilize water via hydrogen bonding, thus forming hydrogels.[13] Many studies have shown that various dipeptides can self-assemble into a gel when the carboxylic acid group of the dipeptide is protonated, allowing more hydrogen bonds to form.[11]

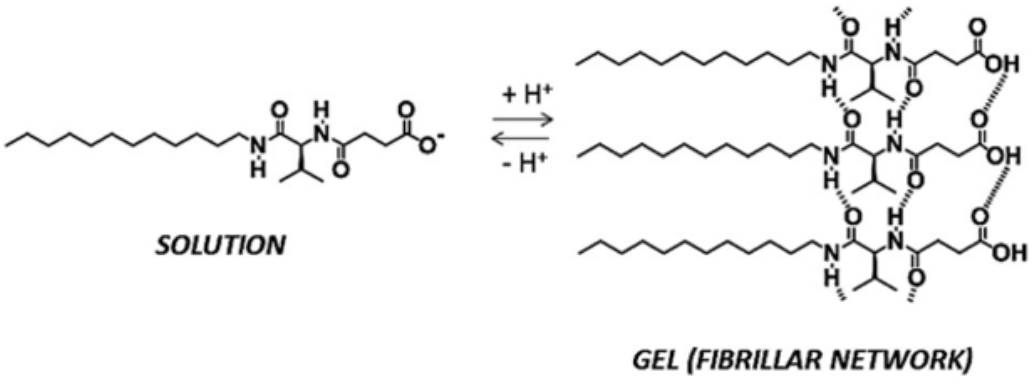

Figure 5. N-acylated amino acid units are assembled into a gel via hydrogen bonding.[22] Reprinted and adapted with permission from ref. 22. Copyright 2016 The Royal Society of Chemistry.

The kinetics of gel assembly and the final structure of the gel are related.[11] Chen *et al*.[23] studied this connection with the Nap-Ala-Val gelator and the help of fluorescent dye, thioflavin-T, which indicates β-sheet structure formation in peptides. Gel formation kinetics was measured by adding the fluorescent dye, whose fluorescence changes with respect to the viscosity of the solution. Nap-Ala-Val formed gel at pH under 5.2 and when the C-terminus was protonated. The properties of the gels depended on the terminal pH. At lower pH values, less β-sheet-type structures were perceived, and the formed fibrils were stiffer.

Johnson *et al*.[24] noticed that the rate of gelation affected the structure and properties of the Fmoc-Leu-Gly gel. Gel formation kinetics was studied by surface plasmon resonance spectroscopy (SPR). The rate of the pH drop affected the gelation time, and as the pH drop rate increased, denser and more heterogeneous gels were obtained.

Exchanging the amino acids at the C- and N-terminus can guide the development of a significantly different product upon gelation. Cheng *et al.*[25] studied the effect of the amino acid sequence on the properties of the hydrogel by comparing two slightly different protected tripeptides, Fmoc–Lys-Leu–Val and Fmoc–Val–Leu–Lys (Figure 6). In both tripeptides, the side chains of the lysine moieties were protected with Boc groups. Fmoc–Val–Leu–Lys assembled into a phase that contained aligned and ordered fibrils, whereas Fmoc–Lys–Leu–Val formed a branched fibril network.

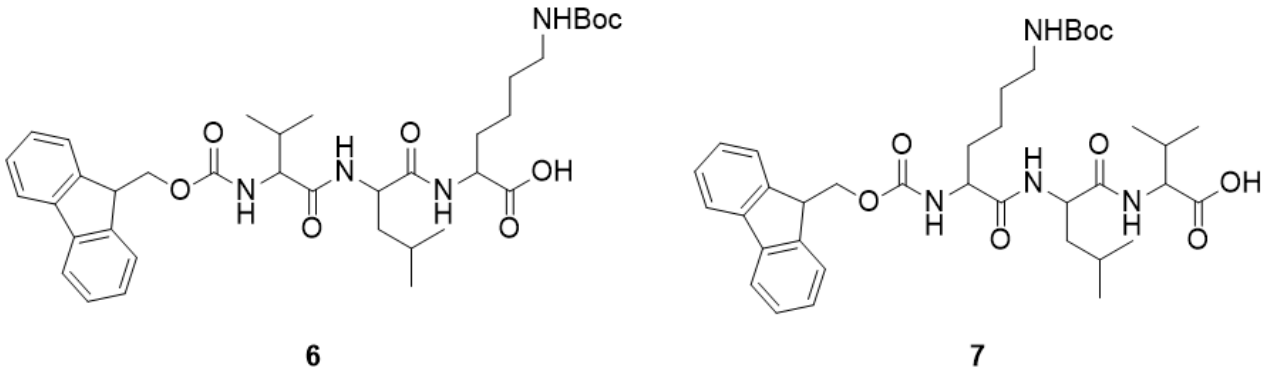

6 **7**

Figure 6. Structures of Fmoc protected tripeptides: Fmoc-Val-Leu-Lys(Boc) **(6)** and Fmoc-Lys(Boc)-Leu-Val **(7)**. In both peptides, the lysine is protected with the Boc group.[25]

Supramolecular hydrogels have also been obtained with the help of enzymes from Fmoc-protected amino acids or dipeptides. Yang *et al.*[26] used phosphatase as an enzyme to dephosphorylate the phosphate group from Fmoc-tyrosine-phosphate, resulting in a hydrogel (Figure 7). When gelation was attempted without alkaline phosphatase, the formation of hydrogel failed. Gelation with enzymes provides a method to observe the presence of enzymes or enzyme inhibitors and determine bacterial types. Such gels can also be used to develop drug delivery systems and new materials for different biomedical approaches.

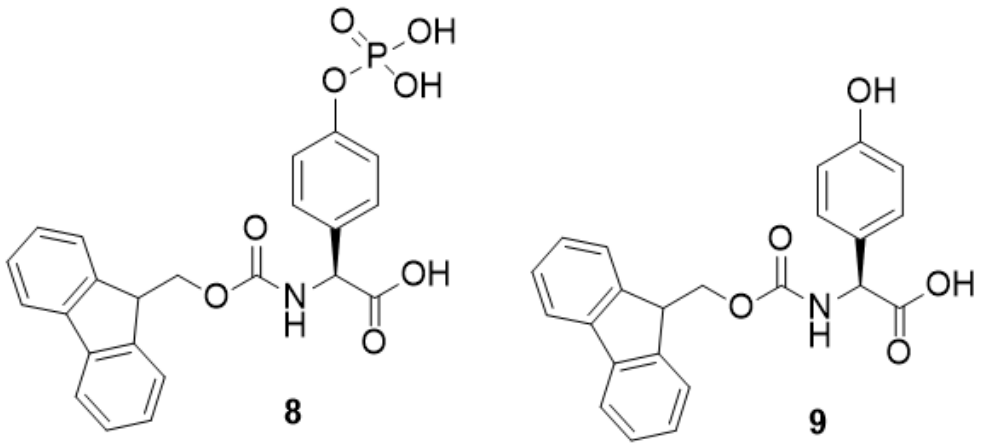

Figure 7. Structures of Fmoc-tyrosine-phosphate precursor **(8)** and Fmoc-tyrosine **(9)** that form hydrogel when the precursor is dephosphorylated.

3 Transient system

Usually, synthetic materials are in equilibrium and do not exchange energy with the environment. In many processes of living organisms, chemical fuel driven dissipative self-assembly is, however, common, making these living organisms transient in nature. These transient processes include cell motility, cell transport, cell proliferation, and morphogenesis. For example, actin and microtubules differ from self-assembled equilibrium systems and materials, as they can use the free energy produced by fuel to form and transport a transient structure.[5] Actins and microtubules use the energy obtained from adenosine triphosphate (ATP) as fuel, which enables them to transform and function as intended. A continuous supply of ATP keeps these transient biomolecular assemblies away from thermodynamic equilibrium. In nature, transient self-assembly structures can also work through these dissipative processes.[27] The behavior of such transient biological processes is driven by the kinetics of fuel consumption rather than thermodynamic stability.[5]

Because natural self-assembly systems are normally in a non-equilibrium state, they need an external energy supply, usually a chemical fuel, to maintain the assembled structures.[28] The chemical fuels convert precursors into self-assembling building blocks that are naturally unstable and revert to their original form (Figure 8). Therefore, according to the second law of thermodynamics, the configurations in question will exist as long as some external energy source is available, giving them a limited lifespan.[4] If the external energy source is removed, the assembled structures return to their original thermodynamically stable state.[28] The formation of the transient assemblies can be controlled by an external fuel supply, as their formation is thermodynamically unfavorable.[3] Transient assemblies are dissipative at the same time, as they are open systems and dissipate energy from the outside. On the other hand, a dissipative system is out of thermodynamic equilibrium and changes energy with the surrounding environment, making it an open and changing system.

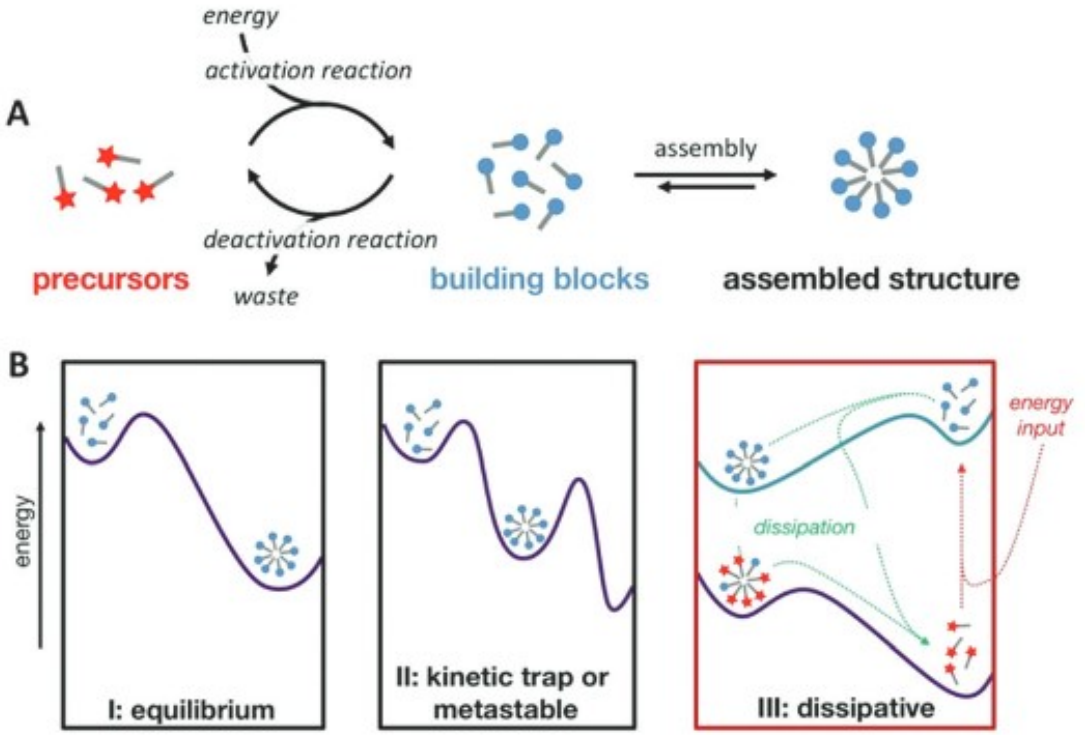

Figure 8. Comparison of energy of equilibrium self-assembly and dissipative self-assembly. In dissipative self-assembly, the system dissipates energy from outside and assembles building blocks from precursors. Building blocks then self-assemble into a designed structure. Formed structures dissolve back to their original form when the external energy supply is halted. Also, waste is usually produced in this prosses, as the equilibrium structures cannot break down back into precursors and then reassemble again into products.[4] Reprinted with permission from ref. 4., Copyright 2017 the Royal Society of Chemistry.

Many biological assemblies drift into a state of non-equilibrium due to the irreversible use of high-energy molecules (ATP). Because of this, they have exquisite dynamic properties such as adjustable lifespan, adaptability, and the ability to self-repair, whereas their synthetic counterparts, which are at or near equilibrium, lack these dynamic properties.[3] This has led to an interesting challenge to prepare synthetic counterparts to these natural transient systems, so-called chemically fueled transient supramolecular materials.[28] The self-assembly of these supramolecular materials is governed by a chemical reaction cycle. In this chemical reaction cycle, an activation reaction converts a precursor, which is first energetically at a minimum, into a building block.[4] The cycle of chemical reactions irreversibly consumes chemical fuel, which is a high-energy reactant, and induces the transition of

the precursor to the high-energy building block state.[3,4] The second reaction is the deactivation reaction which transforms the high-energy building blocks back into precursors.[4]

Successful strategies for constructing synthetic transient assemblies have included, for example, cooperative catalysis, chemically fueled assemblies, pH cycles and various enzyme-programmed reactions. Transient assemblies with tunable lifespans can be prepared by influencing the activation and deactivation kinetics.[28] The lifespan can be adjusted by the amount of chemical fuel, and it also depends on the reactivity of the precursor with the environment.[3,28]

Transient self-assembly systems are becoming more common as they can create unique structures[4] and transfer and store energy, bringing us nearer to realizing the remarkable features of living systems in synthetic systems.[27] These properties are, for example, spatial and temporal control of the activity, adaptability, the ability to self-repair the material, and self-organization into patterns (Figure 9).[4]

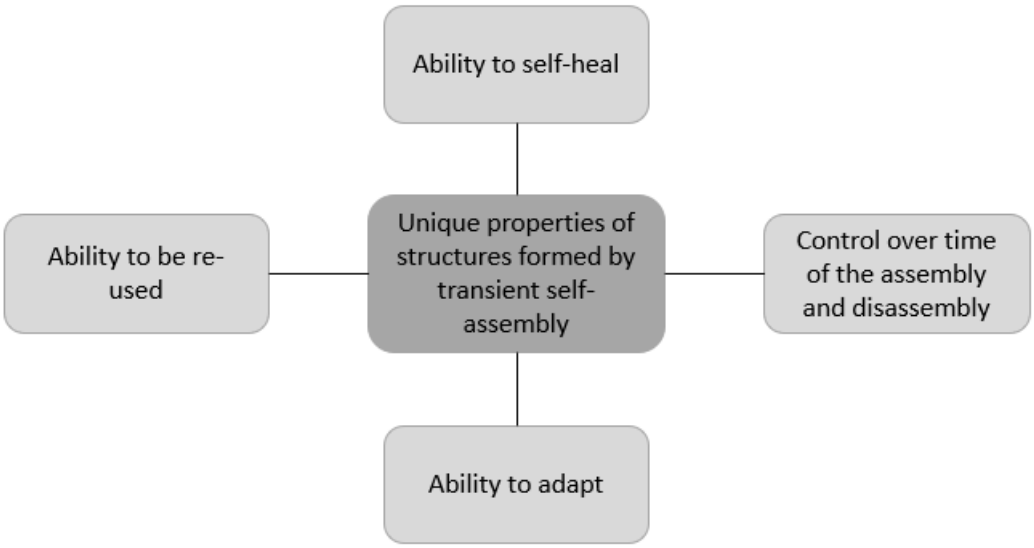

Figure 9. Unique and useful properties of the structures formed by transient self-assembly compared to systems in equilibrium.

4 Transient gels

Supramolecular gels have gained increasing attention as materials for non-equilibrium or energy-dissipative assemblies because they respond to signals such as redox, pH, and temperature changes and the presence of specific ions.[28] Supramolecular hydrogels, which typically do not heal on their own, can regenerate after damage if they form through dissipative self-assembly.[5] These gels have limitations too, such as a narrow pH or temperature range at which the precursor forms a gel.[28] The self-assembly pathway of transient gels is crucial in defining their final supramolecular structure.[29] Usually, the gelation starts relatively quickly (within 30 seconds), and therefore only the kinetics of the disassembly can be controlled, if any.[28]

Self-assembly of transient gels is controlled by a series of chemical reactions and an external energy source. The energy source transforms the precursor into a building block, and when the energy source runs out or changes, the building block transforms back into a precursor. In this way, a transient gel forms, and its lifetime can be adjusted by adjusting the external energy supply.[4] Lifetime can be regulated, for example, by the amount of fuel, the concentration of the precursor used or the concentration of the precursors involved in deactivation.[9] Temperature, pH, light or chemical fuel can be used as an external energy source for the formation and lifetime adjustment of the transient gels.[29]

Chemical reaction cycles in which transient gels are formed have a few basic requirements. The reactions must occur in the same environment and under the same conditions (solvent, temperature, ionic strength). Activation and deactivation reactions need to go along different pathways.[4] A precursor is converted into a product with irreversible consumption of external energy in the activation reaction. While the activation reaction needs to be irreversible, deactivation is a reversible spontaneous reaction which forms the precursor back from the product.[6] It should also be noted that the solvents and reagents that participate in these reactions should not be in contact with one other, at least not significantly.[4]

In the design of transient gels, it is also essential that the activation rate of the assembly is greater than the deactivation rate so that the formed gel withstands before the competing reaction breaks it back into building blocks.[7]

4.1 Fuel-driven transient gels

In fuel-driven reaction cycles forming transient gels, fuel levels and reaction rates define gel properties, such as lifetime and self-regeneration ability. To prepare a fuel-driven transient gel, the self-assembling system must be incorporated into a chemical reaction cycle where activation and deactivation of the system occur.

In fuel-driven reaction cycles, the process also creates waste, the amount of which limits the number of possible cycles.[5,6] When designing the dissipative reaction cycles, a challenge has been finding a chemical method in which the reaction of the fuel with the primary precursor is faster than fuel conversion into waste. Therefore, the reaction cycles can be considered catalysts that simultaneously turn precursors into transient building blocks for self-assembly and chemical fuel into waste (Figure 10). The energy from the fuel is transferred to the waste and temporarily stored in the produced metastable product. The stored energy can later cause dynamic changes in the structure of the intermediate product, for example, its self-organization into fibers and further into a gel.[6]

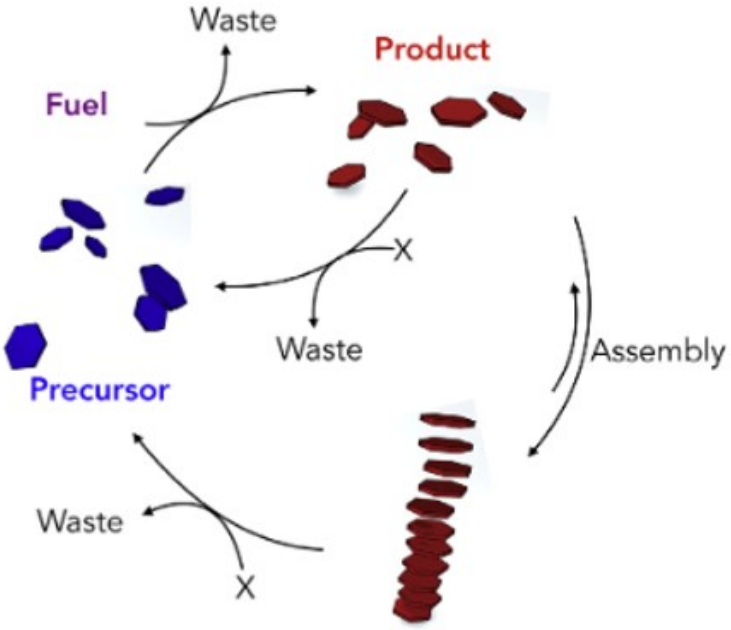

Figure 10. Scheme of transient self-assembly driven by chemical fuel. Precursors change into building blocks by dissipation of the fuel and further self-assemble into supramolecular material.[6]

One effective method for creating transient gels is to use a compound with an ionic charge, in which case the chemical fuel neutralises the precursor charge and forms a neutral compound. Gelators containing anionic carboxylate groups are one example, whereby ester formation is an activation reaction, and ester hydrolysis is a deactivation reaction. Negatively charged carboxylate is neutralised by a reaction with a chemical fuel acting as an alkylating electrophile to form a neutral ester. On the other hand, esters undergo spontaneous hydrolysis in aqueous environments, leading to the reformation of the carboxylate and alcohol, making this system transient (Figure 11). Active ester building blocks form fibers and a self-supporting hydrogel that, over time, collapses and dissolves back into a solution with anionic carboxylates.[5]

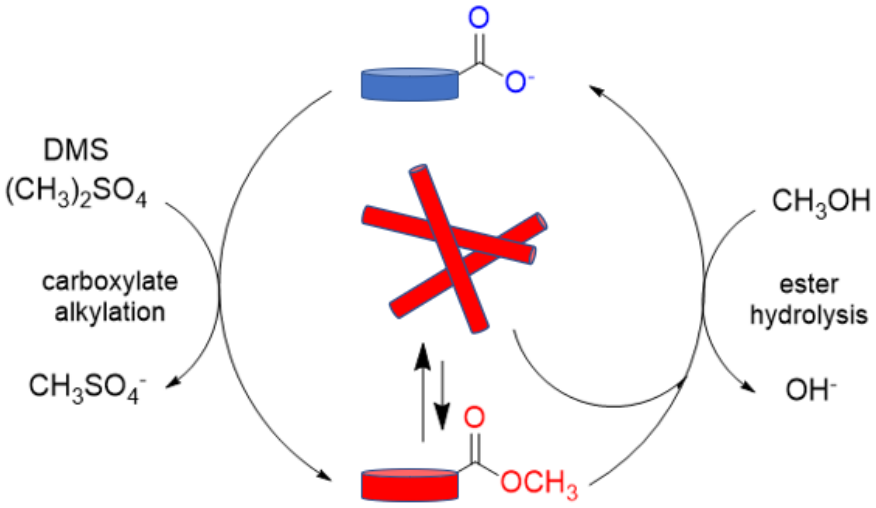

Figure 11. In the reaction cycle, the anionic carboxylates form active building blocks by reaction with alkylating electrophilic fuel (DMS). The building blocks self-assemble into fibers and further to hydrogels or hydrolyze back to inactive building blocks.[5]

Another successful method for producing transient gels is the fuel-driven chemical reaction cycle, which indirectly affects the self-assembly of the precursor. For example, a fuel-powered chemical reaction cycle can momentarily alter the pH of the solution, which causes the self-assembly of the precursor. Here, the building block itself does not react with the fuel but indirectly through a change in pH and thus does not catalyze the conversion of the fuel.[6]

Tena-Solsona *et al*.[30] developed a design that uses a chemical reaction cycle to neutralize the negative charge and cause transient self-assembly of Fmoc-protected peptides and amino acids. In this method, anionic amino acids, i.e., aspartic acid (Asp) or glutamic acid (Glu), were used at the C-terminus of

peptides to balance the self-organizing force caused by the Fmoc, which yielded soluble precursors. The reaction cycle changes the two carboxylates of C-terminal Asp or Glu into respective anhydrides by the hydrolysis of the carbodiimide. Neutralization of charges upon activation causes the products to self-assemble. The product can self-assemble into a hydrogel and form fibers, colloids or spherulites depending on the molecular structure of the precursor.

Transient gels can also be obtained by simultaneous oxidation-reduction reactions. Ogden and Guan[31] reported an out-of-equilibrium system that forms active hydrogel by a controlled mild redox network. In this redox network, they used a disulfide-based hydrogelator and its coupling to form an active hydrogel that assembles and disassembles by oxidation and reduction. Free cysteine thiol (CSH) was used as a precursor, and its dimer, cysteine disulfide (CSSC), was a gelator. Dithiothreitol (DTT) was used as the reducing agent, and hydrogen peroxide as the oxidizing agent. Oxidation of the cysteine precursor to its disulfide dimer induces gelation, while reduction of the disulfide gelator caused the gel to break down as the gelator reverted to the free thiol precursor (Figure 12).

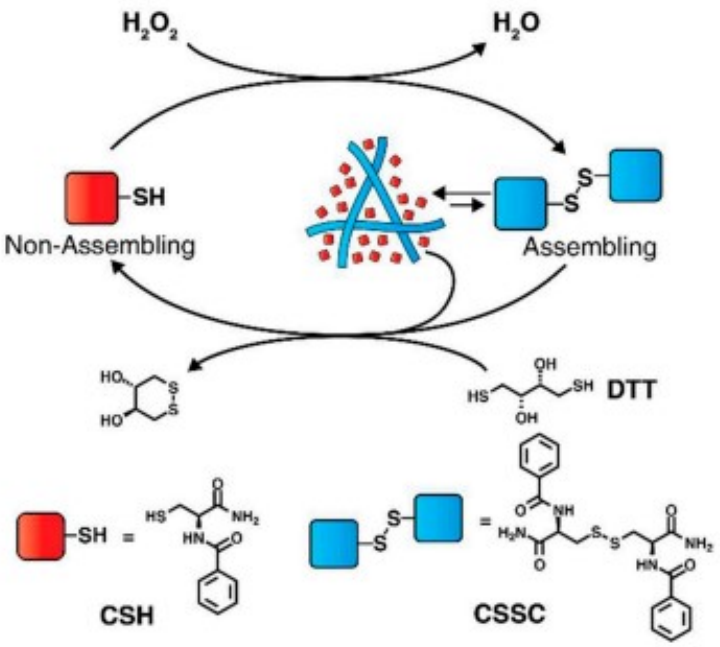

Figure 12. Scheme of the redox network that fuels dissipative self-assembly of an active hydrogel. Inactive precursor (CSH) converts into a gelator building block (CSSC) by oxidation, which assembles into active hydrogel-forming fibers. Hydrogel breaks down by the reduction of gelator molecules.[31] Reprinted with permission from ref. 31., Copyright 2019, with permission from John Wiley & Sons, Inc.

4.2 Light-driven transient gels

UV light is used as an energy source in many transient gelation systems, for example, in constructing gelators and nanoparticles.[31] This means that the reaction cycles that control dissipative self-organization can also be induced by light. The energy consumed in photon absorption controls the reaction cycles, and the light is altered into heat. In activation reactions, the molecule acting as a precursor absorbs a photon, and a photochemical reaction, such as photoisomerization, takes place (Figure 13). Also in this case, deactivation typically occurs spontaneously or through the absorption of another photon.[6] The photosensitive properties of gels are usually achieved by using photoisomerization of certain functional groups. The most often used functional groups are spiropyran and azobenzene.[32]

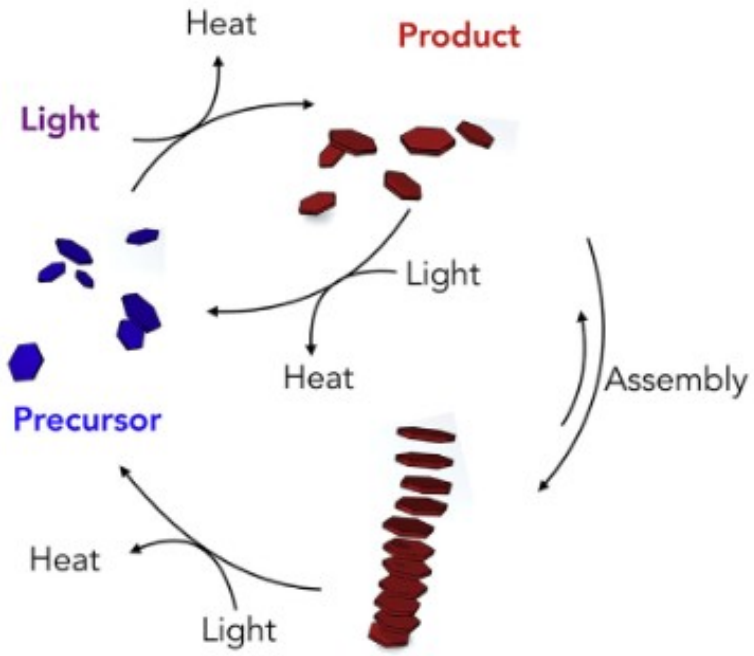

Figure 13. Scheme of dissipative self-assembly driven by light. Precursors change into building blocks (products) by consuming light and further assemble into supramolecular material. No waste is generated, only heat.[6] Reprinted with permission from ref. 6., Copyright 2019, with permission from Elsevier.

These reaction cycles differ from chemical fuel induced reaction cycles in two ways: light-powered reaction cycles do not produce chemical waste, unlike fuel-powered cycles. Since the resulting waste

accumulates and limits the reaction cycles, their number or the assembly process itself, this difference is useful. Light-driven dissipative systems can, therefore, usually perform more reaction cycles compared to fuel-driven ones. Another difference is that light-powered reaction cycles are not catalytic, unlike fuel-powered ones. Because of this, energy is not changed into heat slower or faster, depending on the presence of the precursor.[6] These reaction cycles can be used to regulate the lifetime of dissipative systems more precisely than fuel-powered ones. The energy source is lost as soon as the light source is turned off/removed, and the activation reaction stops, simultaneously stopping the formation of material, while in a fuel-powered cycle, the fuel slowly runs out.[4]

5 Transient peptide gels

The ability of peptides to self-assemble leads to many useful properties, such as structural simplicity and dynamic properties. Because of this, they have been used to create materials that mimic biologically transient systems but with plain structures, enabling a practical approach to the system. These synthetic mimics have led to transient nanostructures and artificial engines powered by chemical fuels and light. The self-assembled peptide nanofibers exhibit dynamic instability, which can be accomplished, for example, by a rival for catalytic peptide formation and hydrolysis, which are the forces of self-assembly and disassembly in the process.[14]

5.1 Acid-controlled transient gelation

Researchers have succeeded in creating transient supramolecular peptide-based gels utilizing pH changes. In these transient gels, the amount of acid controls the transient nature of the gel. The first system mimicking microtubule-formation's transient nature was achieved by Boekhoven *et al.*[33] In their study, the gelation was based on pH-sensitive dibenzoyl-L-cystine (DBC) and its ester form (DBD-$(OMe)_2$). Gel formation was not observed when the pH was above the pKa value of carboxylic acids (about 4.5). This was due to the electrostatic repulsion between the carboxylate groups. However, self-organization of the fibers and further gel formation occurred when the pH was below the pKa of the carboxyl groups. DBC was methylated and neutralized by methyl iodide (MeI) in mild conditions to form esters. In the same conditions, esters spontaneously hydrolyzed and formed the original precursor molecule (Figure 14).

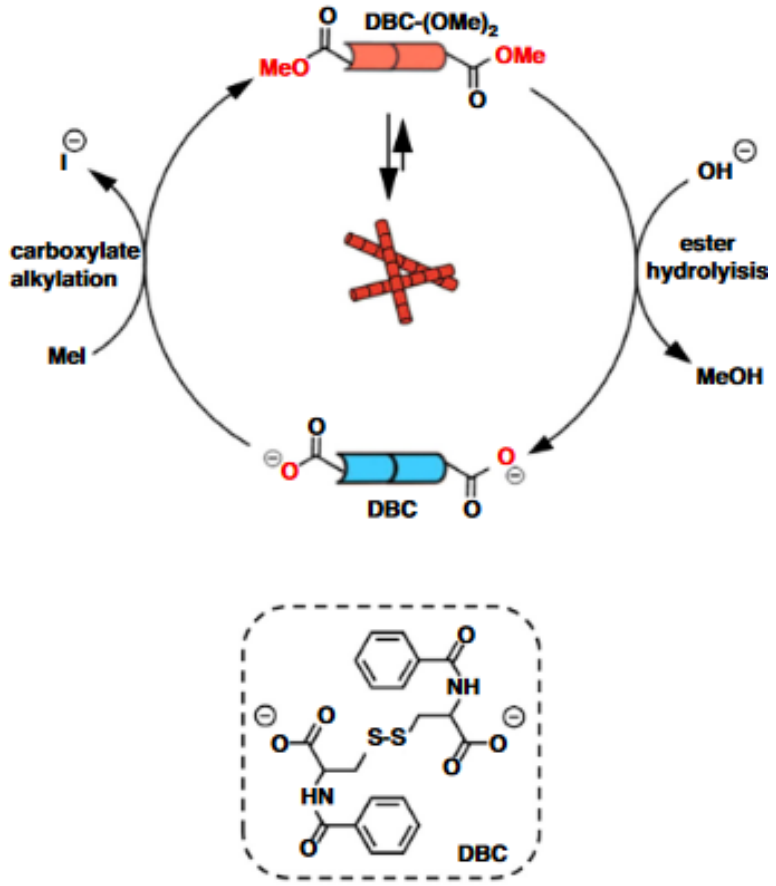

Figure 14. Scheme of transient gelation using DBC precursor. The transient gelation system was formed by the esterification of DBC and its hydrolysis. Dibenzoyl-L-cystines ester form (DBD-$(OMe)_2$) self-assembles into fibers and further into a gel.[33] Reprinted from ref. 35., Copyright 2016, with permission from Elsevier.

The esters formed by methylation self-organize into fibers stabilized by intermolecular hydrogen bonds, which further organize into a gel. The lifetime and properties of the formed gel could be manipulated with the used chemical fuel and control of pH. It was noticed that when low amounts of fuel were used, short-lived and weak gels were obtained, while long-lived and stiff gels were obtained when high fuel concentrations were used.[33]

Other pH-sensitive transient peptide-based gels have also been successfully synthesized. For example, Mondal *et al.*[7] achieved a transient supramolecular hydrogel mimicking a living system in their research, and Chevigny *et al.*[16] succeeded in creating a transient peptide-based organogel whose lifetime could be changed by the amount of acid. In the transient system by Mondal *et al.*,[7] the pH change is a trigger for the self-assembly of phenylalanine and, at the same time, for the disassembly

of the formed fibrils. When acid is added to the reaction, benzyloxy carbonyl-L-phenylalaninate is protonated and forms a hydrogen-bonded dimer that self-assembles to fibrils and further to hydrogel (Figure 15). When urea and urease are added to the reaction, the reaction between them produces NH_3, which in turn causes the fibrils to break down.

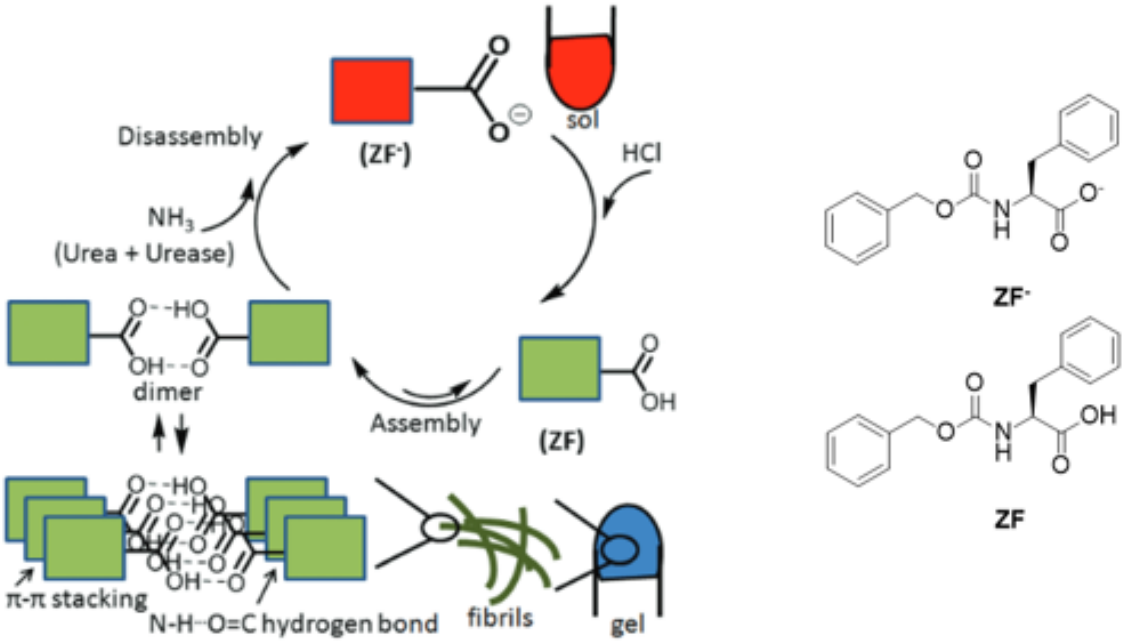

Figure 15. Scheme of acid-induced transient fibril and hydrogel formation and NH_3-induced defibrillation. ((Benzyloxy)carbonyl)-L-phenylalaninate (ZF^-) is protonated by HCl. Protonated ((benzyloxy)carbonyl)-L-phenylalanine (ZF) form dimers that self-assemble into fibrils and hydrogel by π-π stacking and hydrogen bonds. Urease-catalyzed breakdown of urea into ammonia causes the increase in pH and dimers and fibrils to break up.[7] Reprinted with permission from ref. 7., Copyright 2020, with permission from The Royal Society of Chemistry.

Chevigny *et al.*[16] achieved a transient organogel whose lifetime could be controlled with acid and active organic solvent. In this gelation system, Boc-Phe-Phe-O*t*Bu acts as a precursor and sulfuric acid as a gelation trigger (Figure 16). While sulfuric acid triggers the gelation, the solvent used in the gelation, *t*BuOAc, acts as a braking factor. Solvents usually do not have a major role in gelation, but in this case, the solvent had a remarkable effect on the stability of the gel. The lifetime of the organogel could therefore be controlled by the amount of acid and the solvent. By reducing the amount of acid, the lifetime of the gel increased from four days to four weeks. *t*BuOAc prevented the

formation of *t*BuOH, which would cause the gel to break into sol. Therefore, addition of *t*BuOAc increased the stability of the organogel.

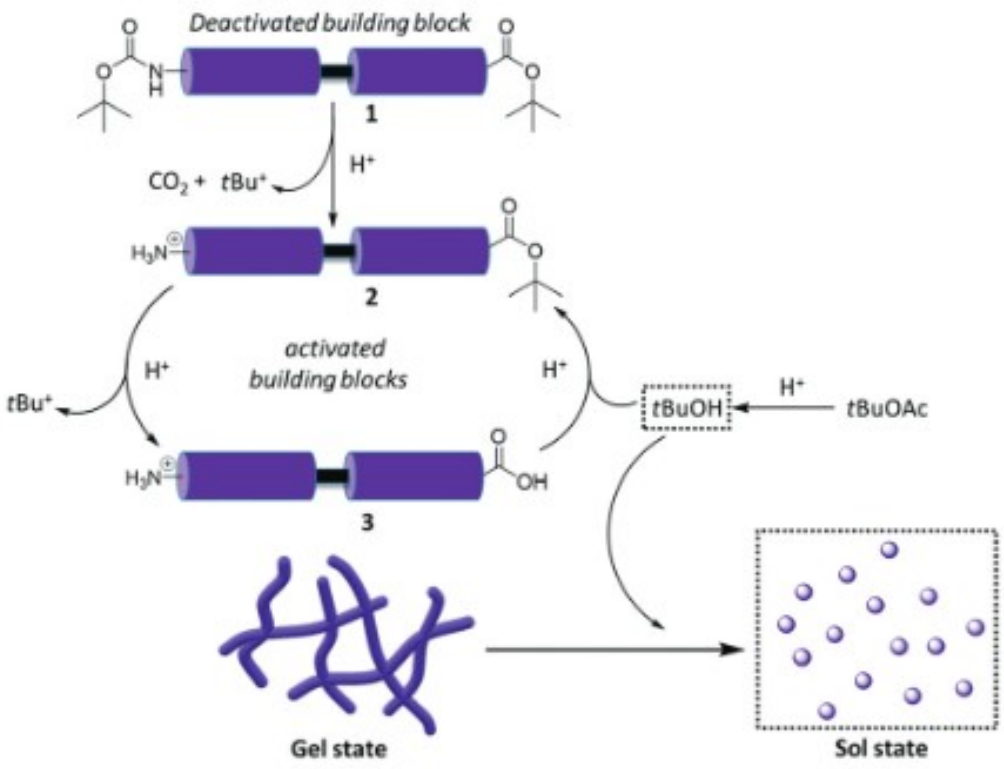

Figure 16. Transient self-assembly of Boc-Phe-Phe-O*t*Bu based organogel. Acid triggers the gelation process by deprotecting the Boc and *tert*-butyl groups. Gelation takes place as a balance of Phe-Phe-O*t*Bu and Phe-Phe. Normally, forming *t*BuOH causes the desolvation of the gel, but *t*BuOAc, as an active solvent acts as a brake and prevents the formation of *t*BuOH and the collapse of the formed gel.[16] Reprinted with permission from ref. 16. Copyright 2021, with permission from The Royal Society of Chemistry.

5.2 Enzyme-controlled transient gelation

Debnath *et al.*[34] formed transient hydrogel, whose formation was based on the gelation properties of naphthalene dipeptides. The formation of the hydrogel was controlled by an enzyme-catalyzed peptide coupling reaction between the methyl ester fuel and the precursor. α-chymotrypsin was used

as an enzyme to catalyze the reactions and form a peptide bond between hydrophobic amino acid X-NH_2 (X = Tyr (Y), Phe (F) or Leu (L)) and naphthalene-protected tyrosine methyl ester (Nap-Tyr-OMe) (Figure 17). Nap-Tyr-OMe acted as an acyl-donor, forming a peptide bond between the ester and the X-NH_2. The same enzyme causes the hydrolysis of the formed peptide building block by catalyzation. After some time, the fuel was consumed, and the hydrolysis of the formed dipeptide to the amino acid precursor took over. This, in turn, led to the collapse of the hydrogel, resulting in a transient hydrogel.

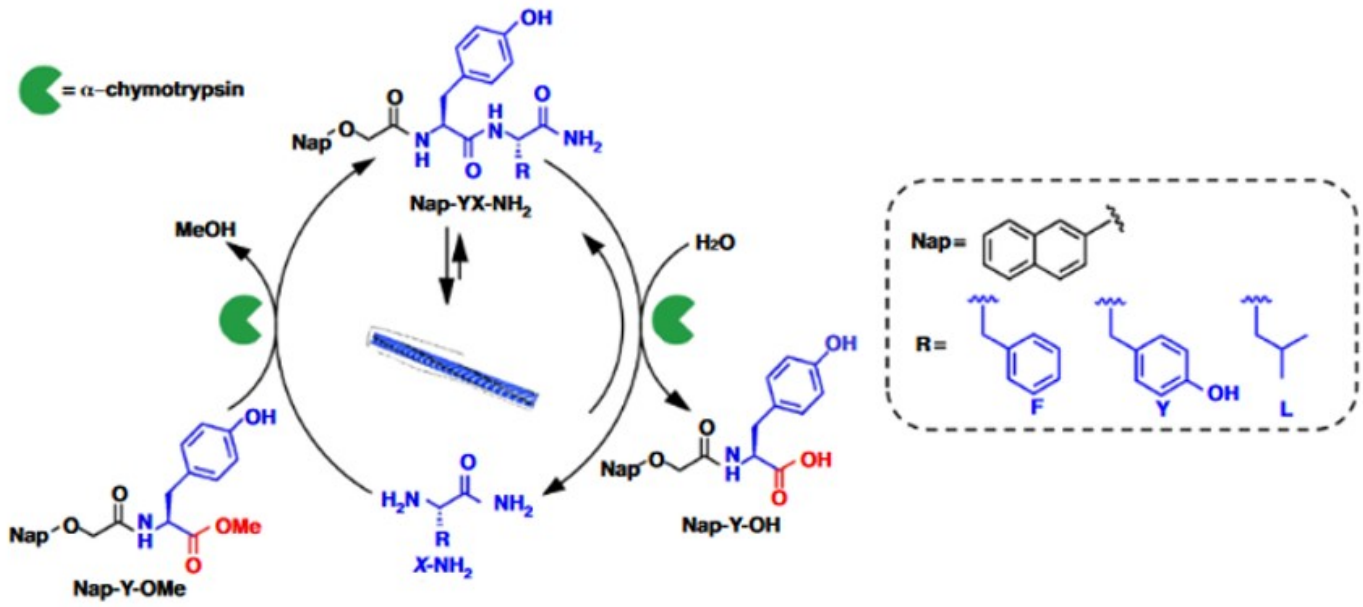

Figure 17. Scheme of enzyme-catalyzed transient self-assembly of naphthalene dipeptide resulting in an active hydrogel. Peptide bond forms between Nap-Tyr(Y)-OMe and hydrophobic amino acid X-NH_2 with the help of α-chymotrypsin as a catalyzing enzyme.[34,35] Reprinted from ref. 35., Copyright 2016, with permission from Elsevier.

Adjusting the lifetime of the formed hydrogel was not easy because the same enzyme catalyzes both activation and deactivation reactions. However, the researchers noticed that the hydrogel's lifetime could be controlled by the concentration of the enzyme. The activation reaction did not change when the concentration of the enzyme was higher than 0.5 mg/ml. Therefore, by increasing the concentration, it was possible to influence the deactivation reaction. At a concentration of 0.5 mg/ml, the hydrogel became liquid within 16 hours, while at a concentration of 3 mg/l, the gel stayed together for only three hours. The deactivation reaction could also be regulated with the help of pH. At more

alkaline pH, hydrolysis occurred faster, and the lifetime of the gel shortened. Finally, an attempt was made to regulate the gel's lifetime by the amount of fuel. When methyl ester fuel was added to the reaction cycle, it increased the number of cycles in which the gel was formed. In this way, it is possible to regulate the lifetime of the gel from minutes to hours.[34]

5.3 Transient peptide gelation depending on the amino acid

Debnath *et al.*[34] noticed that the amino acid used affected whether the system formed a transient or permanent gel. Three different hydrophobic amino acids were used: phenylalanine, leucine and tyrosine. When phenylalanine was used, a permanent gel formed, whereas when leucine and tyrosine were used, transient active gels formed, and their structures broke down over time. When phenylalanine was used, the final concentration of the formed dipeptide gelator, Nap-Tyr-Phe-NH_2, was constantly over the critical gelation concentration (CGC), i.e. the concentration at which a gel forms. The dipeptide gelator with leucine and tyrosine appears only momentarily above the CGC, after which a competing reaction, i.e. hydrolysis, takes place (Figure 18).

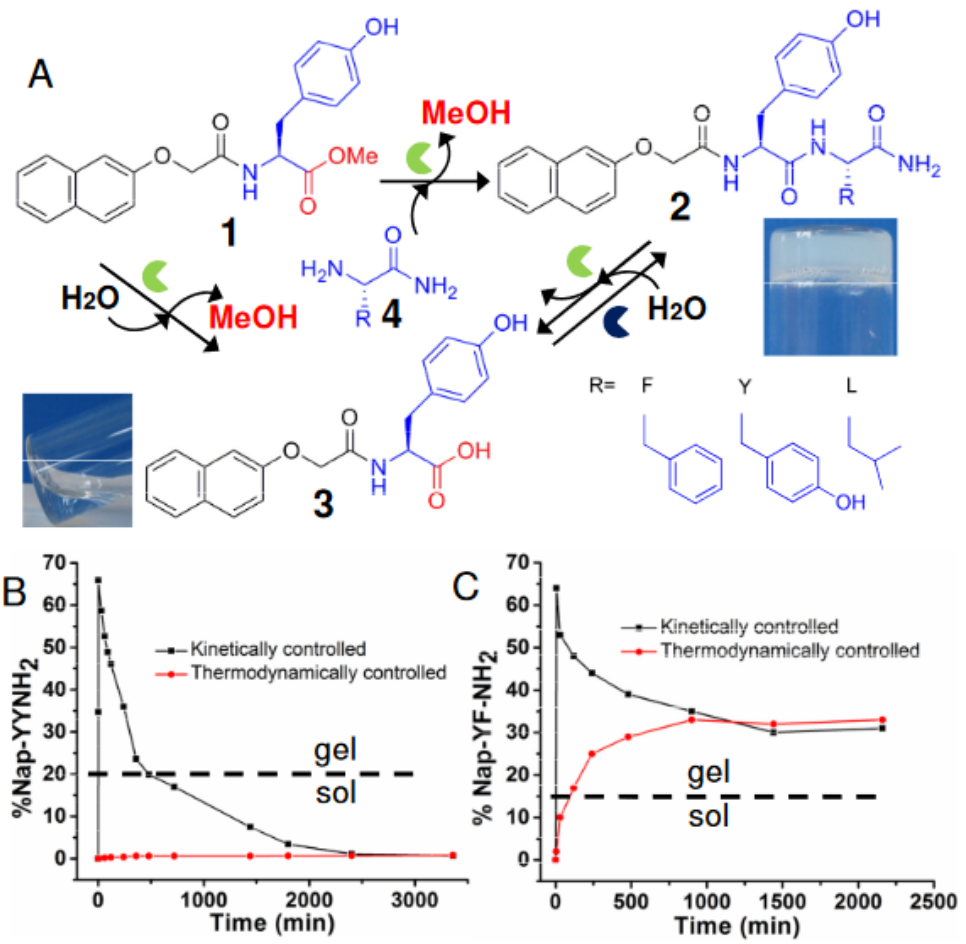

Figure 18. A: Transient enzyme-catalyzed self-assembly of Nap-Tyr-OMe (**1**) with different amide functionalized amino acids (**4**). B: A graph showing kinetically and thermodynamically controlled degradation of the transient gel over time when using tyrosine (Tyr, Y) as an amino acid. C: A graph showing the formation of both kinetically and thermodynamically controlled stable gel when phenylalanine (Phe, F) is used as an amino acid.[34] Reprinted with permission from ref. 34. Copyright 2013 American Chemical Society.

Pappas *et al.*[29] also observed a difference in transient gelation and pathway selection while using different amino acids in the tripeptide hydrogelator. They used aspartic acid/phenylalanine dipeptide methyl ester (Asp-Phe-OMe), known as aspartame, as a precursor and α-chymotrypsin as an enzyme in the reaction network. As the third amino acid, they tried a range of amino acids (Trp, Tyr, Phe, Leu, Val, Ser or Thr). In this tripeptide gelator formation, α-chymotrypsin catalyzes transacylation between the precursor and the third amino acid (Figure 19). Forming tripeptide can exist only transiently, so if it forms, it means that the self-assembly of tripeptide is thermodynamically disfavored and transient gel can self-assemble.

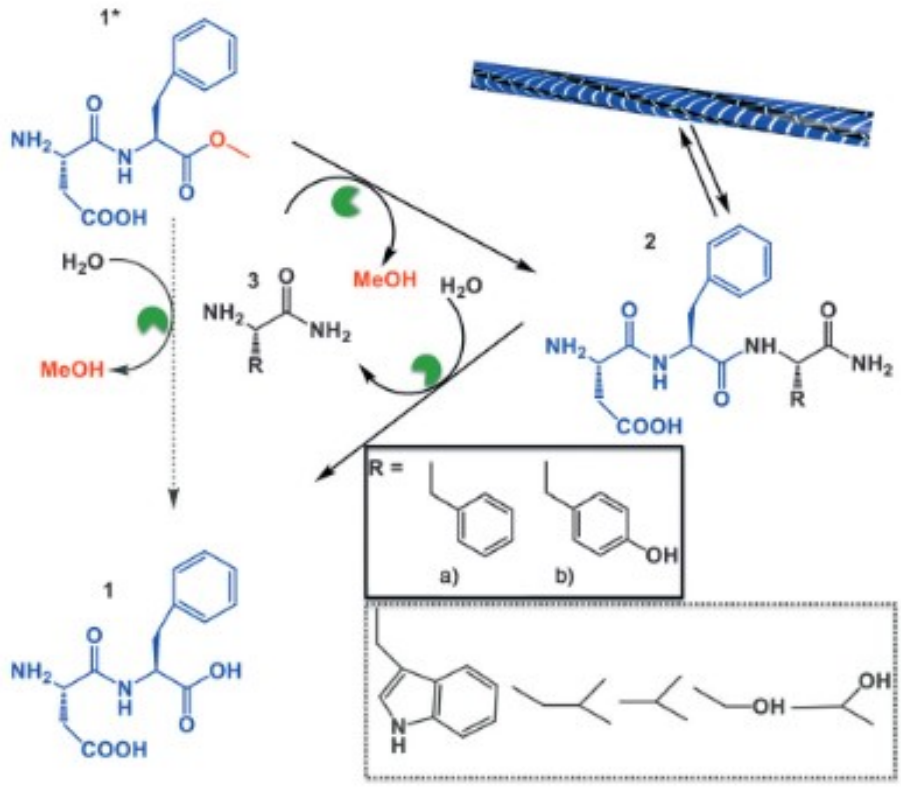

Figure 19. Transient biocatalytic self-assembly of a tripeptide gelator using dipeptide precursor, different amino acids and α-chymotrypsin. α-chymotrypsin catalyzes transacylation of the dipeptide precursors and amino acids and forms a transient hydrogel. The formation of transient hydrogel depended on the used amino acid.[29] Reprinted with permission from ref. 29, Copyright 2015 from John Wiley & Sons, Inc.

No gelation was observed when using Trp, Leu, Val, Ser or Thr as amino acids. Only the formation of Asp-Phe dipeptide was noticed under hydrolysis. However, tripeptide hydrogelator formation and self-assembly of hydrogels were detected when Phe and Tyr were used as amino acids (Phe-NH_2 and Tyr-NH_2). The tripeptides were hydrolyzed gradually, the formed hydrogels broke down, and the dipeptide Asp-Phe formed with the help of the same enzyme.

Replacing phenylalanine with tyrosine caused a significant shortening of the gel's lifespan (from 24 hours to 4 hours). High-performance liquid chromatography (HPLC) analysis of the reaction proved that the tripeptide hydrogelator with tyrosine (Asp-Phe-Tyr-NH_2) was decreased to 40% after 2 h and completely degraded past 10 h. This indicates that the tyrosine peptide has a lower tendency to self-assemble than the phenylalanine peptide.[29] Phenylalanine's ability to form longer-lived gels was also

noticed in the work of Debnath *et al.*[34] above. In their research, however, the phenylalanine-based gelator formed only permanent gels, while in the study of Pappas *et al.*[29], it was able to form a transient gel.

5.4 Light-driven transient peptide gel

As light energy is a good alternative fuel to make transient gels, Liu *et al*.[36] developed a visible-light-driven transient nanofiber hydrogel from peptide-spiropyran (SP) conjugate. They used N-protected tetrapeptide (Fmoc-Lys-Lys(SP)Lys-Phe-NH_2) with a light-responsive nitrospirospyran chromophore at the α-amino lysine sidechain as a gelator. Spiropyrans have two different forms that differ in their properties. Another form of non-polar spiropyran (SP) is the zwitterionic merocyanine (MC) form, which has a relatively large electric dipole moment. In this system, light-responsive nitrospirospyran chromophore acted as a switch to change the peptide's amphiphilicity, which was achieved using the correct amino acid sequence. One side of the structure has two charged lysine side chains, and the other side has hydrophobic phenylalanine and spiropyran side chains (Figure 20). The protonated form of merocyanine (MCH^+) acted as a monomeric resting state and spiropyran as a metastable state from which the nanofibers self-assembled.[36]

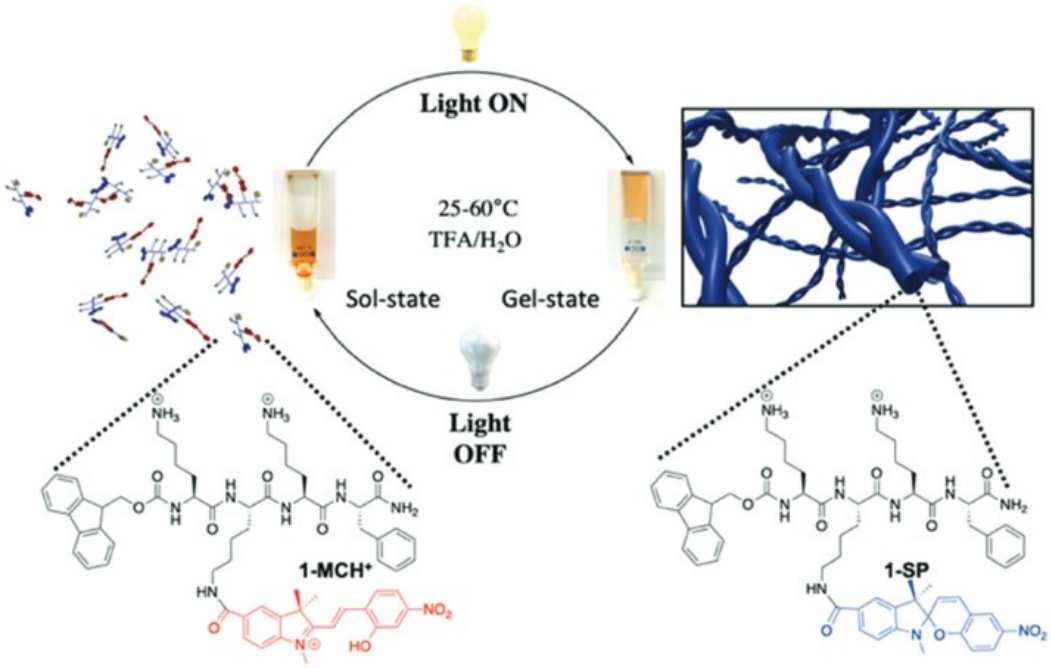

Figure 20. Visible light-driven transient self-assembly of nanofiber hydrogel. The scheme shows the transient nature of the system between the metastable spiropyran (SP) and the resting state (MCH). Sol-to-gel transition is obtained with irradiation of visible light and gel-to-sol transition when continuous irradiation is away.[36] Reprinted with permission from ref. 35. Copyright 2021, with permission from The Royal Society of Chemistry.

6 Applications of transient gels

The applications of transient gels are still in the early years of development, and their application targets are not yet used in real life. However, transient gels have many potential applications that are constantly studied. The attempt to create intelligent synthetic mimics of nature's active materials has led to transient nanostructures and artificial engines powered by chemical fuels.

Being able to synthetically produce fuel-powered active materials by self-assembly processes, such as gels that mimic nature's complex transient materials, could advance the understanding of kinetically controlled dynamic behavior and related spatiotemporal organization. It could also enable applications for drug delivery and active separation, the development of adaptive and self-healing materials and autonomous control of chemical processes.[5] Temporary materials have the property of being switched on and off depending on the fuel supply to the system.[9]

Transient supramolecular gels have been examined for useful and interesting applications in biomedicine, bioscience and material chemistry. These applications include, for example, erasing inks, reusable flexible electric junctions and models to study the structure of matter (Figure 21).[8,9,37] Applications also contain self-abolishing hydrogels and temporary materials that act as delivery devices. By repeating the reaction cycles of transient gels, i.e. sol-gel-sol cycles, transient hydrogels can also be used, for example, in microfluidics to achieve a non-equilibrium state and in tank reactors with continuous mixing. Transient hydrogels also have the potential as a material for soft robotics or microfluidics as temporary fluid controllers.[7]

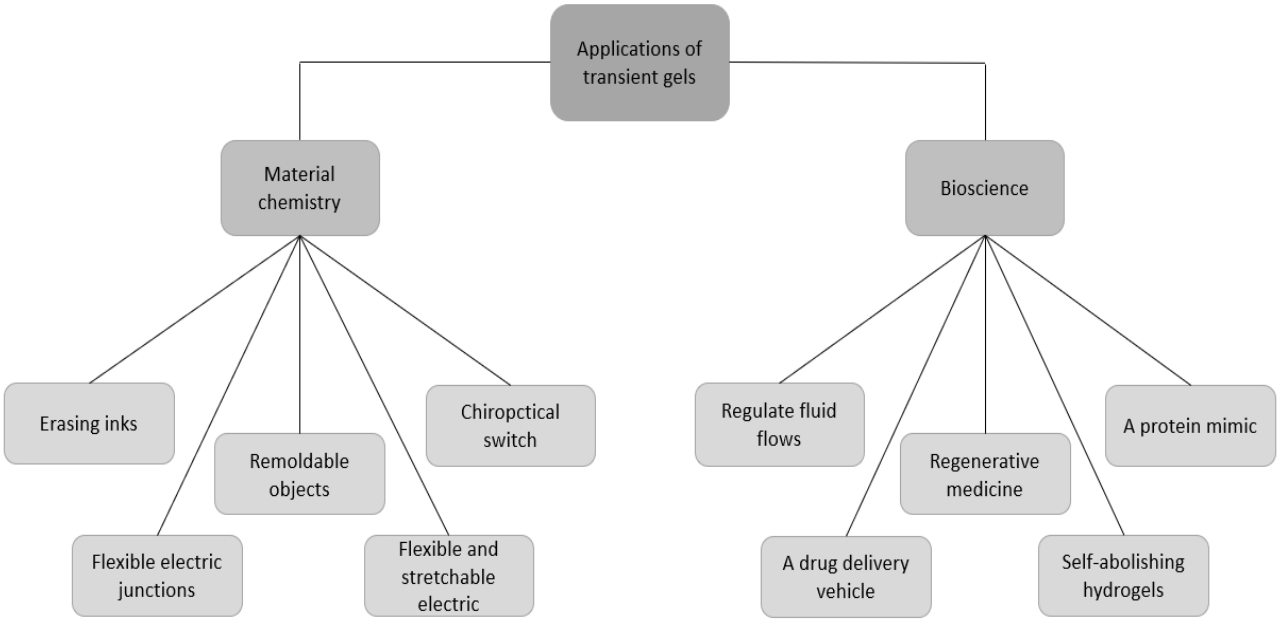

Figure 21. Diagram of possible interesting applications of transient gels in bioscience and material chemistry.

6.1 Applications in bioscience

Hydrogels, as such, have useful properties for biomedical applications, for example, as a support structure for cells or as a platform that regulates the release of drugs. When these useful properties are combined with the properties of dissipative materials, self-abolishing hydrogels are created, whose lifetime can be adjusted from minutes to hours. Self-abolishing hydrogels have potential as biomaterials, for example, in regenerative medicine, because creating a hydrogel that changes its function over time and in which cells can be embedded has been a long-term challenge.[9]

Transient hydrogels could also be used as a drug delivery vehicles. Heuser *et al.*[37] demonstrated product release from a transient hydrogel prepared using a pH-sensitive Fmoc-Leu-Gly hydrogelator, urease enzyme, and citric acid. A transient hydrogel was created by lowering the pH, and the lifetime

was regulated with urease. The formed hydrogel could also release the hydrophilic dye after a pre-programmed time (Figure 22).

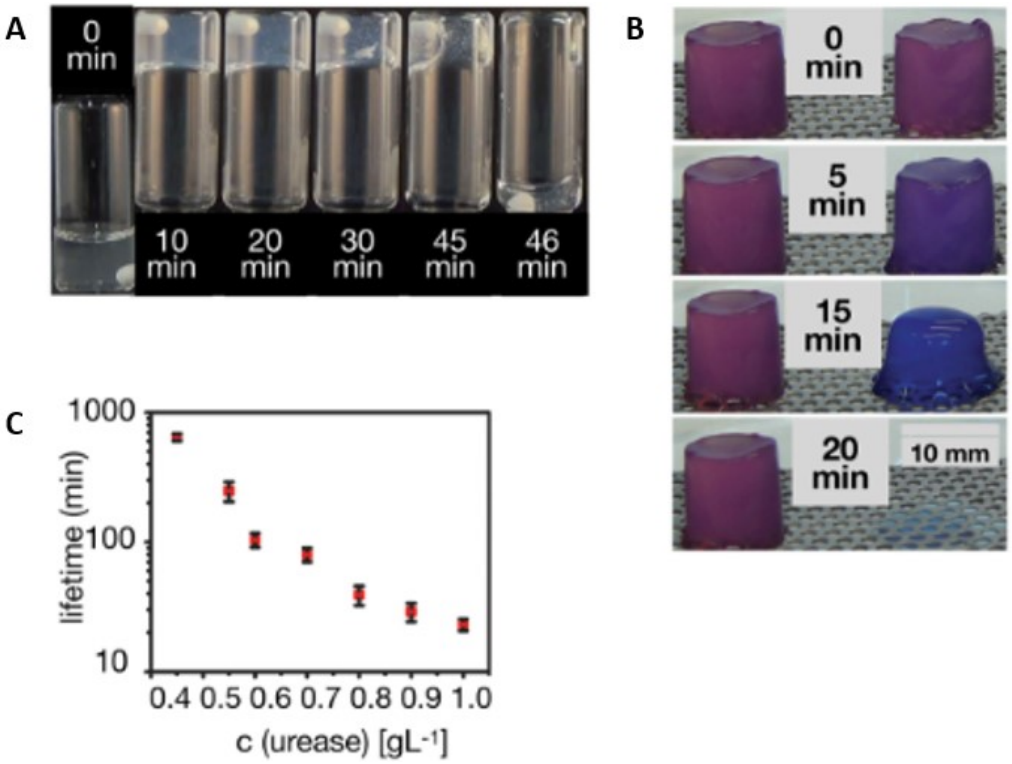

Figure 22. A) Hydrogel at different time points. B) Permanent gel (left) and transient hydrogel (right) at different time points. The transient hydrogel managed to break down after a pre-programmed time and, as a result, released the dye, resazurin, encapsulated within it. C) A plot of the lifetime of the gel versus urease concentration, which tunes its lifetime.[9] Reprinted and adapted with permission from ref. 9., Copyright 2018, from John Wiley & Sons, Inc.

Rieß and Boekhoven[9] also demonstrated the release of the hydrophobic dye from the dissociative supramolecular material. They used Fmoc-protected glutamic acid as a precursor and carbodiimide as a fuel. The lifetime of the formed supramolecular material could be adjusted from 30 to 120 minutes by the amount of fuel, and hydrophobic dyes could be added to the material. The time the dye was added to the dissipative reaction network determined the time at which the dye was released. If the dye was added at the beginning of the cycle, it bound to the core of the material and was released slowly. On the other hand, if the dye was added, for example, 10 minutes after starting the cycle, it bound to the outer parts of the material and was released faster. Therefore, the release of the substance can be controlled by monitoring the amount of the fuel and the time of adding the dye.

pH-sensitive transient hydrogels could also be used as so-called smart drug carriers. The pH of biological tissues varies a lot in the body (alkaline in the intestine and more acidic in the stomach). Therefore, with such a pH-sensitive transient hydrogel, it would be possible to determine in advance at which pH it releases the drug, and the drug is released where it should. The pH-sensitive area of such a hydrogel is easy to regulate by modifying its building blocks and further the structure of the gel. It has also been noticed that cancers cause a pH change in the extracellular space compared to a normal environment. These smart transient hydrogels could, therefore, potentially be used in the targeted administration of cancer drugs.[38]

Transient hydrogels can also be used to regulate various fluid flows. For example, in blood vessels, an interesting application could be preventing blood circulation or guiding it momentarily elsewhere without compression in the event of an accident or during surgery. The ability to temporally control the degradation and reorganization of transient hydrogels would allow them to be degraded and dissolved after a predetermined time.

Other applications where fluid control is needed, such as in industry, are possible.[37] Heuser *et al.*[37] demonstrated fluid flow regulation with a transient hydrogel and device made from poly(dimethyl siloxane) with two different channels for fluid flow: the dominant one and the alternative second one (Figure 23). The transient hydrogel was prepared from pH-sensitive Fmoc-Leu-Gly-OH dipeptide. Acidic buffer acted as an activator for gelation, and urease-catalyzed CO_2 and NH_3 formation from urea acted as a deactivation trigger and degeneration of formed hydrogel. The formed hydrogel is time-programmed.

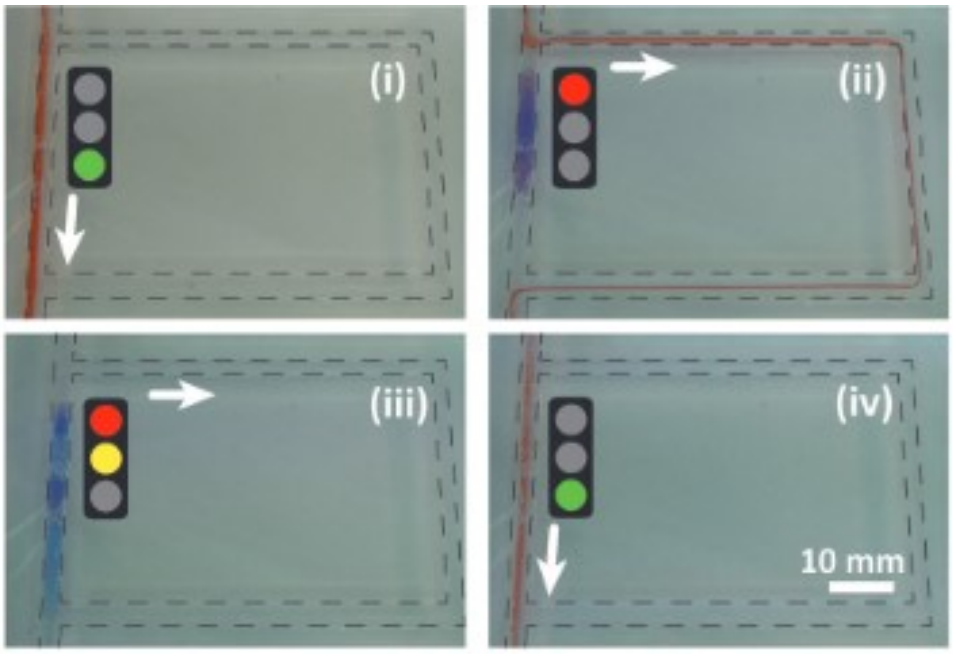

Figure 23. Regulation of fluid flow with the help of transient peptide hydrogel. i) The fluid goes through the dominant channel when no hydrogel is present. ii) The fluid goes through the alternative channel when the transient hydrogel blocks the dominant channel. iii) The hydrogel starts to dissolve. iv) The fluid returns to the original dominant channel when the hydrogel is completely dissolved. The hydrogel is time-programmed.[37] Reprinted with permission from ref. 36., Copyright 2015, from John Wiley & Sons, Inc.

Transient hydrogels that react to different stimuli are interesting materials also in regenerative medicine. For example, they can be used to help repair congenital tissues, in tissue engineering, imaging, and in modulating the tissue environment. Devices built based on transient hydrogels, which react to several different stimuli and have an on-off ability for change, are also an interesting application target. These could potentially be used in, for example, surgical instruments and smart implants that can replace soft tissue such as heart valves.[38] However, research in regenerative medicine is only at the very beginning.

6.2 Applications in material chemistry

In terms of gels, transient systems generally focus on temporary gelation, i.e. sol-gel-sol transition. Olivieri *et al*.[8] studied temporary degelation, i.e. the gel-sol-gel transition and its applications. The researchers used trichloroacetic acid (TCA) as fuel, which temporarily protonates primary neutral amine, which occurs in gel form. TCA, therefore, caused the gel to change back to a solution form. After a while, protonated amine returns to a neutral amine through TCA decarboxylation, and the solution self-assembles again to gel. Two gelators were used for the applications, octadecylamine and O-*tert*-butyl-*L*-tyrosine, which was used more. (Figure 24).

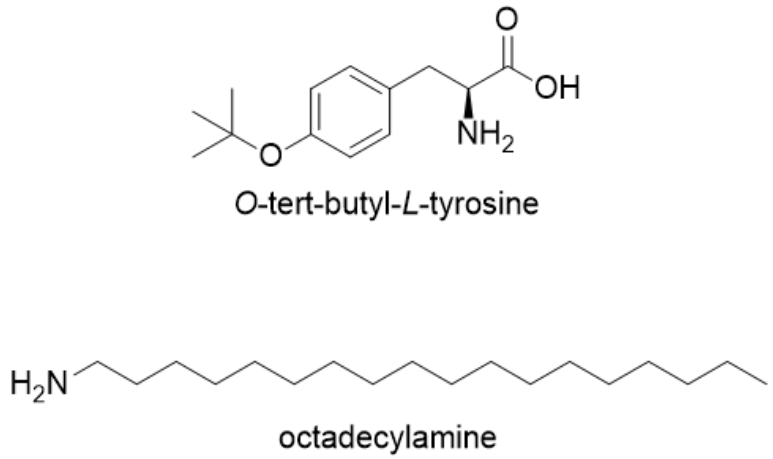

Figure 24. Structures of *O-tert*-butyl-*L*-tyrosine and octadecylamine gelators used in gel-sol-gel transition with TCA fuel.

TCA-fueled gel-sol-gel transition could be used in various material chemistry applications. By using *O-tert*-butyl-*L*-tyrosine as a gelator, a thick gel was created, which was used to prepare multiple active and smart materials. Applications include, for example, erasing inks, remoldable objects, electrical junctions and chiroptical switches (Figure 25).[8]

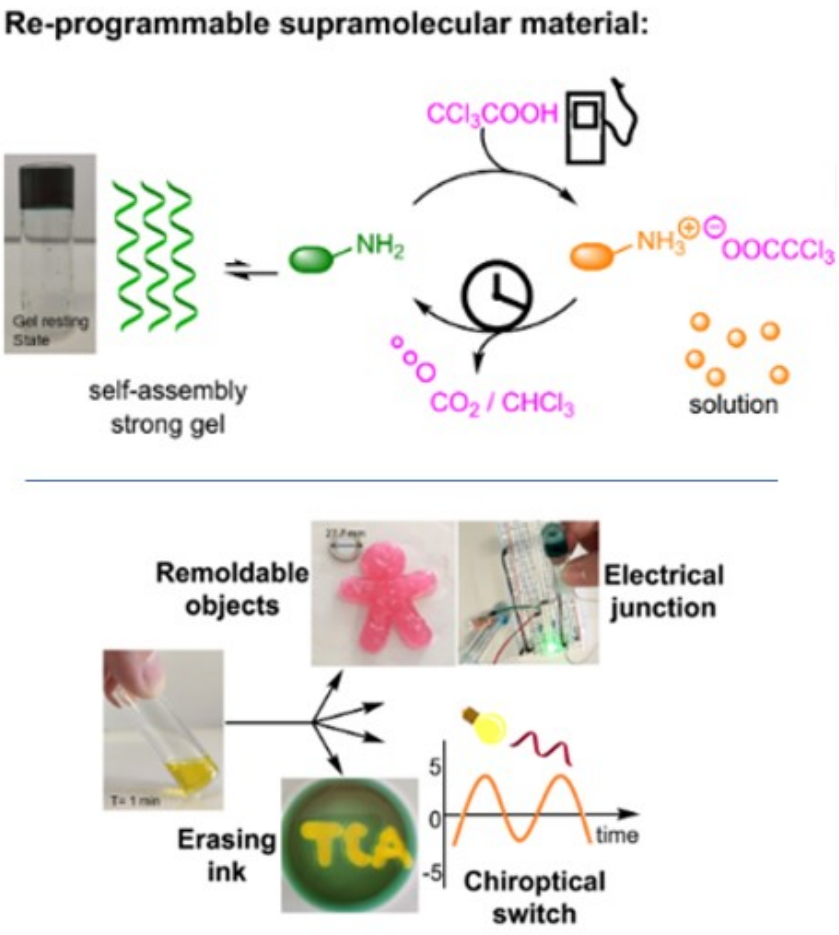

Figure 25. TCA-fueled transient gel-sol-gel system and its various applications. The gel-sol-gel transition is based on the occasional protonation of the amine by TCA, which transforms the rigid gel into a solution. After a certain time, however, the amine returns to a neutral form, and a strong gel is reformed.[8] Reprinted and adapted with permission from ref. 8. Copyright 2022 American Chemical Society.

The gel-sol-gel transition can be used, for example, to create erasing inks and disappearing messages. When the transient gel is used with various acid-sensitive colored additives, TCA can be used as an erasing ink on the surface of the transient gel. A green transient gel system was used as the gel matrix, to which an acid-sensitive colored indicator had been added. The disappearing word was written on the gel by adding TCA solution, causing the parts in touch with the TCA solution to dissolve and turn yellow, while the remaining structure of the gel stayed static and green. After the decarboxylation of TCA, the message vanished as the green gel reformed (Figure 26). The method can be repeated several times, and a completely intact and smooth gel was obtained using an excess of TCA. The technique can be studied, for example, in connection with the application of alternative encryption systems.[8]

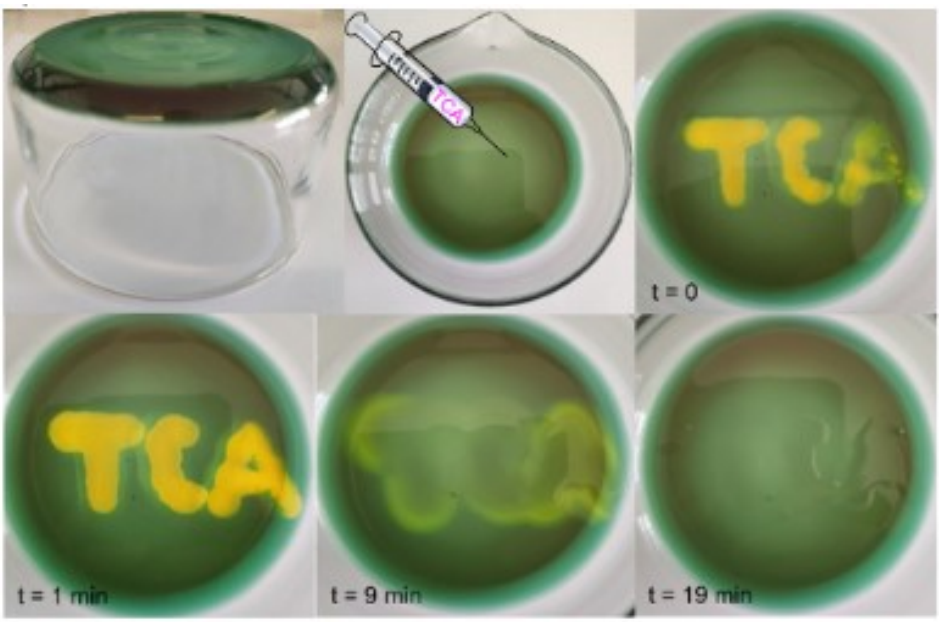

Figure 26. Use of a gel-sol-gel transition to create erasing ink. TCA was added into the solid green gel matrix by syringe. The parts injected with TCA dissolved and turned yellow, revealing the written text. After about 20 minutes, the text disappeared when the dissolved parts gelled again. This could be repeated several times.[8] Reprinted with permission from ref. 8. Copyright 2022 American Chemical Society.

The TCA-fueled gel-sol-gel system designed by Olivier *et al*.[8] can also form remoldable objects. *O*-*tert*-butyl-*L*-tyrosine was used as a gelator to form a strong gel with DMF. When TCA was added to the gel, it dissolved into a solution that could be transferred to the mold. In the mold, the solution gelled again after about 5 minutes. When TCA was added to the gel again, the gel dissolved into a solution and transferred to a new mold. In this way, it was possible to produce a reconfigurable object (Figure 27).

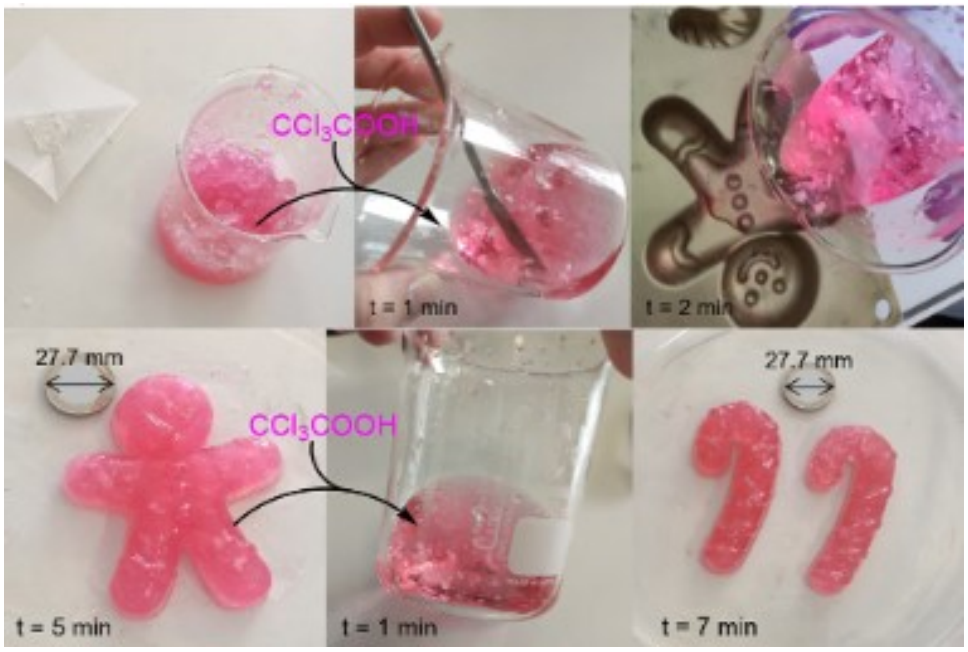

Figure 27. Reconfigurable objects made from transient TCA-fueled gelation system. The gel-sol-gel system could be reproduced about 15 times.[8] Reprinted with permission from ref. 8. Copyright 2022 American Chemical Society.

Hao *et al*.[39] studied a glycerol hydroxyethyl cellulose (GHEC) based macromolecular transient elastomeric gel and its applications in stretchable and flexible electronics. The transient macromolecular elastomer gel has functional hydrogen bonds between hydroxyethyl cellulose (HEC) and glycerol (G). Because of that, the gel has excellent stretchability and the ability to repair itself in surrounding conditions. The transient elastomer gel is also soluble in water, and its decomposition can be controlled by changing the molecular weight of HEC and its ratio to glycerol. The transient gel was studied for various applications, such as self-healing conductors, transient transistors, and electronic shells for robots.[39]

Stretchable and flexible electronics are getting more attention in technology applications. They are used, for example, in personal healthcare, human-computer interaction, and to monitor human activity. However, manufacturing these materials is challenging as they are sensitive to tearing and punctures. Therefore, flexible materials that can self-repair and resist damage are highly desired.[39] Transient gels that can self-repair and change in time have excellent properties for this purpose.[4] The flexible properties also enable connection to non-planar surfaces.[39]

However, such transient assemblies have a limitation, as some waste is always generated in the reaction cycles. The increase in waste limits the number of successful cycles that produce a self-

supporting gel. Mondal *et al.*[7] managed to repeat the gelation cycle three times in their experiment, but the gel was no longer formed on the fourth time the acid was added. Olivier *et al.*[8], on the other hand, managed to repeat the gel-sol-gel cycle 15 times. Despite the challenges of the applications of transient gels, they are nevertheless interesting, and their research is growing.

7 Summary

This literature section discussed transient gels and their applications, focusing more specifically on peptide-based ones. The main difference between systems in living organisms and many artificial self-assembling systems is their transient nature. Most artificial systems are generally passive and static, while self-assembling systems found in nature are active and dynamic. Natural systems have many advantageous properties, so attempts are made to imitate these in plain man-made systems to prepare various active and smart materials.[14] These smart materials can reversibly change their properties in response to external stimuli.[8]

Transient supramolecular gels have a huge potential for various applications as smart materials capable of changing between different states in a given time. Due to transient self-assembly, these gels have unique properties that enable self-healing and adaptive materials for the future. These gels have an exceptional level of autonomy that is not achieved with materials that are in equilibrium.[4] However, regardless of the progress made in recent years, the area is in the early steps, and much more progress is needed before moving to real-world applications. First, simple systems with suitable features must be developed.[8]

Peptide-based transient gels are promising components for active materials because their properties can be modified easily by simply changing the amino acids that act as the building blocks of the gel.[11] Each amino acid has unique properties that can be utilized, especially hydrophobicity and aromaticity, to promote gelation. Phenylalanine is the most commonly used and studied amino acid in creating transient gels. Phenylalanine has excellent gelation ability due to the hydrophobicity and π–π interactions of the phenyl group and the hydrogen bonds formed by the amide group.[2] The most studied dipeptide is diphenylalanine, which has the same properties. π–π interactions and hydrophobic properties can also be achieved by adding aromatic groups to the amino acids, such as the commonly used Fmoc and Nap protecting groups.[11]

Bottom-up made peptides are simple and dynamic, which is also one reason they have been used to create active materials with useful properties. Simpler structures provide an easier approach to better study transient systems found in nature.[14] Peptides can also self-organize. Peptide-based transient gels could be used, for example, to model proteins and their function or to make remoldable objects or control fluid flows.

Transient gels, including peptide-based transient gels, can be prepared by dissipative reaction cycles, for which the necessary energy is generally obtained either as a chemical fuel or as light. Both enzymes and compounds that regulate pH can act as chemical fuel. The choice of fuel can influence the lifetime of the formed transient gel and, thus, its properties.[4,29]

However, gels prepared using transient self-assembly are currently only limited to early-stage studies. The most studied property of transient gels is their formation and control and change of properties over time in a prescribed manner. Self-healing and adaptive materials still need a lot of research.[4] Despite the significant early-stage development of transient supramolecular gels, it is still challenging to develop the properties of materials and systems from ordinary, passive responsiveness to autonomous dynamics and self-regulation.[35,37]

EXPERIMENTAL PART

8 Motivation

Gels have long been used in everyday life, for example, as additives in food products, soaps, cosmetics and healthcare/hygiene products. Gels have also been widely studied for many other applications, such as drug delivery, removal of dyes, tissue engineering and extraction of pollutants.[2] Organogels are soft materials that consist of the organic solvent (liquid phase) and the gelator molecules (solid phase, for example, low molecular weight gelators, LMWGs). In organogels, LMWGs self-assemble, forming a three-dimensional structural network.[40] These polymer-like fibers immobilize the organic solvent to form a gel and the fibers are stabilized by different non-covalent interactions.[41]

Peptide-based gelators have attracted attention due to their biocompatibility and the potential tuning of their chemical properties by functionalizing their core structure.[42] Amino acid-based gels can be prepared in many different ways, of which a simple deprotection reaction is an effective method for the *in situ* preparation of gels.[16,43]

The experimental part of this master's thesis deals with the effect of chemically active organic solvents and acid concentration on the temporal self-assembly, the gelation mechanism and the network of in situ formed organogels during the deprotection reaction of a gelator precursor molecule. The aim of the research work was to create transient gels, based on the previous research by Chevigny *et al*.,[16] using different organic solvents and to study temporal self-assembly. The deprotection reaction (Scheme 1) utilized in this study is based on the protocol of Lin *et al*.,[44] which was further elaborated by Chevigny *et al*.[16] to make transient gels using a chemically active solvent. The Boc group is selectively deprotected from the gelator precursor *N*-*tert*-butyloxycarbonyl (Boc)-L-phenylalanyl-L-phenylalanine *tert*-butyl ester (Boc-Phe-Phe-O*t*Bu) by adding sulfuric acid to the reaction mixture. In the study of Lin *et al*.,[44] the *tert*-butyl group is also deprotected, but the solvent *tert*-butyl acetate (*t*BuOAc) reforms the ester group, making this process reversible while the deprotection of the Boc group is irreversible.

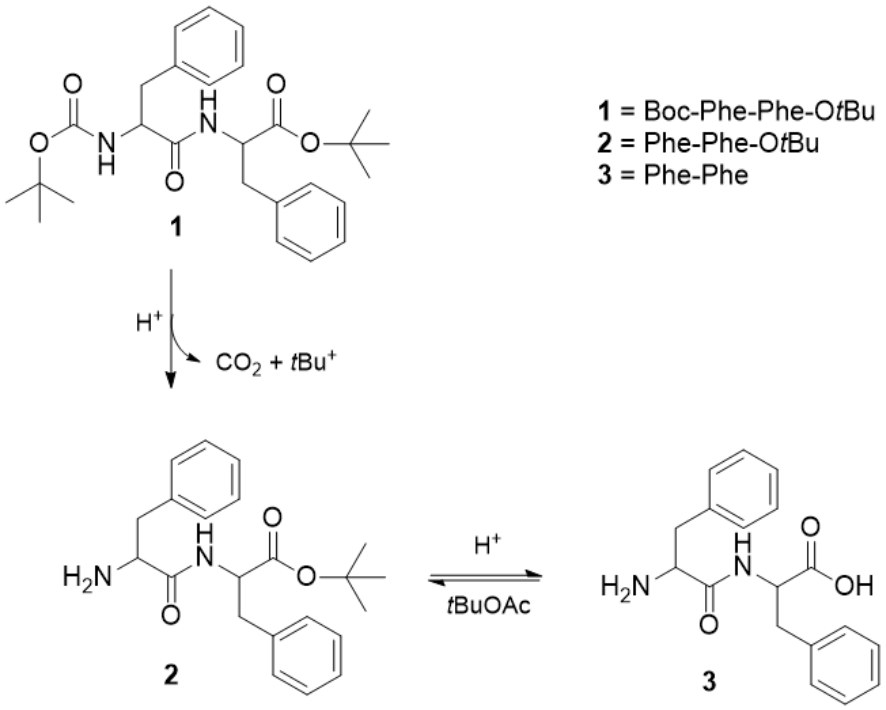

Scheme 1. The proposed reaction mechanism for the reversible deprotection of the Boc group in the presence of the *tert*-butyl group, which leads to *in situ* gelation.[16]

In this study, we assessed five different organic solvents to form organogels using the amino acid-based precursor gelator (Boc-Phe-Phe-O*t*Bu). The selective deprotection of the Boc group in the presence of the *tert*-butyl group was the driving force of the gelation mechanism.[44] One of the solvents has been previously studied,[16] but the impact of others on the gelation process has not been previously explored. The new solvents did not create transient gel systems under the described acidic conditions. Therefore, the study focused on the effect of each solvent and the acid concentration on temporal self-assembly. The novelty of the current work is the assessment of active organic solvents, which not only support the formation of gels per se but engage in the gelation process and affect the spatiotemporal properties (two-dimensional and three-dimensional assemblies over time) of the formed gels.

9 Materials and methods

The chemicals used in this work are presented in Table 1. All chemicals were used without further purification. The saturated aqueous solution of $NaHCO_3$ was prepared by dissolving $NaHCO_3$ in deionized water. 0.1 M HCl solution was diluted from 1 M HCl solution. Hanessian's stain solution used in TLC was prepared by Romain Chevigny on 10.02.2020.

Table 1. Chemicals used in this experiment.

Chemicals	**Mw (g/mol)**	**Manufacturer**	**Purity**
L-Phenylalanyl-L-phenylalanine	312.37	TCI	> 98.0 %
N-(*tert*-Butoxycarbonyl)-L-phenylalanine	265.30	TCI	> 99,0 %
(*S*)-3-Phenylalanine-*tert* butyl ester HCl	257,76	BioSynth	
TBTU (2-(1H-Bentzotriazole-1yl))	321,09	FluoroChem	> 98.0 %
DMF	73,09	Arcos Organics	99,8 %
$NaHCO_3$	84,01	FluoroChem	98,5 %
$MgSO_4$	120,37	Sigma-Alrich	99.0 %
tert-Butyl acetate	116,16	TCI	> 99,0 %
tert-Butyl methyl ether	88,15	TCI	> 99,0 %
tert-Butyl acetoacetate	158,20	TCI	> 95,0 %
tert-Butyl formate	102,13	Sigma-Alrich	99 %
tert-Butyl chloroacetate	150,61	Thermo Scientific	98 %
concentrated H_2SO_4	98,08	Fluka	95–97 %
Ethyl acetate	88,11	VWR chemicals	> 99,5 %
Hexane	86, 18	Honeywell	97 %
Dichloromethane	84,93	VWR chemicals	99,5 %
Toluene	92,14	VWR chemicals	
d_6-DMSO	84,17	Eurisotop	99,80 %

A Mettler Toledo XP205 scale and an Ioniser VWR scale were used to weigh the reagents and net weight of round-bottomed flasks, gels and vials. The solution mixtures and solutions were sonicated

by a Hielscher UP50H ultrasonic processor to assist in dissolution. The melting points of the synthesis products were measured by a Stuart SMP30 instrument, and the transient ($T_{gel\text{-}sol}$) temperatures of the gels were analyzed by a Thermo Scientific block heater. pH values of solvents were measured by a Mettler Toledo instrument.

^{1}H NMR spectra were recorded with Bruker Advance III HD 300 MHz NMR-spectrometer, and ^{13}C and DEPT-135 spectra were recorded with Bruker Advance III HD 500 MHz NMR-spectrometer. The spectra were referenced to d_6-DMSO solvent (δ (d_6-DMSO) = 2.5 ppm for ^{1}H and 39.52 ppm for ^{13}C).

The FT-IR spectra of the starting material and the xerogels were recorded by a Bruker Tensor 27 FTIR spectrophotometer. The spectral range was 400 – 4000 cm^{-1} at a resolution of 4 cm^{-1}. 24 scans were taken for each sample in addition to a background scan.

Scanning electron microscopy (SEM) images were recorded with a Zeiss EVO-50XVP microscope. All xerogel samples were prepared by dipping a carbon film (400 mesh copper grids) into the gel, which dried overnight under a vacuum. The carbon films were purchased from Agar Scientific. SEM imaging was performed by Dr Andreas Johansson.

High-resolution mass spectra (HR-MS) were recorded by an Agilent 6560 Ion mobility Q-TOF mass spectrometer with a dual AJS ESI ion source. Samples were measured with direct infusion (flowrate 5 µl/min) and positive ion mode. For gels, the stock solution was 2 mM in MeOH, and samples were 10 µM in MeOH. The starting material samples were dissolved in DCM (1mg/ml) and diluted in MeOH (5 µl/ml). The data were analyzed using Mass Hunter B.08.00 software (Agilent Technologies, USA). HR-MS spectra were recorded by Dr Anniina Kiesilä.

10 Synthesis

10.1 Synthesis of Boc-Phe-Phe-O*t*Bu 1

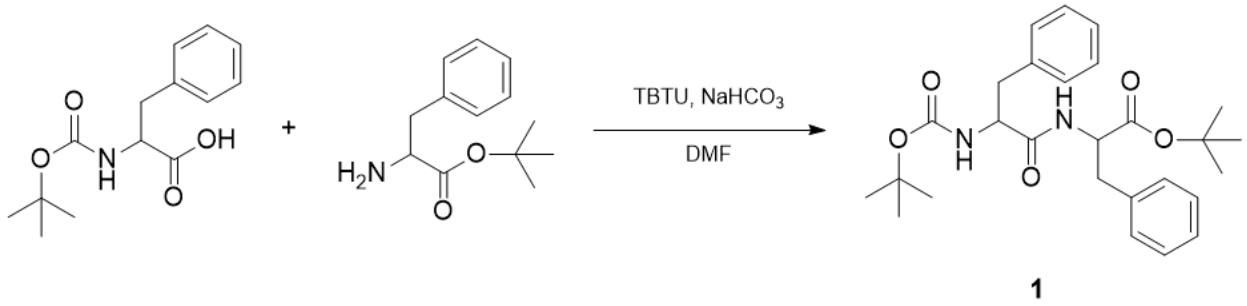

Scheme 2. Synthesis of Boc-Phe-Phe-O*t*Bu.

Boc-phenylalanine (1.13 g, 1.0 eq), TBTU (1.21 g, 1.0 eq), phenylalanine-*tert*-butyl ester (1.07 g, 1.1 eq) and $NaHCO_3$ (0.66 g, 1.1 eq) were added to anhydrous DMF (20 ml) under N_2 atmosphere. The solution was stirred overnight at room temperature under an N_2 atmosphere. The next day, the starting materials were consumed, and a new spot appeared in TLC (Hex:EA = 1:1, Hanessian's stain). The solvent was evaporated under a vacuum (co-evaporation with toluene x3), and the residue was left under a vacuum overnight. The next day the residue was dissolved in DCM. The organic phase was extracted with water (x2) and subsequently washed with HCl (0.1 M), water (x2) and a saturated aqueous solution of $NaHCO_3$. The organic phase was then dried with $MgSO_4$ and evaporated under vacuum, yielding a pale-yellow powder (1.62 g, 81%).

The synthesis was repeated three times, as more starting material was needed for the gelation experiments. Table 2 shows the obtained yields of different synthetic batches.

Table 2. Yields of different synthetic batches of Boc-Phe-Phe-O*t*Bu.

	yield (g)	**yield percentage (%)**	**outcome**
Synthesis 1	1.6217	81	pale yellow powder
Synthesis 2	1.3185	75	white powder
Synthesis 3	1.2239	69	white powder

The ^{1}H NMR spectrum of Boc-Phe-Phe-O*t*Bu (Synthese 1) is given in Figure 28, which is in accordance with the products at all batches. The ^{13}C spectrum of Boc-Phe-Phe-O*t*Bu was not measured, as the measured ^{1}H spectrum was identical to those reported in the literature.

^{1}H NMR (300 MHz, DMSO) δ 8.19 (d, J = 7.6 Hz, 1H, NH), 7.33 – 7.14 (m, 10H, Ar), 6.82 (d, J = 8.8 Hz, 1H, NH), 4.38 (q, J = 7.3 Hz, 1H, CH), 4.24 – 4.13 (m, 1H, CH), 3.02 – 2.88 (m, 4H, CH_2), 1.32 (s, 9H, CH_3), 1.28 (s, 9H, CH_3).

M.P 124-129 ºC.

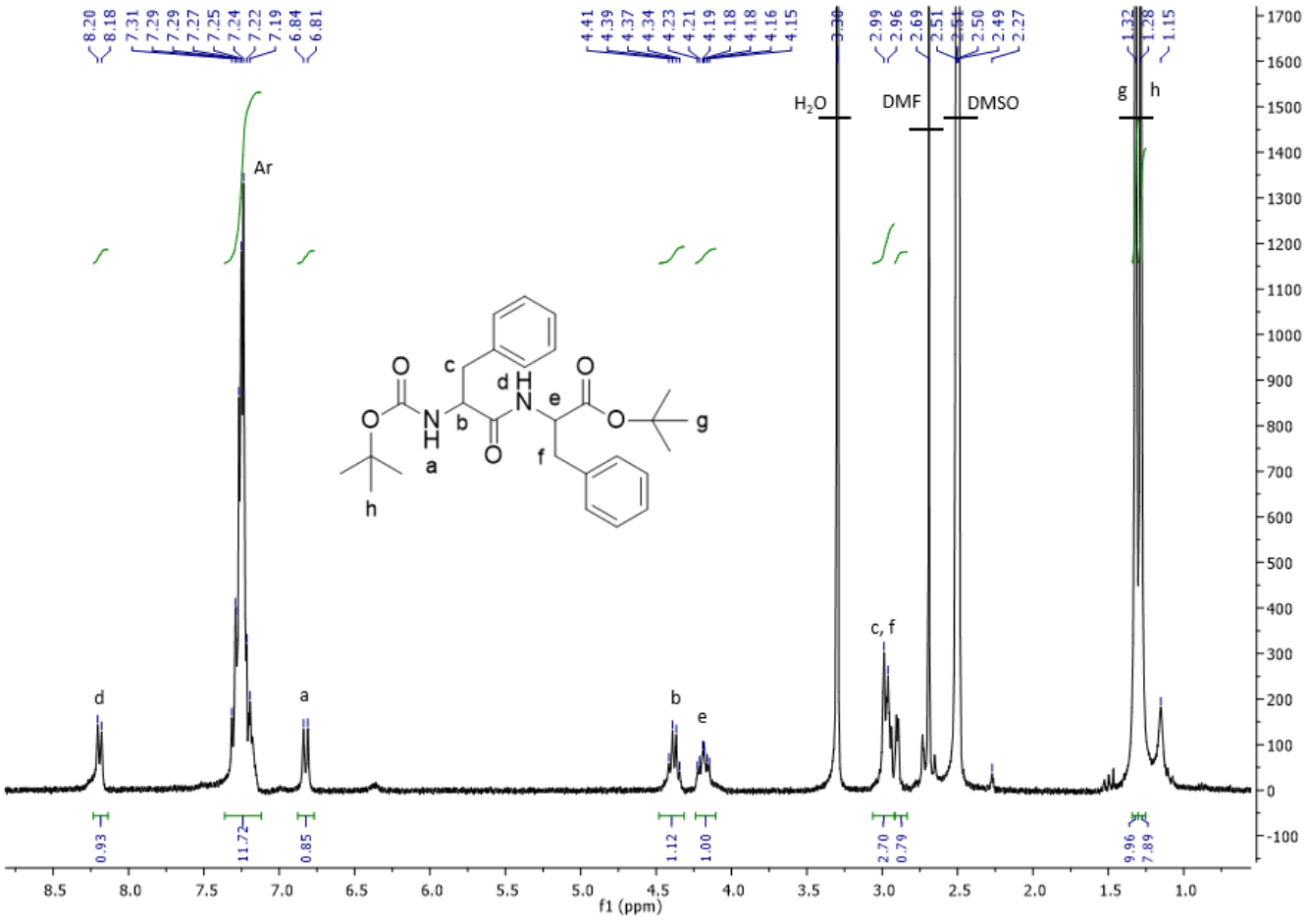

Figure 28. ^{1}H NMR spectrum (300 MHz, d_6-DMSO) of Boc-Phe-Phe-OtBu **1**.

10.2 Synthesis of Phe-Phe-O*t*Bu 2

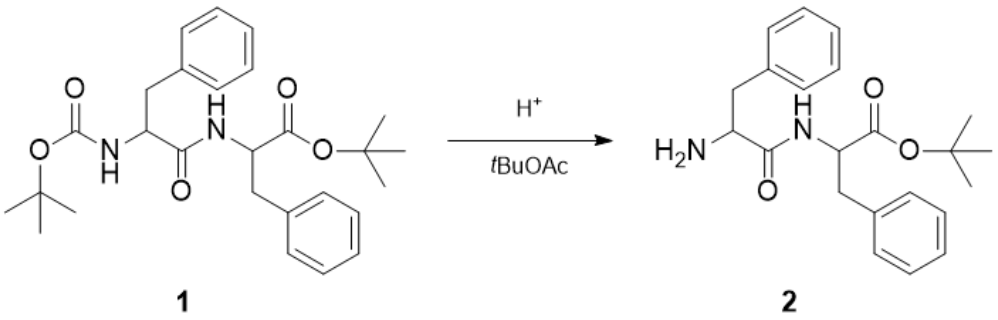

Scheme 3. Synthesis of Boc-Phe-Phe-O*t*Bu **2**.

Boc-Phe-Phe-O*t*Bu (1; 480 mg, 1.0 eq) was suspended in *tert*-butyl acetate (5.1 ml). Concentrated H_2SO_4 (0.16 ml, 3.0 eq) was added dropwise at room temperature. The solution quickly formed a gel. Therefore, additional *tert*-butyl acetate (25 ml) and concentrated H_2SO_4 (total 0.49 ml, 9.0 eq) were added to dissolve the gel, and the solution became transparent. The solution was stirred overnight at room temperature. The next day, the formation of a new compound was confirmed by TLC (Hex:EA = 1:1, Hanessian's stain). The reaction mixture was neutralized with a saturated aqueous solution of $NaHCO_3$. The organic phase was extracted with ethyl acetate and dried with $MgSO_4$. The organic phase was then evaporated under a vacuum. The residue was left under vacuum overnight, yielding a white powder (0.34 g, 89%).

The ^{1}H spectrum of Phe-Phe-O*t*Bu is given in Figure 29. The ^{13}C spectrum of Phe-Phe-O*t*Bu was not measured, as the ^{1}H spectrum was identical to those reported in the literature.

^{1}H NMR (300 MHz, DMSO) δ 8.16 (s, 1H, NH_2), 7.30 – 7.15 (m, 10H, Ar), 7.13 (s, 1H, NH), 4.43 (dd, J = 15.1, 6.0 Hz, 1H, CH), 2.92 (t, J = 8.9 Hz, 3H, CH_2), 2.72 (s, 1H, CH), 2.26 (s, 1H, CH_2), 1.33 (d, J = 1.6 Hz, 10H, CH_3).

M.P. 104-110 ºC

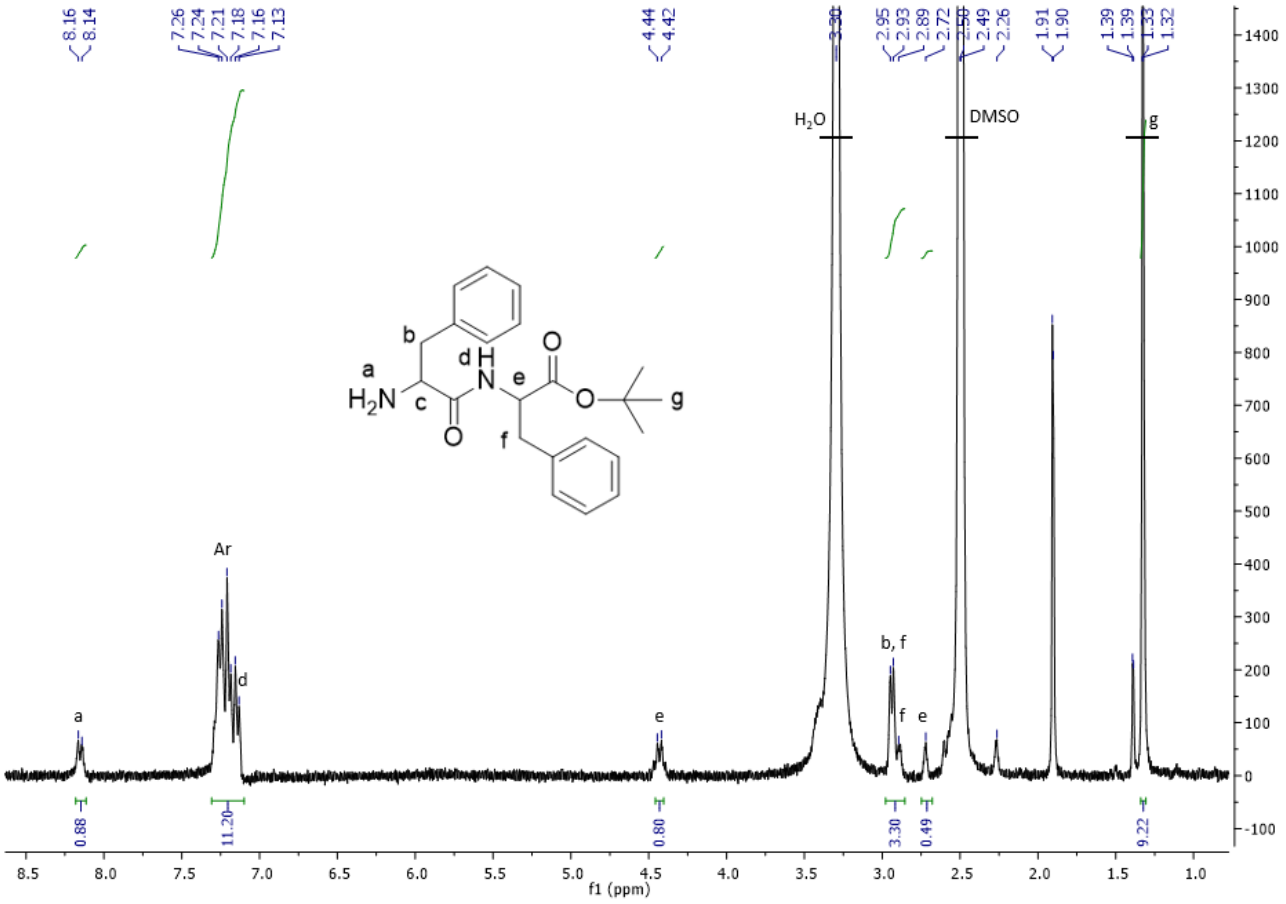

Figure 29. ^{1}H NMR spectrum (300 MHz, d_6-DMSO) of Phe-Phe-O*t*Bu **2**.

11 Gelation experiments

11.1 General gelation protocol

The gelation of precursor gelator Boc-Phe-Phe-O*t*Bu **1** in *tert*-butyl acetate was previously studied[16] while in the current study, four new solvents were tested. In all gelation trials, Boc-Phe-Phe-O*t*Bu **1** (23.5 mg, 0.05M) was dissolved in organic solvents (1.0 ml; *tert*-butyl acetate (*t*BuOAc), *tert*-butyl methyl ether (CH_3O*t*Bu*),* *tert*-butyl chloroacetate ($ClCH_2CO_2$*t*Bu),), *tert*-butyl acetoacetate ($AcCH_2CO_2$*t*Bu) and *tert*-butyl formate (HCO_2*t*Bu); Figure 30). The dissolution of precursor **1** was assisted by ultrasound. Concentrated H_2SO_4 was then added to the solution, and the mixture was swirled. The samples were left at room temperature overnight for gelation to occur. Gelation was verified by the vial inversion method. The gelation trials are summarized in Table 3.

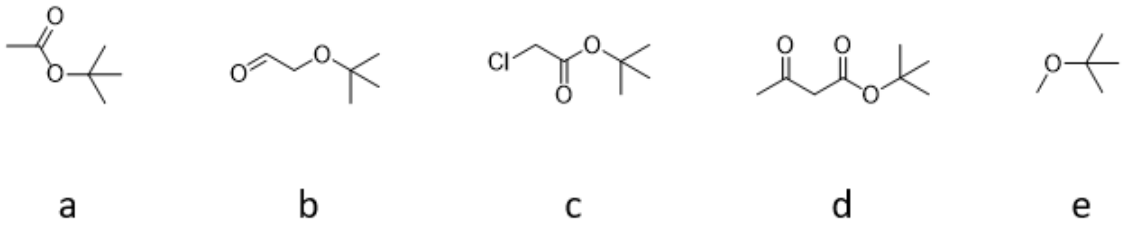

Figure 30. The chemical structure of the organic solvents used in gelation trials: *tert*-butyl acetate (a), *tert*-butyl formate (b), *tert*-butyl chloroacetate (c), *tert*-butyl acetoacetate (d) and *tert*-butyl methyl ether (e).

The gelation trials in *tert*-butyl formate solvent were stopped after the initial gelation test due to its cost and the lack of positive results. Further studies in *tert*-butyl acetoacetate were not pursued either as gelation did not occur.

Table 3. Gelation trials of precursor gelator Boc-Phe-Phe-O*t*Bu **1**. The amount of Boc-Phe-Phe-O*t*Bu was 23.5 mg, 0.05 mol/l in all samples.

Solvent	**H_2SO_4 (eq)**	**H_2SO_4 (µl)**	**Outcome**	**Gelation day**
*t*BuOAc	1.0	2.7	SSG, opaque	day one
*t*BuOAc	0.5	1.35	SSG, opaque	day one
*t*BuOAc	0.18	0.5	SSG, opaque	day one
CH_3O*t*Bu	1.0	2.7	PG	day five
CH_3O*t*Bu	0.5	1.35	PG	day four
CH_3O*t*Bu	0.18	0.5	SSG, transparent	day 13
$ClCH_2CO_2$*t*Bu	1.0	2.7	no gel	-
$ClCH_2CO_2$*t*Bu	0.5	1.35	no gel	-
$ClCH_2CO_2$*t*Bu	0.18	0.5	SSG, opaque	day one
$AcCH_2CO_2$*t*Bu	1.0	2.7	no gel	-
$AcCH_2CO_2$*t*Bu	0.5	1.35	no gel	-
$AcCH_2CO_2$*t*Bu	0.18	0.5	no gel	-
HCO_2*t*Bu	1.0	2.7	no gel	-

SSG = self-supporting gel, PG = partial gel

The pH values of Boc-Phe-Phe-O*t*Bu **1** in different solvents were measured to see potential differences based on the solvent type (Table 4). Boc-Phe-Phe-O*t*Bu **1** (23.5 mg, 0.05M) was dissolved in each solvent (1.0 ml) and sonicated. All solutions were prepared in triplicate. The pH of the *tert*-butyl formate solution was not measured as all tests were already terminated.

Table 4. The pH values of Boc-Phe-Phe-O*t*Bu **1** solutions in different solvents.

Solvent	pH 1	pH 2	pH 3	Average
*t*BuOAc	-	4.94	4.87	4.91
$ClCH_2CO_2tBu$	3.44	3.39	3.30	3.38
$AcCH_2CO_2tBu$	5.17	5.14	5.12	5.14
CH_3OtBu	5.21	5.22	5.23	5.22

The results show that *tert*-butyl chloroacetate has the lowest pH value, from which it can be concluded that it would need less acid for gelation than other solvents. The same amount of acid in this solvent as in the others would result in a much lower final pH. This is also seen in the gelation results, as gelation occurred only with 0.18 eq of acid in *tert*-butyl chloroacetate, while with other solvents, a partial gel or self-supporting gel was also obtained with higher equivalents of acid.

11.2 Phase transition temperature ($T_{gel-sol}$) measurements

Based on the results of the initial gelation experiments (Table 3), three different organogels were prepared for the $T_{gel-sol}$ measurements, namely in *tert*-butyl acetate (0.05 M, 0.5 eq of acid), in *tert*-butyl chloroacetate (0.05 M, 0.18 eq of acid) and in *ter*t-butyl methyl ether (0.05 M, 0.18 eq of acid). The organogels were heated in a block heater, and the temperature was raised by 5 ºC in 10 minutes intervals starting from 30 ºC. After each temperature increase step, the organogels were assessed by the vial inversion method. The organogels in *tert*-butyl acetate (0.5 eq of acid) broke at 55-60 ºC, in *tert*-butyl chloroacetate (0.18 eq of acid) at 50-55 ºC, and those in *tert*-butyl methyl ether (0.18 eq of acid) at 50-55 ºC. All gels reformed after cooling overnight (gel-to-sol-gel), verifying that they are thermoreversible in nature (Figure 31).

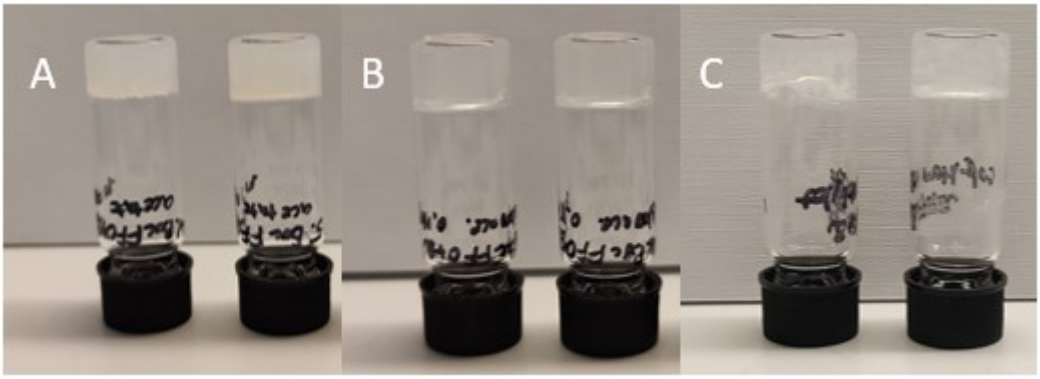

Figure 31. Reformed organogels after cooling overnight in A: *tert*-butyl acetate, 0.5 eq of acid, 0.05 M, B: *tert*-butyl chloroacetate, 0.18 eq of acid, 0.05 M, and C: *tert*-butyl methyl ether, 0.18 eq of acid, 0.05 M.

11.3 Swelling tests

Swelling experiments were performed on two different organogels: in *tert*-butyl acetate (0.05 M, 0.5 eq of acid) and *tert*-butyl chloroacetate (0.05 M, 0.18 eq of acid). First, the initial weights (net weight) of the gels were weighed before the addition of solvent (*tert*-butyl acetate 500 µl and *tert*-butyl chloroacetate 200 µl, respectively) on the surface of the gels. After 24 hours, the added solvent was removed, and the swollen organogel was weighed. The weight measurement was performed daily for three weeks (excluding weekends).

The swelling degree (SD%) was calculated with equation (1):

$$SD(\%) = \frac{w_t}{w_0} \cdot 100\ \%\ , \qquad (1)$$

where w_t is the measured weight of the swollen gel, and w_0 is the weight of the initial organogel.

Figure 32 presents the differences in swelling behavior between the two organogels. Organogel in *tert*-butyl chloroacetate swelled during the first 10 days, after which the weight started to decrease

because there is a limit in swelling after which the gel collapses. However, the gel did not break down completely at any stage. The organogel in *tert*-butyl acetate remained stable throughout the swelling trials and did not swell, meaning the gel is in equilibrium. Organogel in *tert*-butyl chloroacetate is, therefore, more elastic compared to *tert*-butyl acetate one.

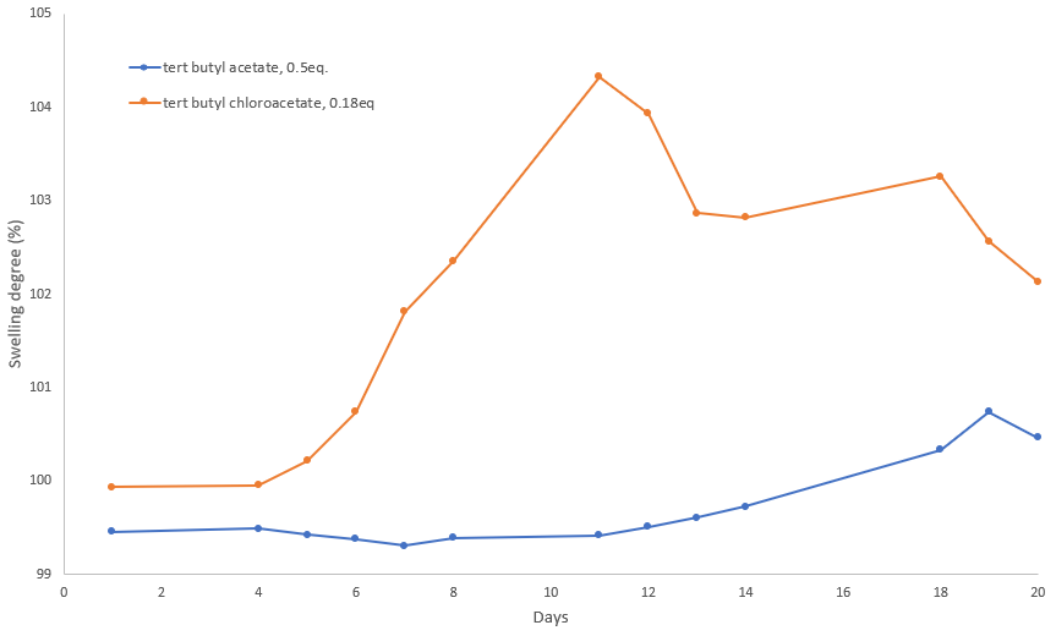

Figure 32. Swelling profiles vs time of organogels in *tert*-butyl acetate (0.05 M, 0.5 eq) and in *tert*-butyl chloroacetate (0.05 M, 018 eq).

11.4 Gelation control experiments

Gelation control experiments were performed with Phe-Phe-O*t*Bu **2** and Phe-Phe **3** in *tert*-butyl acetate, *tert*-butyl methyl ether and *tert*-butyl chloroacetate, to identify which of the *in situ* formed compounds, **2** or **3**, acts as an organogelator (Scheme 1). Gelation trials were performed following the protocol mentioned above. The results are presented in Tables 5 and 6 below.

Table 5. Gelation control trials of Phe-Phe-O*t*Bu **2**. The amount of Phe-Phe-OtBu **2** was kept constant (18.5 mg, 0.05 mol/l).

Solvent	**H_2SO_4 (eq.)**	**H_2SO_4 (µl)**	**Outcome**	**Gelation time**
*t*BuOAc	0.5	1.06	SSG	day one
CH_3OtBu	0.18	0.38	SSG	immediately
$ClCH_2CO_2tBu$	0.18	0.38	sol	-

Table 6. Gelation control trials of Phe-Phe **3**. The amount of Phe-Phe **3** was kept constant (15.6 mg, 0.05 mol/l).

Solvent	**H_2SO_4 (eq)**	**H_2SO_4 (µl)**	**Outcome**	**Gelation time**
*t*BuOAc	0.5	0.90	sol	-
CH_3OtBu	0.18	0.32	SSG	day one
$ClCH_2CO_2tBu$	0.18	0.32	SSG	day one

Phe-Phe-O*t*Bu **2** formed a self-supporting gel in *tert*-butyl acetate at day one and in *tert*-butyl methyl ether immediately after stirring with ultrasound. The formation of a self-supporting gel in *tert*-butyl chloroacetate was not observed. This may be due to the sonication of the solution after acid addition or solubility of the gelator in *tert*-butyl chloroacetate compared with other solvents. Phe-Phe **3**, however, formed a self-supporting gel in *tert*-butyl methyl ether and *tert*-butyl chloroacetate at day one but not in *tert*-butyl acetate, as was observed in previous studies[16]. These observations suggest that both Phe-Phe-O*t*Bu **2** and Phe-Phe **3** can form self-supporting gels in *tert*-butyl methyl ether and their ability to gel depends on the solvent type. Based on previous research, for *tert*-butyl acetate, both Phe-Phe-O*t*Bu **2** and Phe-Phe **3** are required to produce a self-supporting gel, as gelation is driven by the balance between these two compounds.[16] The gelation results can also be seen in Figure 33.

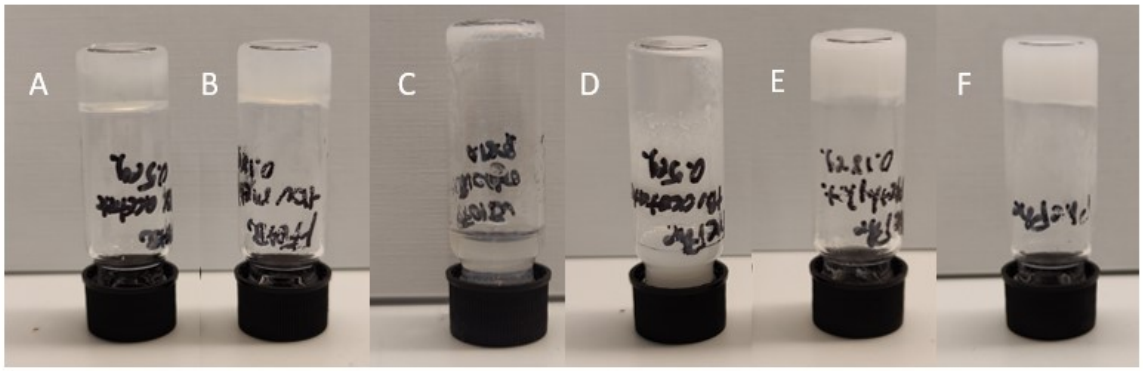

Figure 33. Phe-Phe-O*t*Bu **2** and Phe-Phe **3** gelation tests: (A) Phe-Phe-O*t*Bu in *tert*-butyl acetate, (B) Phe-Phe-O*t*Bu in *tert*-butyl methyl ether, (C) Phe-Phe-OtBu in *tert*-butyl chloroacetate (D) Phe-Phe in *tert*-butyl acetate (E) Phe-Phe in *tert*-butyl methyl ether and (D) Phe-Phe in *tert*-butyl chloroacetate.

12 Results and discussion

12.1 Gelation results

All organogels were prepared by dissolving 23.5 mg of Boc-Phe-Phe-O*t*Bu **1** in 1 ml of each organic solvent (0.05 M). The amount of acid was deliberately changed to investigate the effect of acid concentration on gelation. Three solvents yielded self-supporting gels, *t*BuOAc, $ClCH_2CO_2tBu$ and CH_3OtBu (Table 7). In *tert*-butyl acetoacetate ($AcCH_2CO_2tBu$), gel formation was not observed at any tested condition. Therefore, further studies were not pursued. In addition, gelation trials with *tert*-butyl formate (HCO_2tBu) were abandoned due to its high cost and the negative obtained preliminary gelation results.

Table 7. Gelation results of gelator precursor Boc-Phe-Phe-O*t*Bu **1**.

Solvent	**H_2SO_4 (eq)**	**H_2SO_4 (µl)**	**Outcome**	**Tgel-sol (°C)**	**Lifetime**	**Comment**
*t*BuOAc	1.0	2.7	SSG, opaque		6 days	
*t*BuOAc	0.5	1.35	SSG, opaque	55–60	9 days	
*t*BuOAc	0.18	0.5	SSG, PG, opaque	50–55	14 days	
$ClCH_2CO_2tBu$	0.18	0.5	SSG, opaque	50–55	-	
CH_3OtBu	0.18	0.5	SSG, transparent	50–55	-	Formed on day 13
CH_3OtBu	1.0	2.7	PG		-	Formed on day 5
CH_3OtBu	0.5	1.35	PG		-	Formed on day 4

In *tert*-butyl acetate all trials resulted in self-supporting, opaque gels on day one. The organogels prepared using 1.0 eq of acid broke on day 6, and those with 0.5 eq of acid broke on day 9. The tested sample (triplicate) using 0.18 eq of acid formed two self-supporting gels and one partial gel, which

broke on day 14. *tert*-Butyl chloroacetate solvent induced gelation only with 0.18 eq of acid. From the *tert*-butyl methyl ether solvent, only the sample with 0.18 eq of acid formed a self-supporting gel on day 13. Other equivalences formed partial gels on day 5 (1.0 eq of acid) and on day 4 (0.5 eq of acid). The only gels that broke were gels in *tert*-butyl acetate. Gels made with other organic solvents ($ClCH_2CO_2tBu$ and CH_3OtBu) did not break, so the transient nature of the gels could not be demonstrated with these solvents. Figure 34 presents the obtained self-supporting and partially formed gels.

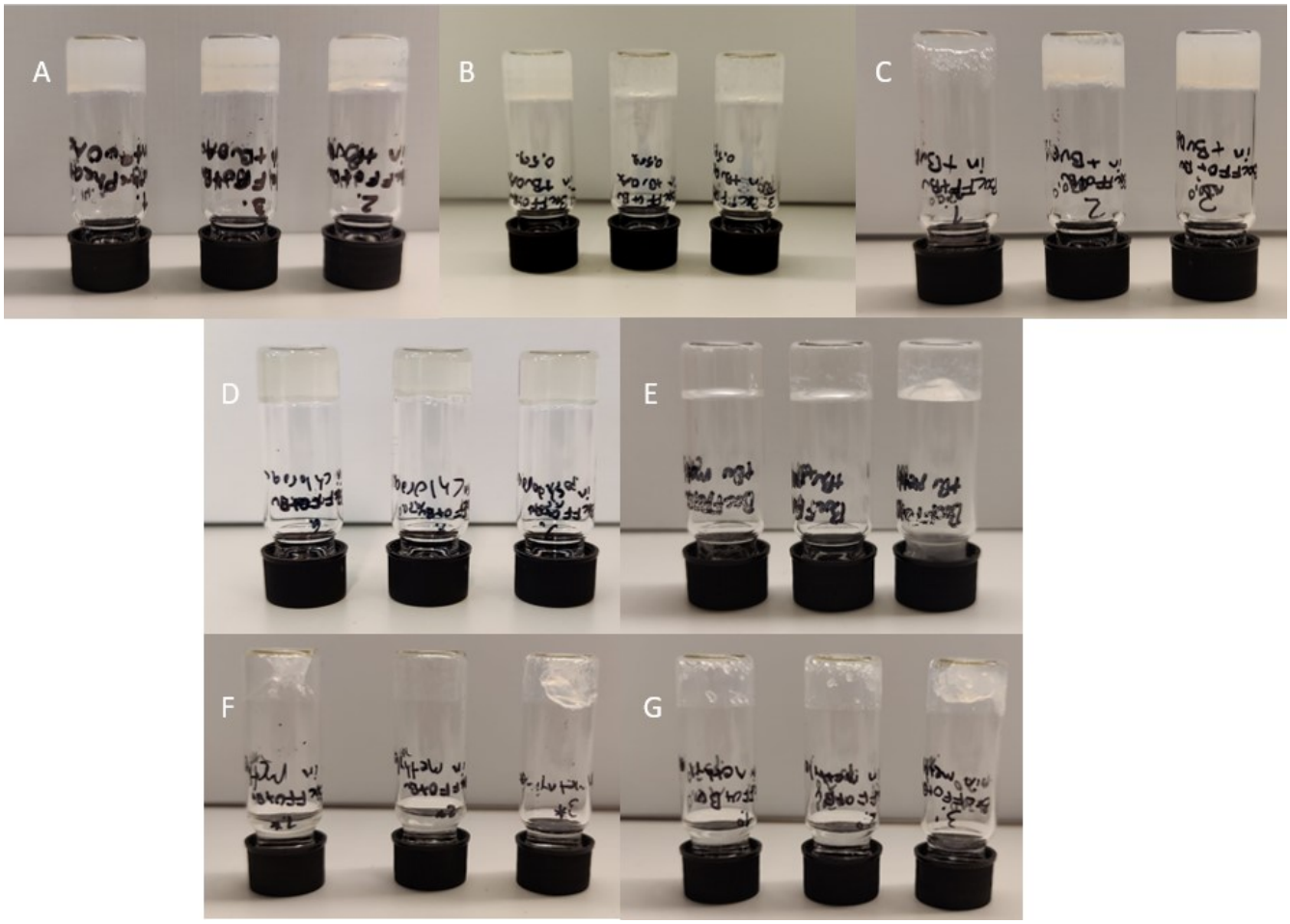

Figure 34. Self-supporting gels of Boc-Phe-Phe-O*t*Bu **1** in: (A) *tert*-butyl acetate (1.0 eq of acid), (B) *tert*-butyl acetate (0.5 eq of acid), (C) *tert*-butyl acetate (0.18 eq of acid), (D), *tert*-butyl chloroacetate (0.18 eq of acid) and (E) *tert*-butyl methyl ether (0.18 eq of acid). Partial gels in *tert*-butyl methyl ether: (F) 0.5 eq of acid and (G) 1.0 eq of acid.

From these observations, it can be concluded that the acid concentration affects the gelation process. However, the effect was different in different solvents. For example, in *tert*-butyl acetate, reducing the amount of acid impaired gelation. With 0.18 eq of acid, one of the replicates did not gel properly, and one formed gel on day 2, while in other equivalences, all replicates formed self-supporting gels on day one. In the other two solvents ($ClCH_2CO_2tBu$ and CH_3OtBu), reducing the amount of acid improved the gelation result, and only self-supporting gels were obtained with 0.18 eq of acid. Only partial gels (CH_3OtBu) or no gels ($ClCH_2CO_2tBu$) were obtained with higher acid equivalents.

It is of note that the gelation in *tert*-butyl methyl ether took considerably longer time than in the other two solvents. This is probably due to the structure of the *tert*-butyl methyl ether solvent, which is the only ether solvent, while other solvents are ester-based. Esters are known to be more reactive than ethers because they contain a polar carbonyl group. The lower reactivity of the solvent may have affected the gelation time.

In previous studies, the solvent (*t*BuOAc) played an important role in gelation as a chemically active solvent since it acted as a brake (breaking the gel network), whereas the acid was an accelerator in the gelation process inducing gelation (Scheme 1).[16] Under acidic conditions, *tert*-butyl acetate solvent reversed the ester deprotection of **2** while it formed *tert*-butanol, a secondary antagonist solvent, which causes the dissolution of the two-component **2**/**3** organogel. In this study, the self-supporting gels prepared with the new organic solvents ($ClCH_2CO_2tBu$ and CH_3OtBu) did not break, so it can be concluded that under the given conditions, the amount of the antagonist solvent *tert*-butanol is not sufficient to cause the dissolution of the gels, although in NMR spectra we do observe the -OH of *tert*-butanol.

12.2 NMR analysis

NMR analysis was performed to compare differences between the gel (gel) and solution (sol) phases of the materials (sol-to-gel). The solutions refer to materials after the addition of acid and before gelation occurs (sol-to-gel transition). Therefore, NMR spectra of the formed gels and the corresponding solutions were recorded. Additionally, differences amongst solvent types, and partial/self-supporting gels were assessed.

NMR samples of the formed gels and corresponding solutions were prepared by drying under a vacuum overnight and dissolving the dried samples in deuterated DMSO. The dissolved samples were then transferred to NMR tubes. All xerogels (dried self-supporting gels) contained both Boc-Phe-Phe-O*t*Bu **1** and Phe-Phe-O*t*Bu **2** in different ratios and some solvent impurities. Some xerogels also contained Phe-Phe **3** but in small amounts. In all xerogels, the formation of *tert*-butanol is also observed.[45] ^{13}C NMR spectra of the xerogels and corresponding solutions (day 1) and ^{1}H and ^{13}C spectra of Phe-Phe **3** are shown in appendices (1-5).

12.2.1 Comparison of xerogel and solution (sol-to-gel transition) in *tert*-butyl methyl ether

The ^{1}H NMR spectra of Boc-Phe-Phe-O*t*Bu **1** in *tert*-butyl methyl ether (0.05 M, 0.18 eq of acid) that formed a gel at day 13 (A) and a sample of Boc-Phe-Phe-O*t*Bu **1** in *tert*-butyl methyl ether (0.05M, 0.18 eq of acid) at day one (B) in the sol phase are presented in Figure 35. Both gel and sol phases showed NH protons from **1** (8.19 and 6.82 ppm) and NH peaks approximately at 8.89 ppm, which do not appear in any of the starting materials (neat materials **1**, **2** and **3** in powder form). These protons originate from Phe-Phe-O*t*Bu **2** (8.89 ppm) and Phe-Phe **3** (8.83 ppm), which form *in situ* by the deprotection of **1** under acidic conditions (Scheme 1). Both also give a new larger peak at 8.07 ppm belonging to protonated NH_3^+ group of the Phe-Phe-O*t*Bu **2**. The hydroxyl group of *tert*-butanol gives a peak at 4.9 ppm in the gel phase and 4.7 ppm in the sol, but the intensity in the sol phase (B) is higher. The Boc group signals are seen in both samples at 1.28 ppm and the *tert*-butyl group at 1.32 ppm. In gel, the *tert*-butyl group gives a doublet signal, which suggests two conformations of **1** or **2**.

The findings suggest that the gel and corresponding sol phases contain unreacted Boc-Phe-Phe-O*t*Bu **1**, Phe-Phe-O*t*Bu **2** and Phe-Phe **3**, which form *in situ*. Boc-Phe-Phe-O*t*Bu **1** and Phe-Phe-O*t*Bu **2** are approximately in a 1:1 ratio in the gel phase (A) and a 1:1.4 ratio in the sol phase (B) (Figure 35). Both also contain a small amount of Phe-Phe **3**. The ratios show that the amount of unreacted precursor **1** decreases when the gel is formed.

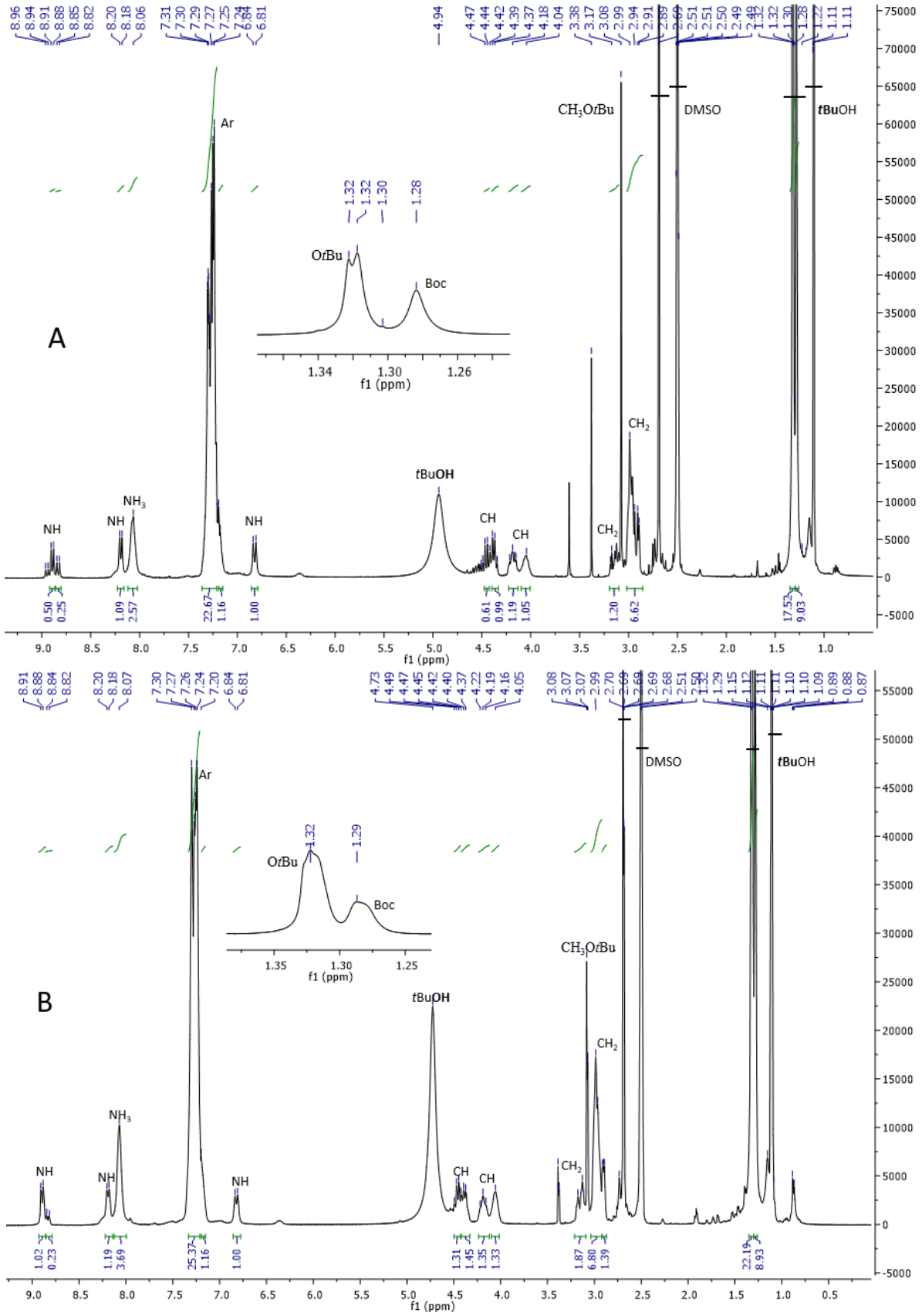

Figure 35. ^{1}H NMR (300 MHz, d_6-DMSO) spectra of Boc-Phe-Phe-O*t*Bu **1** materials in the gel and sol phases. (A) xerogel in *tert*-butyl methyl ether (0.05 M, 0.18 eq) and (B) sol in *tert*-butyl methyl ether (0.05 M, 0.18 eq).

12.2.2 Comparison of xerogel in *tert*-butyl methyl ether with different equivalents of acid

The ^{1}H NMR spectra of Boc-Phe-Phe-O*t*Bu **1** self-supporting gel in *ter*t-butyl methyl ether (0.05 M, 0.18 eq) formed at day 13 (A) and Boc-Phe-Phe-O*t*Bu **1** partial gel in *ter*t-butyl methyl ether (0.05 M, 0.5 eq) formed at day four (B) are presented in Figure 36. Besides the difference in gelation time, there are also differences in the corresponding ^{1}H NMR spectra. The NH protons from the Boc-Phe-Phe-O*t*Bu **1** and Phe-Phe-O*t*Bu **2** have different chemical shifts and intensities. When adding 0.18 eq of acid, the NH peak at 8.89 ppm gives a multiplet, while when adding 0.5 eq of acid, the NH signal at 8.92 ppm gives a double doublet signal with different intensities. The addition of 0.5 eq of acid gives a partial gel, in which the NH proton at 8.92 ppm is from Phe-Phe-O*t*Bu **2** and at 8.85 ppm from Phe-Phe **3**. Both spectra show protonated NH_3^+ protons at 8.06 and 8.07 ppm from the Phe-Phe-O*t*Bu **2** and Phe-Phe **3**. The *tert*-butyl alcohol hydroxyl group gives a signal approximately at 4.9 ppm in self-supporting gels (0.18 eq) and at 4.18 ppm in partially formed gels (0.5eq). Both equivalents of acids give materials (fully formed and partial gels) which have the CH proton from the *in situ* formation of Phe-Phe-O*t*Bu **2** approximately at 4.45 ppm and the CH protons from unreacted precursor Boc-Phe-Phe-O*t*Bu **1**. The CH protons from Boc-Phe-Phe-O*t*Bu **1** cannot be distinguished in the partial gel due to overlapping *tert*-butanol in the same area. The CH_2 protons also showed different intensities in the partial gel (0.5 eq), as the protons from Boc-Phe-Phe-O*t*Bu **1** at 2.90 ppm have smaller intensity.

Both gels (partial and fully formed) have a Boc group at 1.28 ppm and a *tert*-butyl group at 1.32 ppm. However, in the gel from 0.18 eq of acid, the *tert*-butyl group gives a doublet, indicating possibly two different conformations in the gel phase. The ratio of Boc-Phe-Phe-O*t*Bu **1** and Phe-Phe-O*t*Bu **2** is approximately 1:1 in the fully formed gel (A) and 0.25:1 in the partial gel (B; Figure 36). From the ratios, it can be concluded that when increasing the acid concentration, the amount of precursor **1** decreases as more **2** and **3** are formed *in situ*. Thus, the amount of acid does affect the gelation and acts as an accelerator in the gelation project, as mentioned in previous studies.[16] In addition, both samples contain a small amount of Phe-Phe **3**, but much less than compounds **1** and **2**.

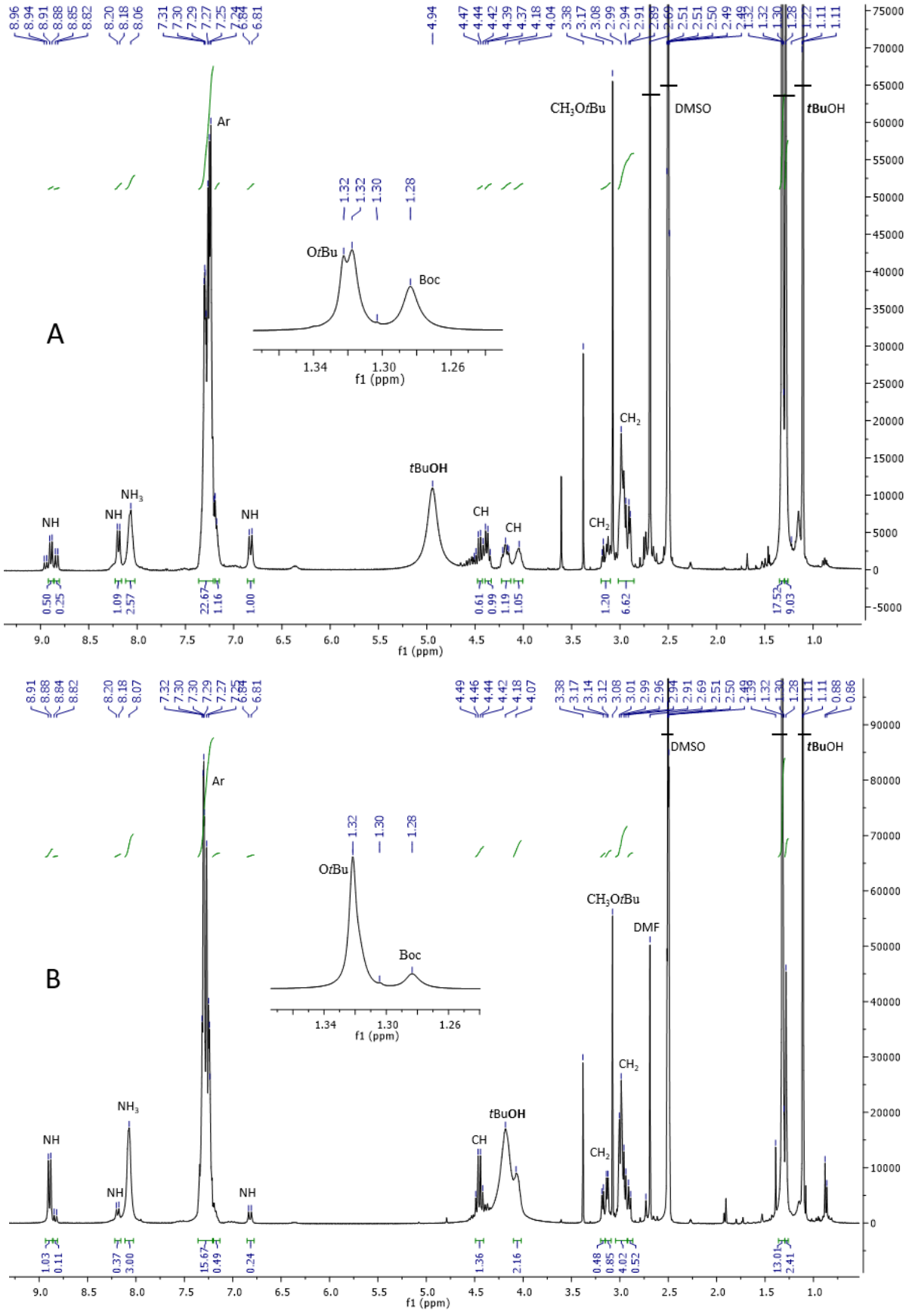

Figure 36. ^{1}H NMR (300 MHz, d_6-DMSO) spectra of formed gels in *tert*-butyl methyl ether (0.05 M): (A) 0.18 eq of acid, fully formed gel and (B) 0.5 eq of acid, partially formed gel.

12.2.3 Comparison of gels in different solvents using the same amount of acid

The ^{1}H NMR spectra of gel samples (0.05 M, 0.18 eq) formed in *tert*-butyl methyl ether on day 13 (A) and in *tert*-butyl chloroacetate on day one (B) are presented in Figure 37. Both spectra give signals of NH protons from the Boc-Phe-Phe-O*t*Bu **1** at 8.19 ppm and 6.82 ppm. In addition, the protonated NH_3^+ signal from Phe-Phe-O*t*Bu **2** at 8.08 and 8.06 ppm was observed. The main difference between the two gel samples is observed in NH proton signals approximately at 8.89 ppm, where the peak is a doublet in *tert*-butyl chloroacetate, whereas in *tert*-butyl methyl ether, the signal is a triplicate doublet. This suggests the absence of Phe-Phe **3** in the gel obtained from *tert*-butyl chloroacetate (B). Another difference between the two samples is the presence of *tert*-butanol, seen only in the gel obtained from *tert*-butyl methyl ether at 4.95 and 1.1 ppm. In the gel obtained from *tert*-butyl chloroacetate, the *tert*-butanol signal is shifted approximately at 6.25 ppm, but the peak has a significantly lower intensity. The peak from the *tert*-butyl chloroacetate sample (4.2 ppm) overlaps with the CH proton peaks of the gel (B). Both samples show CH_2 protons from the Boc-Phe-Phe-O*t*Bu **1** and Phe-Phe-OtBu **2** approximately centered at 3.18 ppm and 2.95 ppm. The Boc and tert-butyl groups are seen at 1.28 and 1.32 ppm in both gels, respectively. The signal of the *tert*-butyl group gives a doublet suggesting the presence of two conformations in the gel phase.

The NMR studies show a considerable amount of unreacted precursor **1** in the gel phase. The ratio of Boc-Phe-Phe-O*t*Bu **1** and Phe-Phe-O*t*Bu **2** is approximately 1:1 in both samples (Figure 37), which indicates that the solvent does not affect the amount of remaining precursor **1,** while acid concentration seemed to influence it. The most significant difference between the gels is the presence of Phe-Phe **3** and *tert*-butanol in the gel obtained with *tert*-butyl methyl ether (A). The low acid concentration cannot explain the difference, as the acid content is the same in both solvents. Therefore, solvents seem to affect the gelation.

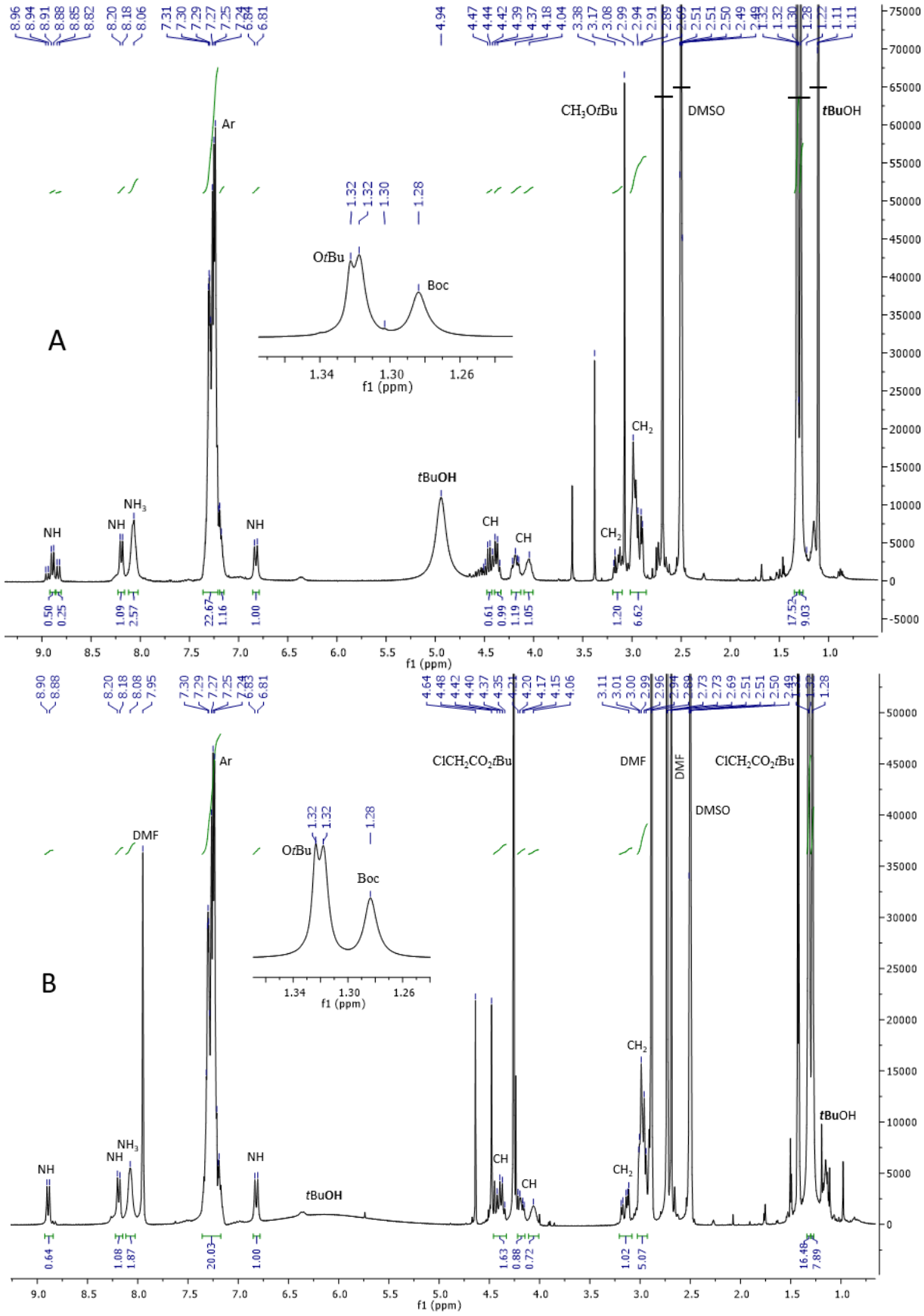

Figure 37. ^{1}H NMR (300 MHz, d_6-DMSO) spectra of gels (0.05 M): (A) in *tert*-butyl methyl ether, 0.18 eq, SSG and (B) and *tert*-butyl chloroacetate, 0.18 eq, SSG.

13.3 FT-IR analysis

Fourier-transform infrared spectroscopy (FT-IR) analysis was performed to study the secondary structure of the formed gels. The main areas of interest are the amide A (around 3300 cm^{-1}), amide I (1600-1690 cm^{-1}) and amide II (1480-1575 cm^{-1}) areas. The amide A band is caused by N-H stretching vibration, the amide I band by C=O stretching vibrations, and the amide II band is due to the N-H bending and C-N stretching vibrations.[46]

The samples for FT-IR analysis were prepared by drying the gels (preparation of xerogels) on a petri dish on top of a glass plate. The FT-IR spectra were recorded from the xerogels of the corresponding self-supporting gels (fully formed gels). In addition, the precursor Boc-Phe-Phe-O*t*Bu **1** and *in situ* formed Phe-Phe-O*t*Bu **2** and Phe-Phe **3** gelators were also analyzed as neat materials (powder form) for reference.

13.3.1 FT-IR analysis of Boc-Phe-Phe-O*t*Bu, Phe-Phe-O*t*Bu and Phe-Phe

The FT-IR spectra of Boc-Phe-Phe-O*t*Bu **1**, Phe-Phe-O*t*Bu **2** and Phe-Phe **3** (neat powders) are given in Figure 38. Each compound showed absorption at the amide A region although slightly shifted (3287 (**1**), 3338 (**2**) and 3252 (**3**) cm^{-1}, respectively). The spectra also showed aromatic C-H stretching vibrations around 3000 cm^{-1} (2978 (**1**), 2936 (**2**) and 2977 (**3**) cm^{-1}, respectively). The C=O group gives stretching vibrations at 1732 cm^{-1} for Boc-Phe-Phe-O*t*Bu **1** and Phe-Phe-O*t*Bu **2**, but for Phe-Phe **3** it is downshifted to 1684 cm^{-1}. The spectra of Boc-Phe-Phe-O*t*Bu **1** and Phe-Phe-O*t*Bu **2** have amide I peaks (C=O stretching) at 1650 and 1678 cm^{-1}, but in Phe-Phe at 1613 cm^{-1}. Finally, amide II vibrations (N-H bending) are found in all three compounds at 1522 (**1**), 1536 (**2**) and 1551 (**3**) cm^{-1}.

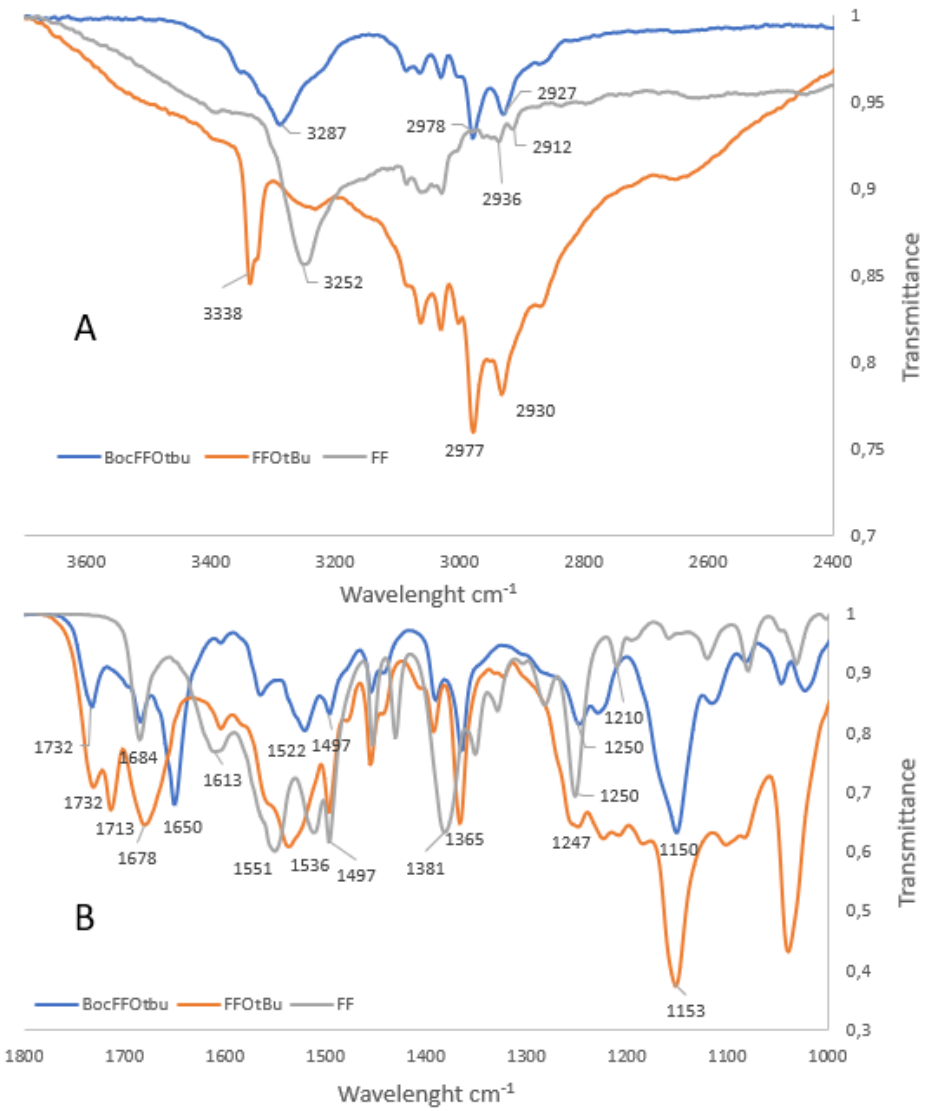

Figure 38. FT-IR spectra of Boc-Phe-Phe-O*t*Bu **1** (blue), Phe-Phe-O*t*Bu **2** (orange) and Phe-Phe **3** (grey). A) spectrum width 2600 – 3500 cm^{-1} (B) spectrum width 1000 – 1800 cm^{-1}.

Boc-Phe-Phe-O*t*Bu **1** and Phe-Phe-O*t*Bu **2** also give rise to the ester group C-O stretching peak at 1153 and 1150 cm^{-1}, while Phe-Phe **3** showed the C-O stretching peak of the carboxylic group at 1210 cm^{-1}. Phe-Phe **3** shows a sharp peak at 1250 cm^{-1}, assigned to the C-N stretching. In the spectra of Boc-Phe-Phe-O*t*Bu **1**, the C-N stretch band is shown at 1250 cm^{-1} and for Phe-Phe-O*t*Bu **2**, C-N stretch is shown as a shoulder peak at 1247 cm^{-1}, which is merged with the ester group C-O stretching peak.

13.3.2 FT-IR analysis of Boc-Phe-Phe-O*t*Bu xerogels in different solvents

The Boc-Phe-Phe-O*t*Bu xerogel obtained from *tert*-butyl chloroacetate and *tert*-butyl methyl ether (0.05 M, 0.18 eq) were analyzed by Fourier transformation infrared (FTIR) spectroscopy (Figure 39). The spectra are qualitatively similar, and there are no significant differences in peak positions between different solvents in xerogels with the same acid concentration. In both xerogels, the amide A region shows stretching vibration bands at 3323 and 3291 cm^{-1}. The amide I band, associated with the C=O stretching frequency, showed peaks in both xerogels at 1654 and 1651 cm^{-1}. This suggests that both xerogels form an α-helical like structure.[46] The ester groups C=O have stretching vibrations at 1732 cm^{-1} and 1736 cm^{-1} in *tert*-butyl chloroacetate and *tert*-butyl methyl ether xerogels, respectively. The absorptions are almost the same as in the neat powder samples (neat starting material) of Boc-Phe-Phe-O*t*Bu **1** and Phe-Phe-O*t*Bu **2**. At the amide II region, the N-H bending vibration band is found in both xerogels at 1521 and 1522 cm^{-1}. A sharp peak at 1151 cm^{-1} is associated with the ester C-O vibration. The peak is merged to larger peaks, approximately at 1223 cm^{-1} and 1219 cm^{-1}, associated with the amine C-N. Both spectra have a C-H bend at 1365 cm^{-1}, indicating the unreacted Boc-Phe-Phe-O*t*Bu **1**, unlike in previous studies by Chevigny *et al.*[16]

Due to the similarity of the spectra and as both gels contain an α-helical-like structure, it can be concluded that the solvent does not significantly affect the secondary structure or the self-assembly of precursor gelator **1**.

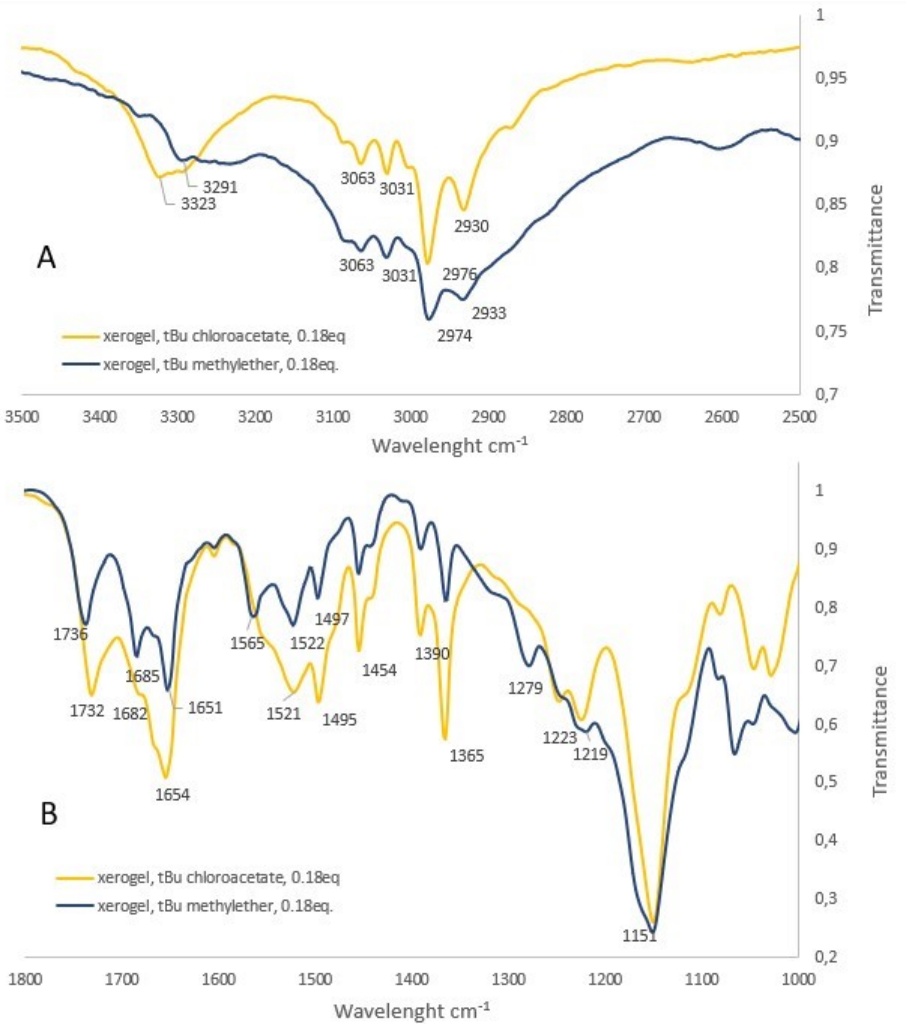

Figure 39. FT-IR analysis of the Boc-Phe-Phe-O*t*Bu xerogels in *tert*-butyl chloroacetate (yellow) and *tert*-butyl methyl ether (blue), 0,05 M, 0.18 eq: (A) wavelength area 2600 – 3500 cm^{-1} (B) wavelength area 1000 – 1800 cm^{-1}.

13.3.3 FT-IR analysis of Boc-Phe-Phe-O*t*Bu xerogels using different equivalence of acid

The Boc-Phe-Phe-O*t*Bu xerogels in *tert*-butyl acetate (0.05 M) were analyzed and compared by FTIR spectroscopy. For the preparation of the gels, two different equivalents of acid (0.5 eq and 1.0 eq; Figure 40) were used. The amide A region shows stretching vibration bands at 3325 cm^{-1} and C=O stretching vibrations of the ester group are observed at 1711 cm^{-1} in both xerogels. The peak at 1604

cm^{-1} is due to the N-H bending. In both xerogels, the C-O and C-N stretching peaks are merged into a broad band centered at 1154 cm^{-1}. This peak has shoulder peaks at 1209, 1257 and 1211 cm^{-1}.

The main difference in spectra is seen in the amide I region: With the sample of 0.5 eq acid, the peak is at 1651 cm^{-1}, and in 1.0 eq upshifted to 1691 cm^{-1}. These observations suggest that the xerogel obtained from 0.5 eq of acid forms an α-helical-like structure, while the xerogel obtained from 1.0 eq of acid forms a β-sheet like secondary structure.[46] Compared to the powder (neat starting material), the location of the amide I band indicates that the xerogel with 0.5 eq of acid still contains unreacted Boc-Phe-Phe-O*t*Bu **1**. The amide II band also has a slight difference between the xerogels, as the 0.5 eq sample shows a peak at 1519 cm^{-1} and that of 1.0 eq at 1546 cm^{-1}.

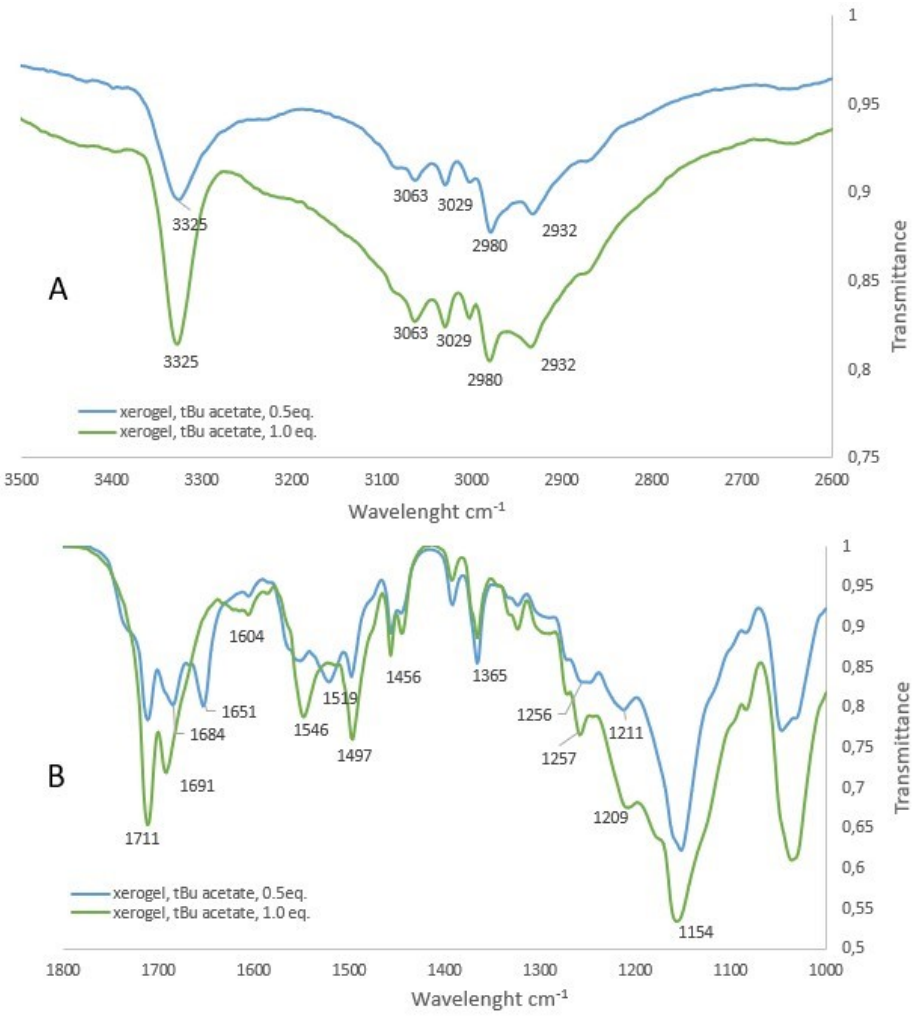

Figure 40. FT-IR analysis of xerogels in *tert*-butyl acetate, 0.05 M, 0.5 eq of acid (blue) and 1.0 eq of acid (green): (A) wavelength area 2600 – 3500 cm^{-1} (B) wavelength area 1000 – 1800 cm^{-1}.

These observations suggest that unreacted Boc-Phe-Phe-O*t*Bu **1** is still left in the xerogel obtained from 0.5 eq of acid, while the xerogel derived by adding 1.0 eq of acid does not contain the starting material. This suggests that 0.5 eq of acid is insufficient to deprotect all precursor gelator **1**, while 1.0 eq of acid is enough. The two gels also form different in their secondary structures. Thus, it can be concluded that the amount of acid also affects the secondary structure and the self-assembly of the **1**.

13.4 HR-MS

High-resolution mass spectrometry (HR-MS) was used to detect the presence of Boc-Phe-Phe-O*t*Bu **1**, Phe-Phe-O*t*Bu **2** and Phe-Phe **3** in the xerogels. HR-MS spectra were recorded from three different self-supporting gels: a gel made in *tert*-butyl acetate with 0.5 eq of acid (xerogel 1), a gel made in *tert*-butyl chloroacetate with 0.18 eq of acid (xerogel 2) and a gel made in *tert*-butyl methyl ether with 0.18 eq of acid (xerogel 3). The information from HR-MS spectra is presented in Table 8. Comparative spectra and information of Boc-Phe-Phe-O*t*Bu and Phe-Phe-O*t*Bu were obtained from the study of Chevigny *et al.*[16] Mass accuracy was calculated with equation (2):

$$\Delta m/z = m/z_{\text{theor}} - m/z_{\text{exp}} \quad (2)$$

, where m/z_{theor} is the calculated theoretical mass and m/z_{exp} is the accurate mass from the experimental work.

Table 8. m/z values, molecular formulas, and mass accuracies of samples. Theoretical *m/z* values are from ChemDraw.

sample	**molecular formula**	**ion**	***m/z* (theor)**	***m/z* (exp)**	**mass accuracy (mDa)**
Boc-Phe-Phe-O*t*Bu	$C_{27}H_{36}N_2O_5$	[**1**+H]$^+$	469.2697	469.2675	2.2
		[**1**+Na]$^+$	491.2516	491.2495	2.1
		[**1**+K]$^+$	507.2256	507.2236	2.0
Phe-Phe-O*t*Bu	$C_{22}H_{28}N_2O_3$	[**2**+H]$^+$	369.2173	369.2161	1.2
		[**2**+Na]$^+$	391.1992	391.1978	1.4
xerogel 1	$C_{27}H_{36}N_2O_5$	[**1**+Na]$^+$	491.2516	491.251	0.6
	$C_{27}H_{36}N_2O_5$	[**1**+K]$^+$	507.2256	507.2248	0.8
	$C_{22}H_{28}N_2O_3$	[**2**+H]$^+$	369.2173	369.2164	0.9
	$C_{18}H_{20}N_2O_3$	[**3**+H]$^+$	313.1531	313.1553	-2.2
xerogel 2	$C_{27}H_{36}N_2O_5$	[**1**+Na]$^+$	491.2516	491.252	-0.4
	$C_{27}H_{36}N_2O_5$	[**1**+K]$^+$	507.2256	507.2258	-0.2
	$C_{22}H_{28}N_2O_3$	[**2**+H]$^+$	369.2173	369.2167	0.6
	$C_{18}H_{20}N_2O_3$	[**3**+H]$^+$	313.1531	313.1575	-4.4
xerogel 3	$C_{27}H_{36}N_2O_5$	[**1**+Na]$^+$	491.2516	491.2509	0.7
	$C_{27}H_{36}N_2O_5$	[**1**+K]$^+$	507.2256	507.2248	0.8
	$C_{22}H_{28}N_2O_3$	[**2**+H]$^+$	369.2173	369.2164	0.9
	$C_{18}H_{20}N_2O_3$	[**3**+H]$^+$	313.1531	313.154	-0.9

The HR-MS spectra of the xerogels confirm the information obtained from ^{1}H NMR and FT-IR spectra. Boc-Phe-Phe-O*t*Bu **1**, Phe-Phe-O*t*Bu **2**, Phe-Phe **3**, and ions (H^+, Na^+ and K^+ adducts) corresponding to literature values are seen in all xerogels (Table 8). The spectrum of xerogel in *tert*-butyl chloroacetate (xerogel 3) also gives information that the ^{1}H NMR spectra did not show: Based on the HR-MS spectrum, the gel also potentially contains Phe-Phe **3** (*m/z* of $C_{18}H_{20}N_2O_3$ found 313.154). Thus, based on HR-MS spectra, all gels contain Boc-Phe-Phe-O*t*Bu **1**, Phe-Phe-O*t*Bu **2** and some Phe-Phe **3**. The HR-MS spectra of the xerogels and neat compounds Boc-Phe-Phe-O*t*Bu **1** and Phe-Phe-O*t*Bu **2** are given in Appendices 6-10.

13.5 SEM microscopy

To assess the network of the formed self-supporting gels scanning electron microscopy imaging (SEM) was performed (Figure 41). SEM imaging was done on three gels: Boc-Phe-Phe-O*t*Bu xerogel in *tert*-butyl methyl ether (0.5 eq of acid), in *tert*-butyl acetate (1.0 eq of acid) and in *tert*-butyl chloroacetate (0.18 eq of acid). The xerogel samples were prepared by dipping a carbon film into the gel and letting it dry overnight under a vacuum.

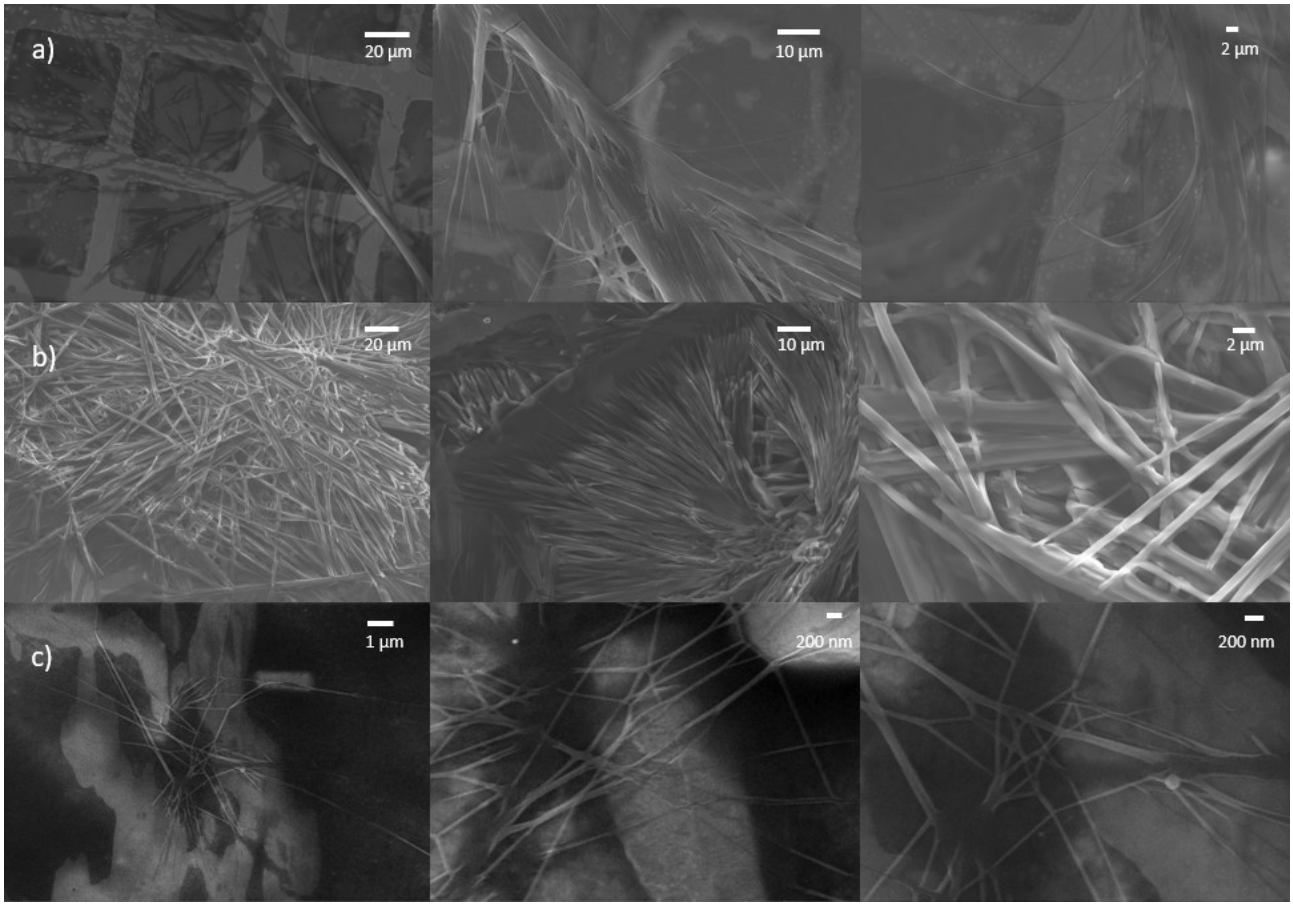

Figure 41. SEM images of xerogels in a) *tert*-butyl methyl ether (0.5 eq of acid), b) *tert*-butyl acetate (1.0 eq of acid) and c) *tert*-butyl chloroacetate (0.18 eq of acid). Three different images are presented for each sample at different magnifications.

The xerogels showed three-dimensional networks that consist of ribbons and fibers as in the corresponding organogels.[41] The xerogel in *tert*-butyl methyl ether (0.5 eq of acid) consists of fine fibers that assemble into thicker units. The fibers are visible as well-curved lines in the SEM images.

The xerogels in *tert*-butyl acetate (1.0 eq of acid) and *tert*-butyl chloroacetate (0.18 eq of acid) consist of ribbons as a unit. Some of these ribbons are packed together to make thicker ribbons.

The differences in the three-dimensional structure of the gels could be due to the solvents and their structural differences. This conclusion is supported by a previous study by Chevigny *et al*.,[16] where the three-dimensional structure of the gel changed when the solvent was added on top of it and the gel was let to swell. Also, the sample preparation may cause differences, as the samples of xerogel in *tert*-butyl acetate and in *tert*-butyl chloroacetate were prepared on the first day of gelation (day 1), while the sample of xerogel in *tert*-butyl methyl ether was prepared on day 6 since the gel formed on day 5 (partial gel).

14 Conclusions

The aim of the experimental part was to form self-supporting gels using an amino acid-based precursor gelator (Boc-Phe-Phe-O*t*Bu **1**), different organic solvents and sulfuric acid. The purpose was to study how different organic solvents and acid concentrations affect the gelation and the structure of the gel. Selective deprotection of the Boc group in the presence of the *tert*-butyl group was used as a gelation mechanism. This method in gelation has been used before by Lin *et al.*[44] and Chevigny *et al.*[16]

In this study, we managed to form thermoreversible self-supporting gels from three different organic solvents: *tert*-butyl acetate, *tert*-butyl chloroacetate and *tert*-butyl methyl ether. Gelation conditions and results differ between the solvents. As stated previously[16], the acid acts as an accelerator in the gelation process, removing the Boc group. Therefore, the acid concentration affects the amount of starting material (Boc-Phe-Phe-O*t*Bu **1**) in the gel. This is seen in the ^{1}H NMR spectra, where the xerogel in *tert*-butyl methyl ether and 0.5 eq of acid contains less Boc-Phe-Phe-O*t*Bu **1** than the xerogel with 0.18 eq of acid. The same observation can also be made from the FT-IR spectra, where the Boc group is completely absent in the xerogel from *tert*-butyl acetate and 1.0 eq of acid, whereas in the xerogel with 0.5 eq of acid, it is still present.

Based on the gelation results and NMR spectra, there are differences between the used solvents. The gelation times between the solvents differed significantly. In *tert*-butyl methyl ether, the self-supporting gels only formed after approximately two weeks, while other gels formed on day one. The structure of *tert*-butyl methyl ether is different from the other used solvents, as it is the only ether and has lower reactivity, which may affect the gelation. Based on the ^{1}H NMR spectra, the gels from *tert*-butyl chloroacetate do not contain *tert*-butanol as much as other gels in other solvents. HR-MS confirms that the gels contain all three compounds: Boc-Phe-Phe-O*t*Bu **1**, Phe-Phe-O*t*Bu **2** and Phe-Phe **3**. HR-MS also confirmed the presence of Phe-Phe **3** in xerogel from *tert*-butyl chloroacetate, which was not seen in ^{1}H NMR spectra.

Although the solvent appears to affect the gelation process and the amount of *tert*-butanol, it does not significantly affect the secondary structure or self-assembly process of the gel, as seen in the FT-IR spectra. The SEM images show that the gels form a three-dimensional network consisting of ribbons and fibers typical for organogels. Xerogel from *tert*-butyl methyl ether consist of fine fibers, and xerogels from *tert*-butyl acetate and *tert*-butyl chloroacetate have ribbons as a unit. This suggests that the solvent affects the three-dimensional network and structure of the formed gel.

Based on this study, it can be concluded that the solvent affects the gelation process and gel network. As for the acid, it can be concluded that it accelerates the gelation process and affects the gelation. Regarding the solvents that did not produce a self-supporting gel, other gelation conditions should be investigated. The transient nature of self-supporting gels can also be achieved by changing the gelation conditions, such as molarity and the amount of acid. This topic needs more research to accurately answer these questions regarding the active involvement of the solvents in the gelation process.

References

1. Ferry, J. D., Protein Gels. Anson, M. L. ja Edsall, J. T. (edit.), *Adv. in Prot. Chem.*, Academic Press, **1948**, vol. 4, ss. 1–78.
2. Das, T.; Häring, M.; Haldar, D. ja Díaz, D. D., Phenylalanine and derivatives as versatile low-molecular-weight gelators: design, structure and tailored function, *Biomater. Sci.*, **2018**, *6*, 38–59.
3. Schnitter, F.; Bergmann, A. M.; Winkeljann, B.; Rodon Fores, J.; Lieleg, O. ja Boekhoven, J., Synthesis and characterization of chemically fueled supramolecular materials driven by carbodiimide-based fuels, *Nat. Protoc.*, **2021**, *16*, 3901–3932.
4. Rossum, S. A. P. van; Tena-Solsona, M.; Esch, J. H. van; Eelkema, R. ja Boekhoven, J., Dissipative out-of-equilibrium assembly of man-made supramolecular materials, *Chem. Soc. Rev.*, **2017**, *46*, 5519–5535.
5. Boekhoven, J.; Hendriksen, W. E.; Koper, G. J. M.; Eelkema, R. ja van Esch, J. H., Transient assembly of active materials fueled by a chemical reaction, *Sci.*, **2015**, *349*, 1075–1079.
6. Rieß, B.; Grötsch, R. K. ja Boekhoven, J., The Design of Dissipative Molecular Assemblies Driven by Chemical Reaction Cycles, *Chem*, **2020**, *6*, 552–578.
7. Mondal, S.; Podder, D.; Kumar Nandi, S.; Chowdhury, S. R. ja Haldar, D., Acid-responsive fibrillation and urease-assisted defibrillation of phenylalanine: a transient supramolecular hydrogel, *Soft Mat.*, **2020**, *16*, 10115–10121.
8. Olivieri, E.; Gasch, B.; Quintard, G.; Naubron, J.-V. ja Quintard, A., Dissipative Acid-Fueled Reprogrammable Supramolecular Materials, *ACS Appl. Mater. Interfaces*, **2022**, *14*, 24720–24728.
9. Rieß, B. ja Boekhoven, J., Applications of Dissipative Supramolecular Materials with a Tunable Lifetime, *ChemNanoMat*, **2018**, *4*, 710–719.
10. Tomasini, C. ja Castellucci, N., Peptides and peptidomimetics that behave as low molecular weight gelators, *Chem. Soc. Rev.*, **2013**, *42*, 156–172.
11. K. Johnson, E.; J. Adams, D. ja J. Cameron, P., Peptide based low molecular weight gelators, *J. Mater. Chem.*, **2011**, *21*, 2024–2027.
12. Pramanik, B. ja Ahmed, S., Peptide-Based Low Molecular Weight Photosensitive Supramolecular Gelators, *Gels*, **2022**, *8*, 533.
13. Shen, J.-S.; Mao, G.-J.; Zhou, Y.-H.; Jiang, Y.-B. ja Zhang, H.-W., A ligand-chirality controlled supramolecular hydrogel, *Dalton Trans.*, **2010**, *39*, 7054–7058.
14. Singh, N.; Kumar, M.; Miravet, J. F.; Ulijn, R. V. ja Escuder, B., Peptide-Based Molecular Hydrogels as Supramolecular Protein Mimics, *Chem. Eur. J.*, **2017**, *23*, 981–993.
15. Das, S. ja Das, D., Rational Design of Peptide-based Smart Hydrogels for Therapeutic Applications, *Front. Chem.*, **2021**, *9*, 770102.
16. Chevigny, R.; Schirmer, J.; C. Piras, C.; Johansson, A.; Kalenius, E.; K. Smith, D.; Pettersson, M.; D. Sitsanidis, E. ja Nissinen, M., Triggering a transient organo-gelation system in a chemically active solvent, *Chem. Commun.*, **2021**, *57*, 10375–10378.

17. Kar, T.; Mandal, S. K. ja Das, P. K., Organogel–Hydrogel Transformation by Simple Removal or Inclusion of N-Boc-Protection, *Chem. Eur. J.*, **2011**, *17*, 14952–14961.

18. Yang, Z.; Wang, L.; Wang, J.; Gao, P. ja Xu, B., Phenyl groups in supramolecular nanofibers confer hydrogels with high elasticity and rapid recovery, *J. Mater. Chem.*, **2010**, *20*, 2128–2132.

19. J. Bowerman, C.; M. Ryan, D.; A. Nissan, D. ja L. Nilsson, B., The effect of increasing hydrophobicity on the self-assembly of amphipathic β-sheet peptides, *Mol. Biosyst.*, **2009**, *5*, 1058–1069.

20. Nebot, V. J.; Armengol, J.; Smets, J.; Prieto, S. F.; Escuder, B. ja Miravet, J. F., Molecular Hydrogels from Bolaform Amino Acid Derivatives: A Structure–Properties Study Based on the Thermodynamics of Gel Solubilization, *Chem. Eur. J.*, **2012**, *18*, 4063–4072.

21. Debnath, S.; Shome, A.; Das, D. ja Das, P. K., Hydrogelation Through Self-Assembly of Fmoc-Peptide Functionalized Cationic Amphiphiles: Potent Antibacterial Agent, *J. Phys. Chem. B*, **2010**, *114*, 4407–4415.

22. A. Angulo-Pachón, C. ja F. Miravet, J., Sucrose-fueled, energy dissipative, transient formation of molecular hydrogels mediated by yeast activity, *Chem. Commun.*, **2016**, *52*, 5398–5401.

23. Chen, L.; Morris, K.; Laybourn, A.; Elias, D.; Hicks, M. R.; Rodger, A.; Serpell, L. ja Adams, D. J., Self-Assembly Mechanism for a Naphthalene−Dipeptide Leading to Hydrogelation, *Langmuir*, **2010**, *26*, 5232–5242.

24. Johnson, E. K.; Adams, D. J. ja Cameron, P. J., Directed Self-Assembly of Dipeptides to Form Ultrathin Hydrogel Membranes, *J. Am. Chem. Soc.*, **2010**, *132*, 5130–5136.

25. Cheng, G.; Castelletto, V.; Moulton, C. M.; Newby, G. E. ja Hamley, I. W., Hydrogelation and Self-Assembly of Fmoc-Tripeptides: Unexpected Influence of Sequence on Self-Assembled Fibril Structure, and Hydrogel Modulus and Anisotropy, *Langmuir*, **2010**, *26*, 4990–4998.

26. Yang, Z.; Gu, H.; Fu, D.; Gao, P.; Lam, J. K. ja Xu, B., Enzymatic Formation of Supramolecular Hydrogels, *Adv. Mater.*, **2004**, *16*, 1440–1444.

27. Ragazzon, G. ja Prins, L. J., Energy consumption in chemical fuel-driven self-assembly, *Nat. Nanotechnol*, **2018**, *13*, 882–889.

28. Panja, S.; Patterson, C. ja Adams, D. J., Temporally-Programmed Transient Supramolecular Gels, *Macromol. Rapid Commun.*, **2019**, *40*, 1900251.

29. Pappas, C. G.; Sasselli, I. R. ja Ulijn, R. V., Biocatalytic Pathway Selection in Transient Tripeptide Nanostructures, *Angew Chem. Int. Ed.*, **2015**, *127*, 8237–8241.

30. Tena-Solsona, M.; Rieß, B.; Grötsch, R. K.; Löhrer, F. C.; Wanzke, C.; Käsdorf, B.; Bausch, A. R.; Müller-Buschbaum, P.; Lieleg, O. ja Boekhoven, J., Non-equilibrium dissipative supramolecular materials with a tunable lifetime, *Nat. Commun.*, **2017**, *8*, 15895.

31. Ogden, W. A. ja Guan, Z., Redox Chemical-Fueled Dissipative Self-Assembly of Active Materials, *ChemSystemsChem*, **2020**, *2*, e1900030.

32. Wang, Z.; Li, Y.; Wang, X.; Pi, M.; Yan, B. ja Ran, R., A rapidly responsive, controllable, and reversible photo-thermal dual response hydrogel, *Polymer*, **2021**, *237*, 124344.

33. Boekhoven, J.; Brizard, A. M.; Kowlgi, K. N. K.; Koper, G. J. M.; Eelkema, R. ja van Esch, J. H., Dissipative Self-Assembly of a Molecular Gelator by Using a Chemical Fuel, *Angew Chem. Int. Ed.*, **2010**, *122*, 4935–4938.

34. Debnath, S.; Roy, S. ja Ulijn, R. V., Peptide Nanofibers with Dynamic Instability through Nonequilibrium Biocatalytic Assembly, *J. Am. Chem. Soc.*, **2013**, *135*, 16789–16792.

35. della Sala, F.; Neri, S.; Maiti, S.; Chen, J. L.-Y. ja Prins, L. J., Transient self-assembly of molecular nanostructures driven by chemical fuels, *Curr. Opin. Biotechnol.*, **2017**, *46*, 27–33.

36. Liu, M.; N. Creemer, C.; J. Reardon, T. ja R. Parquette, J., Light-driven dissipative self-assembly of a peptide hydrogel, *Chem. Commun.*, **2021**, *57*, 13776–13779.

37. Heuser, T.; Weyandt, E. ja Walther, A., Biocatalytic Feedback-Driven Temporal Programming of Self-Regulating Peptide Hydrogels, *Angew Chem. Int. Ed.*, **2015**, *127*, 13456–13460.

38. Hoque, J.; Sangaj, N. ja Varghese, S., Stimuli-Responsive Supramolecular Hydrogels and Their Applications in Regenerative Medicine, *Macromol. Biosci.,* **2019**, *19*, 1800259.

39. Hao, M.; Li, L.; Wang, S.; Sun, F.; Bai, Y.; Cao, Z.; Qu, C. ja Zhang, T., Stretchable, self-healing, transient macromolecular elastomeric gel for wearable electronics, *Microsyst. Nanoeng.*, **2019**, *5*, 1–10.

40. Abdallah, D. J. ja Weiss, R. G., Organogels and Low Molecular Mass Organic Gelators, *Adv. Mater.*, **2000**, *12*, 1237–1247.

41. Shapiro, Y. E., Structure and dynamics of hydrogels and organogels: An NMR spectroscopy approach, *Prog. Polym. Sci.*, **2011**, *36*, 1184–1253.

42. Marchesan, S.; Vargiu, A. V. ja Styan, K. E., The Phe-Phe Motif for Peptide Self-Assembly in Nanomedicine, *Molecules*, **2015**, *20*, 19775–19788.

43. Aykent, G.; Zeytun, C.; Marion, A. ja Özçubukçu, S., Simple Tyrosine Derivatives Act as Low Molecular Weight Organogelators, *Sci. Rep.*, **2019**, *9*, 4893.

44. Lin, L. S.; Lanza, T.; de Laszlo, S. E.; Truong, Q.; Kamenecka, T. ja Hagmann, W. K., Deprotection of N-tert-butoxycarbonyl (Boc) groups in the presence of tert-butyl esters, *Tetrahedron Lett.*, **2000**, *41*, 7013–7016.

45. Fulmer, G. R.; Miller, A. J. M.; Sherden, N. H.; Gottlieb, H. E.; Nudelman, A.; Stoltz, B. M.; Bercaw, J. E. ja Goldberg, K. I., NMR Chemical Shifts of Trace Impurities: Common Laboratory Solvents, Organics, and Gases in Deuterated Solvents Relevant to the Organometallic Chemist, *Organometallics*, **2010**, *29*, 2176–2179.

46. Kong, J. ja Yu, S., Fourier Transform Infrared Spectroscopic Analysis of Protein Secondary Structures, *Acta Biochim. Biophys.* **2007**, *39*, 549–559.

Appendices

APPENDIX 1

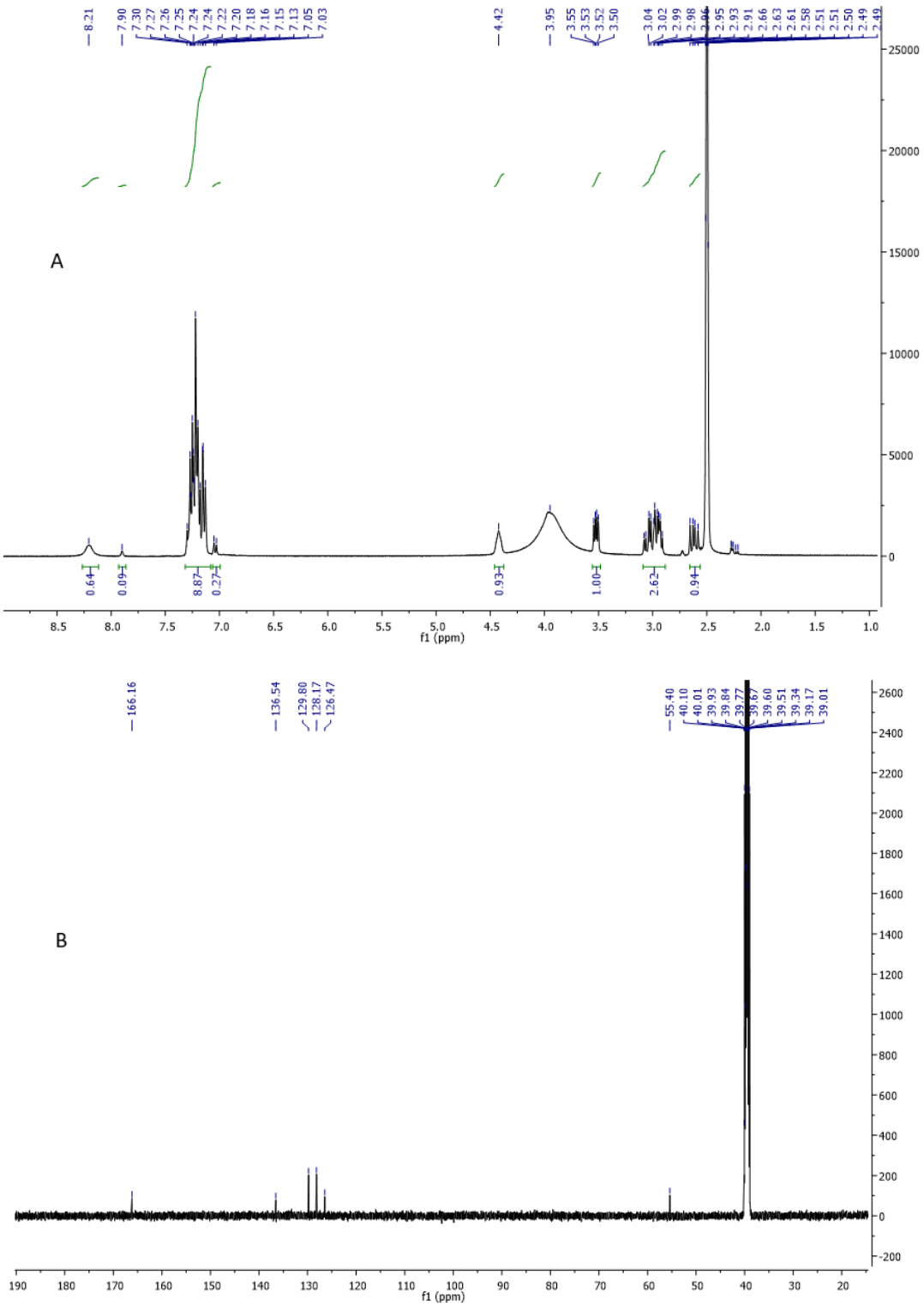

Figure A1. ^{1}H (A) and ^{13}C (B) NMR spectra of Phe-Phe: ^{1}H NMR (300 MHz, DMSO) δ 8.21 (s, 1H), 7.90 (s, 1H), 7.22 (tdd, J = 14.5, 9.2, 7.3 Hz, 10H), 7.04 (d, J = 6.8 Hz, 1H), 4.42 (s, 1H), 3.52 (dd, J = 8.4, 4.5 Hz, 1H), 3.11 – 2.88 (m, 2H), 2.62 (dd, J = 13.6, 8.4 Hz, 2H). ^{13}C NMR (126 MHz, DMSO) δ 166.16 (s), 136.54 (s), 129.80 (s), 128.17 (s), 126.47 (s), 55.40 (s).

APPENDIX 2

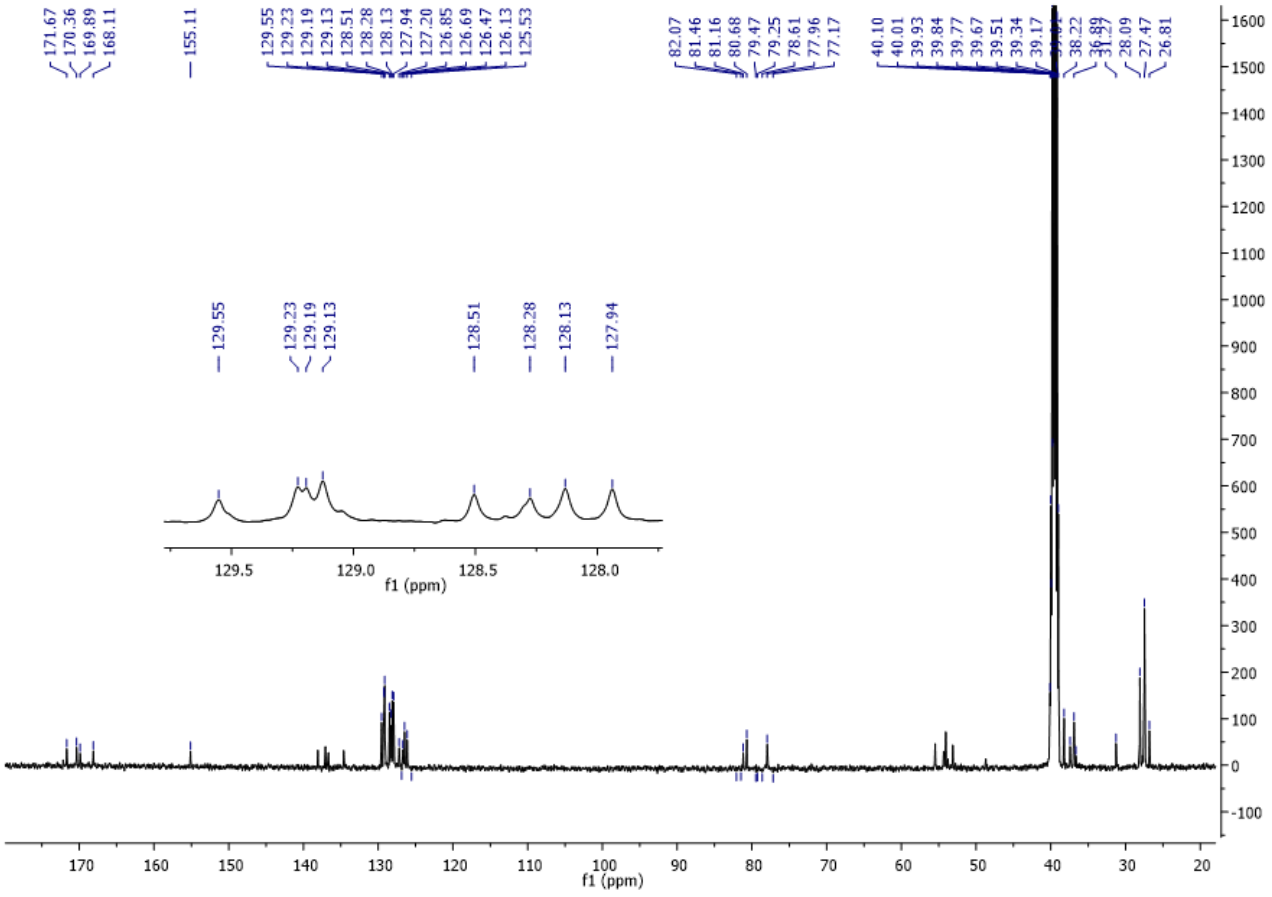

Figure A2. ^{13}C spectra of xerogel in *tert*-butyl methyl ether (0.18 eq of acid). ^{13}C NMR (126 MHz, DMSO) δ 171.67 (s), 170.36 (s), 169.89 (s), 168.11 (s), 155.11 (s), 138.08 (s), 137.06 (s), 136.55 (s), 134.61 (s), 129.55 (s), 129.34 – 128.96 (m), 128.51 (s), 128.28 (s), 128.13 (s), 127.94 (s), 127.20 (s), 126.69 (s), 126.47 (s), 126.13 (s), 81.16 (s), 80.43 (s), 77.96 (s), 55.26 (d, J = 56.6 Hz), 54.17 – 53.54 (m), 53.15 – 52.64 (m), 38.22 (s), 37.42 (s), 36.89 (s), 36.65 (s), 31.27 (s), 28.09 (s), 27.47 (s), 26.81 (s).

APPENDIX 3

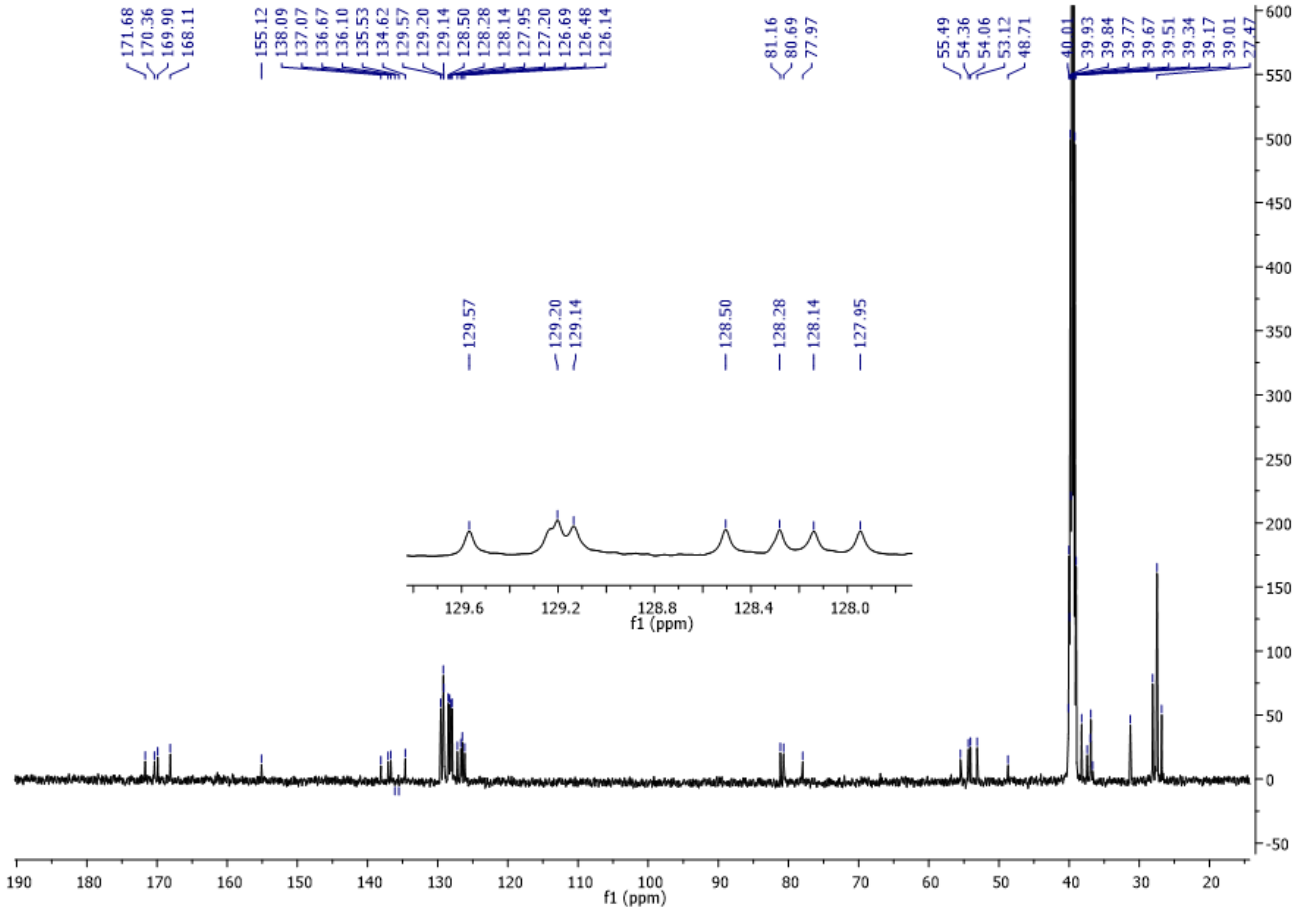

Figure A3. ^{13}C spectra of Boc-Phe-Phe-OtBu in *tert*-butyl methyl ether (0.18 eq of acid, solution). ^{13}C NMR (126 MHz, DMSO) δ 171.68 (s), 170.36 (s), 169.90 (s), 168.11 (s), 155.12 (s), 138.09 (s), 137.07 (s), 136.67 (s), 134.62 (s), 129.57 (s), 129.17 (d, J = 8.4 Hz), 128.50 (s), 128.28 (s), 128.14 (s), 127.95 (s), 127.20 (s), 126.69 (s), 126.48 (s), 126.14 (s), 81.16 (s), 80.69 (s), 77.97 (s), 55.49 (s), 54.36 (s), 54.06 (s), 53.12 (s), 48.71 (s), 38.22 (s), 37.43 (s), 36.94 (d, J = 9.5 Hz), 36.65 (s), 31.28 (s), 28.09 (s), 27.47 (s), 26.81 (s).

APPENDIX 4

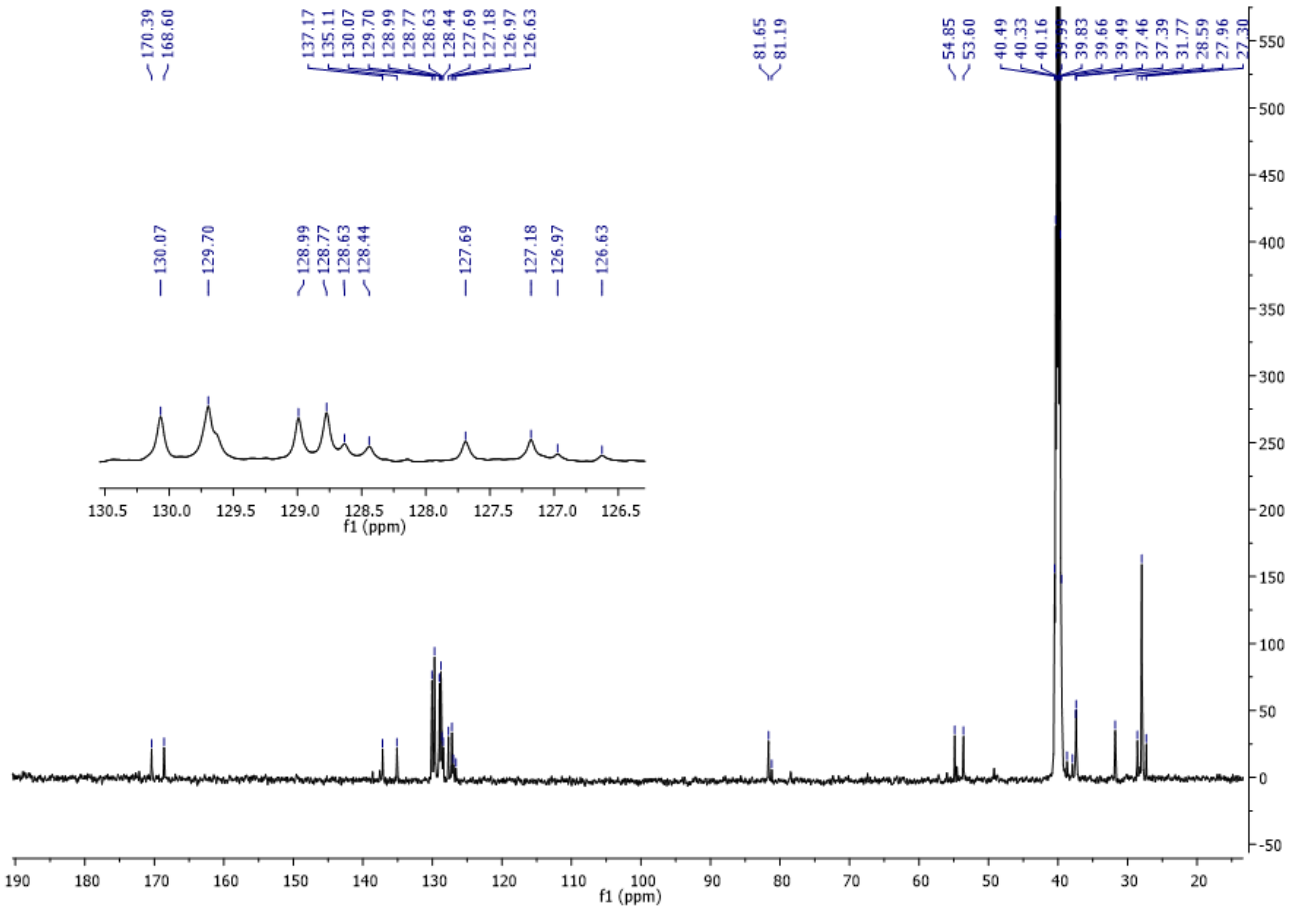

Figure A4. ^{13}C spectra of xerogel in *ter*t-butyl methyl ether (0.5 eq of acid). ^{13}C NMR (126 MHz, DMSO) δ 170.39 (s), 168.60 (s), 137.17 (s), 135.11 (s), 130.07 (s), 129.70 (s), 128.71 (dd, J = 43.4, 25.9 Hz), 127.69 (s), 127.08 (d, J = 26.2 Hz), 126.63 (s), 81.65 (s), 81.19 (s), 54.85 (s), 53.60 (s), 38.71 (s), 37.91 – 37.81 (m), 37.42 (d, J = 9.3 Hz), 31.77 (s), 28.59 (s), 27.96 (s), 27.30 (s).

APPENDIX 5

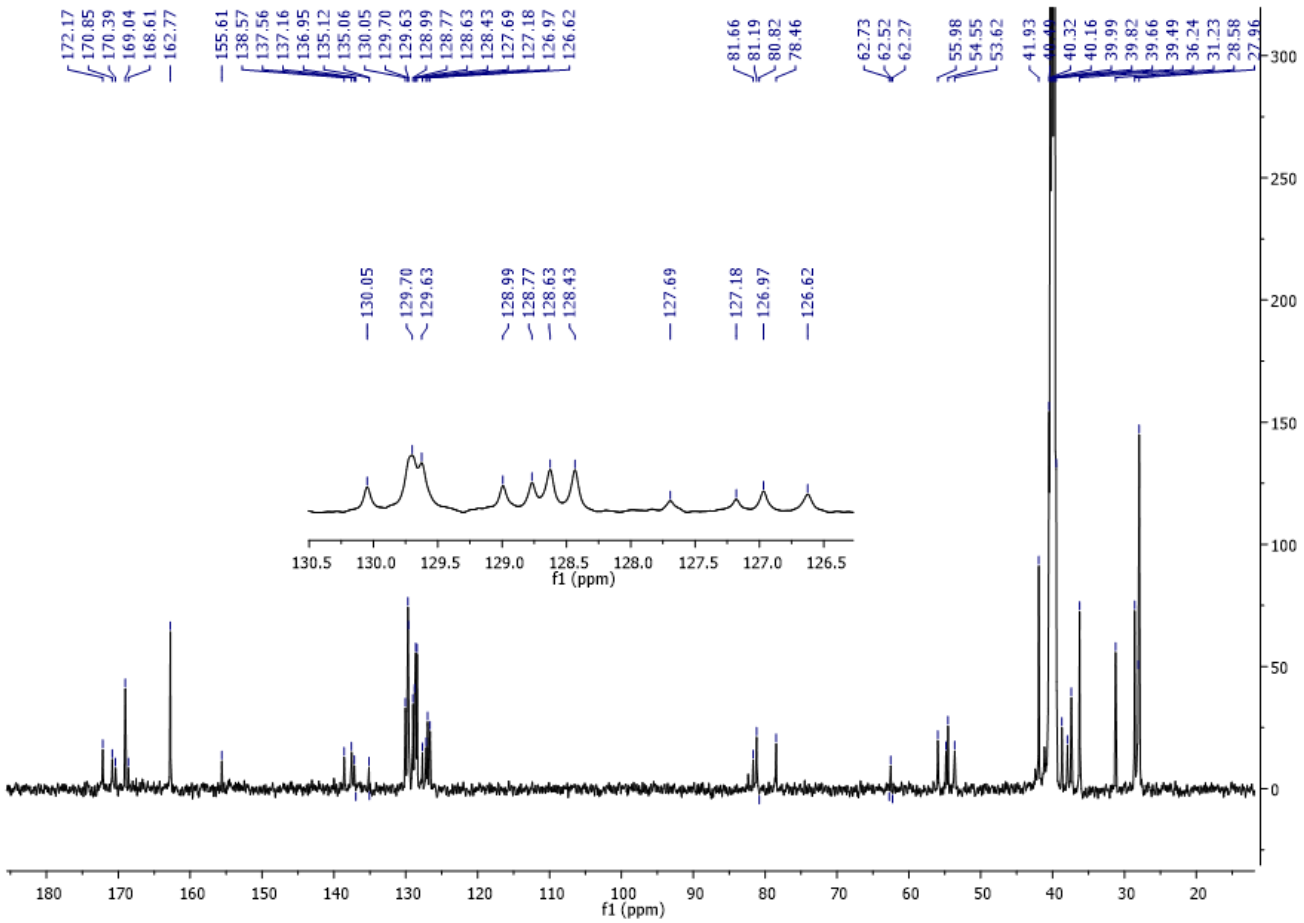

Figure A5. ^{13}C spectra of xerogel in *tert*-butyl chloroacetate (0.18 eq of acid). ^{13}C NMR (126 MHz, DMSO) δ 172.17 (s), 170.85 (s), 170.39 (s), 169.04 (s), 168.58 – 168.35 (m), 162.77 (s), 155.61 (s), 138.57 (s), 137.56 (s), 137.16 (s), 135.12 (s), 130.05 (s), 129.66 (d, J = 9.2 Hz), 128.99 (s), 128.70 (d, J = 17.7 Hz), 128.43 (s), 127.69 (s), 127.18 (s), 126.97 (s), 126.62 (s), 81.66 (s), 81.19 (s), 78.46 (s), 62.52 (s), 55.98 (s), 54.70 (d, J = 37.2 Hz), 53.62 (s), 41.93 (s), 38.70 (s), 37.93 (s), 37.39 (s), 36.24 (s), 31.23 (s), 28.58 (s), 28.02 (d, J = 16.0 Hz).

APPENDIX 6

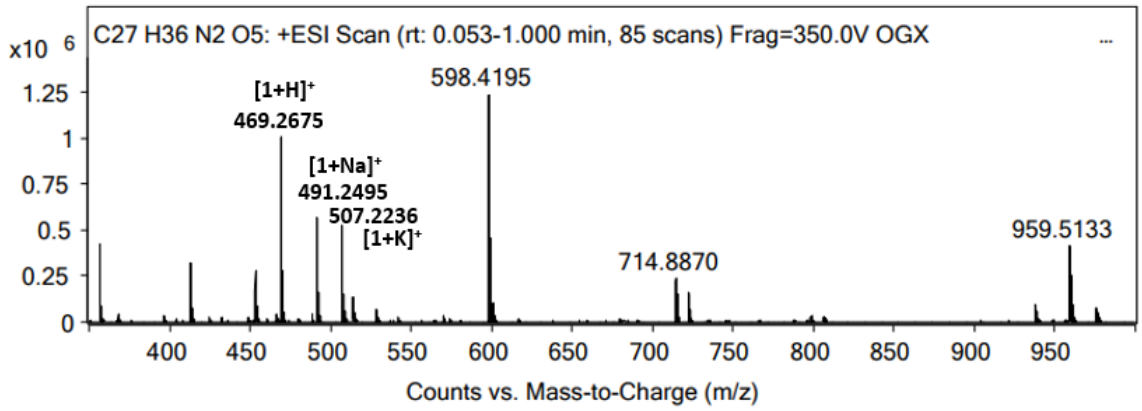

Peak List

m/z	z	Abund	Formula	Ion
130.1573		521689.91		
313.1525	1	597440.59	C15 H22 N O6	(M+H)+
357.1425	1	449518.38	C19 H20 N2 O5	(M+H)+
413.2058	1	321748.02	C23 H28 N2 O5	(M+H)+
469.2675	1	1059430.44	C27 H36 N2 O5	(M+H)+
491.2495	1	575523.38	C29 H34 N2 O5	(M+H)+
507.2236	1	529553.08	C32 H30 N2 O4	(M+H)+
598.4195	1	1301037.8		
599.4235	1	477798.81		
959.5133	1	428614.02		

Formula Calculator Results

Formula	Best	Mass	Tgt Mass	Diff (ppm)	Ion Species	Score
C15 H22 N O6	True	312.1455	312.1447	-2.62	C15 H23 N O6	97.79
C18 H20 N2 O3	False	312.1455	312.1474	5.95	C18 H21 N2 O3	91.14
C19 H20 N2 O5	True	356.1354	356.1372	4.98	C19 H21 N2 O5	95.75
C26 H16 N2	False	356.1354	356.1313	-11.44	C26 H17 N2	73.02
C23 H28 N2 O5	True	412.1987	412.1998	2.7	C23 H29 N2 O5	98.41
C30 H24 N2	False	412.1987	412.1939	-11.5	C30 H25 N2	75.81
C27 H36 N2 O4	True	452.2666	452.2675	2.02	C27 H37 N2 O4	99
C32 H36 O2	False	452.2665	452.2715	11.03	C32 H37 O2	83.05
C27 H36 N2 O5	True	468.2605	468.2624	4.06	C27 H37 N2 O5	94.97
C34 H32 N2	False	468.2605	468.2565	-8.45	C34 H33 N2	76.24
C30 H33 N O5	True	487.2365	487.2359	-1.22	C30 H34 N O5	81.76
C33 H31 N2 O2	False	487.2365	487.2386	4.26	C33 H32 N2 O2	73.47
C29 H34 N2 O5	True	490.2424	490.2468	8.88	C29 H35 N2 O5	88.48
C36 H30 N2	False	490.2424	490.2409	-3.06	C36 H31 N2	82.95
C33 H32 N O3	False	490.2424	490.2382	-8.51	C33 H33 N O3	82.92
C32 H30 N2 O4	True	506.2162	506.2206	8.63	C32 H31 N2 O4	74.64
C36 H28 N O2	False	506.2161	506.212	-8.18	C36 H29 N O2	70.3
C40 H24 O6	True	600.1588	600.1573	-2.46	C40 H25 O6	83.62

Figure A6. HR-MS spectra and mass accuracies of Boc-Phe-Phe-O*t*Bu. Spectra and mass accuracies of Boc-Phe-Phe-O*t*Bu are from Chevigny *et al.*[16]

APPENDIX 7

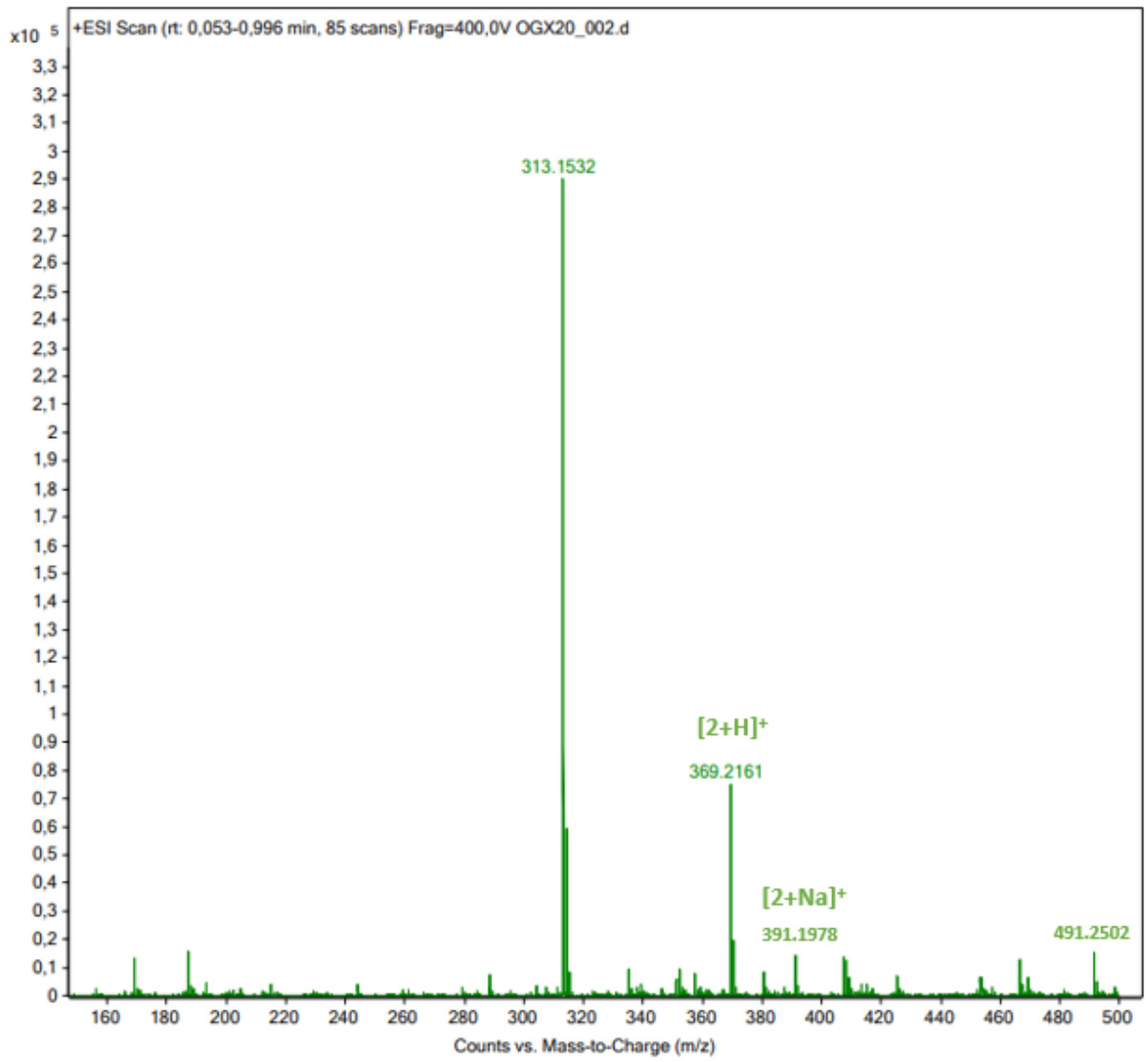

Figure A7. HR-MS spectra of Phe-Phe-O*t*Bu. Spectra of Phe-Phe-O*t*Bu is from Chevigny *et al.*[16]

APPENDIX 8

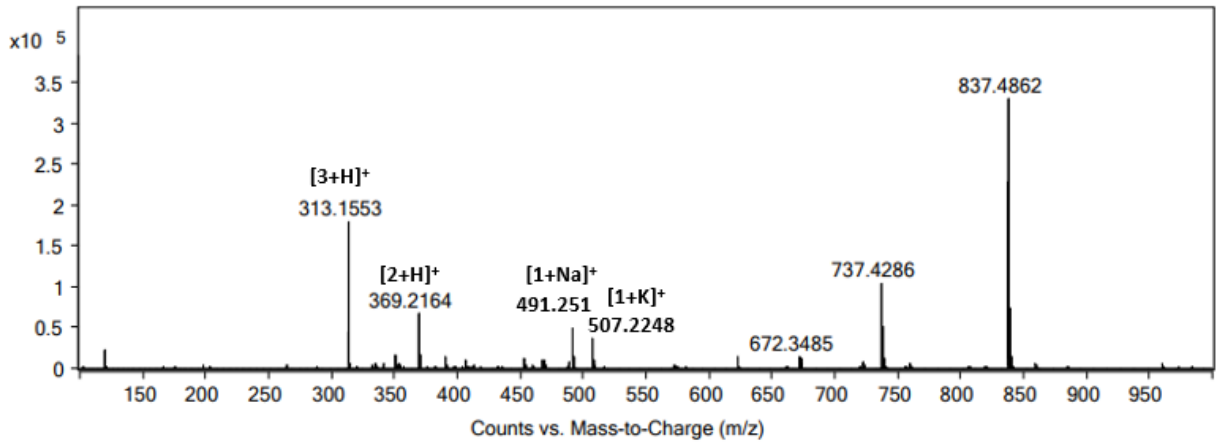

Peak List

m/z	z	Abund	Formula	Ion
313.1553	1	180721.33		
314.157	1	43999.68		
369.2164	1	68138.3		
491.251	1	48769.77	C27 H36 N2 O5	(M+Na)+
507.2248	1	37682.48	C27 H36 N2 O5	(M+K)+
737.4286	1	104932.2		
738.4314	1	52470.86		
837.4862	1	336949.73		
838.4871	1	229557.81		
839.488	1	75149.23		

Figure A8. HR-MS spectra of xerogel in *tert* butyl acetate (0.5 eq of acid).

APPENDIX 9

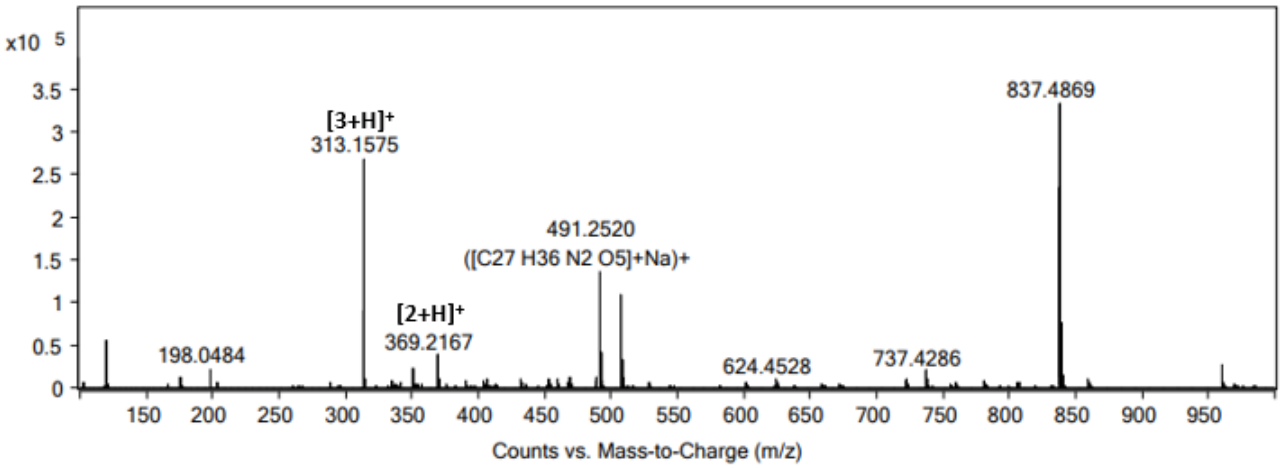

Peak List

m/z	z	Abund	Formula	Ion
120.0799	1	55287.19		
313.1575	1	269410.01		
314.1576	1	90258.73		
369.2167	1	38570.81		
491.252	1	137106.43	C27 H36 N2 O5	(M+Na)+
492.2544	1	41988.19	C27 H36 N2 O5	(M+Na)+
507.2258	1	111665.87	C27 H36 N2 O5	(M+K)+
837.4869	1	341996.37		
838.4877	1	235964.89		
839.4884	1	77235.2		

Figure A9. HR-MS spectra of xerogel in *tert*-butyl chloroacetate (0.18 eq of acid).

APPENDIX 10

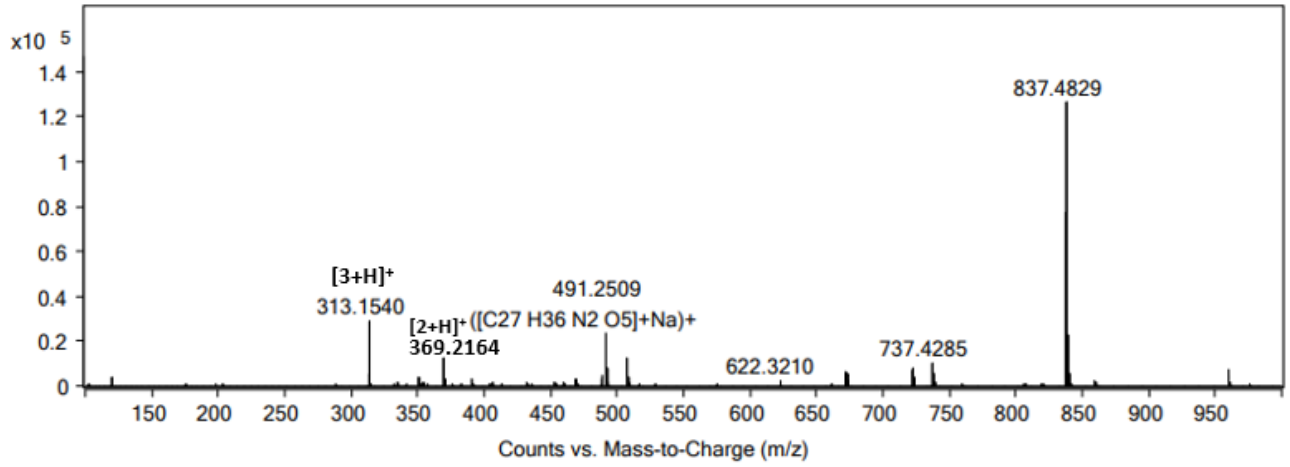

Peak List

m/z	z	Abund	Formula	Ion
313.154	1	28958.26		
369.2164	1	12755.82		
491.2509	1	23857.11	C27 H36 N2 O5	(M+Na)+
492.2544	1	7598.18	C27 H36 N2 O5	(M+Na)+
507.2248	1	13190.32	C27 H36 N2 O5	(M+K)+
722.3747	2	8003.29		
737.4285	1	10091.26		
837.4829	1	128559.38		
838.4852	1	77239.49		
839.4878	1	23183.24		

Figure A10. HR-MS spectra of xerogel in *tert*-butyl methyl ether (0.18 eq of acid).